Morphological effects of pulsed Doppler diagnostic ultrasound on rat adult lung and fetal tissues

A thesis presented in fulfillment of the requirements
for the degree of Master of Science in
Physiology and Anatomy at
Massey University

Stanica Milan Dulović

1999

TABLE OF CONTENTS

Abstract
Acknowledgments
CHAPTER 1 INTRODUCTION

1.1	**Use of ultrasound in medicine**	1.1
1.2	**Physics of ultrasound**	1.2
1.2.1	**Ultrasound (sound) wave**	1.2
	Cycle	1.2
	Period	1.2
	Frequency	1.2
	Wavelength	1.3
	Frequency and wave length	1.3
	Displacement amplitude	1.3
	Propagation speed	1.3
	Density of a medium	1.3
	Stiffness of a medium	1.3
1.2.2	**Acoustic pressure and pressure amplitude**	1.3
1.2.3	**Acoustic power and ultrasound (sound) intensity**	1.4
	Acoustic power output	1.4
1.2.4	**Propagation of ultrasound through a medium**	1.4
	Acoustic impedance of medium	1.4
	Reflection and refraction of ultrasound	1.5
	Absorption of ultrasound energy	1.5
	Attenuation of ultrasound energy	1.5
1.2.5	**Source of ultrasound (transducer)**	1.6
	Focusing an ultrasound beam (focal depth)	1.6
1.2.6	**Ultrasound scanning**	1.6
1.2.7	**Operating mode in ultrasound imaging**	1.7
1.2.8	**Doppler ultrasound**	1.8
	Doppler shift	1.8
	Doppler ultrasound imaging	1.8
	Pulse repetition frequency	1.8
1.2.9	**Mechanical index (MI)**	1.9

1.3	**Risk of using ultrasound in medicine**	1.9
1.3.1	**General opinions**	1.9
1.3.2	**Previous studies in adult lung**	1.10
1.3.3	**Previous studies in fetuses**	1.11
1.4	**Aim of the present study**	1.12
	TABLES	1.13
	FIGURES	1.16
CHAPTER 2	**MATERIAL AND METHODS**	2.1
2.1	**Experimental animals**	2.1
2.2	**Ultrasound machine**	2.1
2.2.1	**General information**	2.1
2.2.2	**Adjustment of focal depth**	2.2
2.3	**Experimetal procedures**	2.2
2.3.1	**Anaesthesia**	2.2
2.3.2	**Shaving and depilation**	2.2
2.3.3	**Ultrasound exposure**	2.2
	General features of exposure	2.2
	Specific features of exposure of the adult rat lungs	2.3
	Specific features of exposure of fetuses	2.3
2.3.4	**Euthanasia**	2.3
2.4	**Light microscopy**	2.4
2.4.1	**Adult lung**	2.4
	Transversly sectioned lobes	2.4
2.4.2	**Fetuses**	2.4
	Serially sectioned fetuses	2.4
2.5	**Statistics**	2.5
2.5.1	**Scoring of microscopical findings**	2.5
2.5.2	**Statistical methods**	2.5
	Mantel-Haenszel method	2.5
	Logistic regression analysis	2.5
	TABLES	2.6
	FIGURES	2.8

CHAPTER 3	RESULTS FOR ADULT RAT LUNGS	3.1
	Introduction	3.1
3.1	Normal rat lungs	3.1
3.1.1	Anatomy	3.1
3.1.2	Structure	3.2
	Blood supply	3.2
3.1.3	Ultrastructure	3.3
3.2	Lung haemorrhage	3.3
3.2.1	General features of the haemorrhage	3.3
3.2.2	Type of haemorrhage	3.3
	Frank haemorrhage	3.3
	Microscopically detected haemorrhage	3.4
	Artefactual haemorrhage	3.4
	Doubtful haemorrhage	3.4
	Haemorrhage in the control lung	3.4
3.2.3	Location of haemorrhage within a lung	3.4
3.2.4	Threshold study	3.5
	TABLES	3.6
	FIGURES	3.7
CHAPTER 4	RESULTS FOR FETUSES	4.1
	Introduction	4.1
4.1	Results in fetal rat lung	4.1
4.1.1	Normal lung in the last third of gestation	4.1
4.1.2	Fetal lung haemorrhage	4.2
4.2	Non-lung fetal haemorrhage	4.2
4.3	Effect of varying mechanical index (MI) on the incidence of fetal haemorrhage	4.3
4.3.1	Fetuses with lung haemorrhage	4.3
4.3.2	Fetuses with haemorrhage in any tissue	4.3
4.4	Effect of method of exposure on the incidence of fetal haemorrhage	4.4

4.5	**Effect of fetal age on haemorrhage**	4.4
4.6	**Results for serially sectioned fetuses.**	4.4
	TABLES	4.5
	FIGURES	4.10
CHAPTER 5	DISCUSSION	5.1
5.1	**Experimental methods as a model of clinical conditions**	5.1
5.1.1	**Experimental equipment**	5.1
5.1.2	**Mechanical index (MI) as a threshold parameter**	5.1
5.1.3	**Adjustment of the ultrasound machine for use with small labaratory animals**	5.1
5.2	**Damage in adult rat lungs**	5.2
5.2.1	**Lung haemorrhage**	5.2
	Anaesthesia and lung haemorrhage	5.2
5.2.2	**Possible sources of variations within experimental groups**	5.3
	Pregnancy	5.3
	Variations in experimental procedures on experimental rats	5.3
5.3	**Damage in the tissues of rat fetuses**	5.3
5.3.1	**General observations**	5.3
5.3.2	**Fetal lung haemorrhage**	5.4
5.3.3	**Haemorrhage in fetal tissues other than lungs**	5.4
5.3.4	**Effect of age on fetal haemorrhage**	5.4
5.4	**Possible pathophysiology of haemorrhage produced by ultrasound**	5.5
5.4.1	**Cavitation hypothesis**	5.5
5.4.2	**Hypothesis on the association of developing bone with fetal haemorrhage**	5.6
5.4.3	**Speculations on possible pathomechanism**	5.7
	Vulnerability of tissues	5.7
	Site of extravasation	5.7
	Heat	5.7
	Relative motion	5.8
	Blast injury	5.8

	Rapid volume and pressure changes	5.8
5.4.4	**Ultrasound induced haemorrhage and the repair process**	5.10
5.4.5	**The animal as a model for human being**	5.10
5.5	**Precautionary conclusion**	5.10

REFERENCES

This work is dedicated to my mother who had struggled with heart failure and died in her fifties. This motivated me to choose medicine and medical science as my life occupation.

ABSTRACT

This study investigated morphological effects of diagnostic pulsed Doppler ultrasound on adult and fetal rat lungs from 16 to 22 days gestation. A clinical ultrasound machine with two types of focused transducers (3.5 MHz, 5MHz) was used with an adjustment for an experimental animal as small as a rat. Three levels of exposure were represented by a mechanical index (MI) of 0.5, 0.6 and 1.0. Subpleural multifocal intra-alveolar haemorrhage was found to a significant degree in exposed adult rat lung and less significantly in fetal lung. The threshold for adult lung haemorrhage was considered to be between MI 0.5 and 0.6.

Fetal lungs were microscopically investigated by sectioning through the whole fetal body, which facilitated the discovery of haemorrhage at other sites. The percentage of exposed fetuses with haemorrhage is significant.

A threshold for fetal haemorrhage could not be determined because a significant variation due to age within each exposure group affected the results. The oldest 21 and 22 day old fetuses had no lung haemorrhage or significant non-lung haemorrhage. The risk for haemorrhage at all three exposure levels is more than double that of non exposed fetuses. Fetuses with lung in the canalicular stage of development (18-19 day) showed the greatest degree of lung haemorrhage.

Following laparotomy of the dam to achieve a precise and uniform exposure, a small number of fetuses within each exposure group was exposed directly. There was no higher degree of haemorrhage in these fetuses than in others indirectly exposed through the dam's abdominal wall.

The fetal age dependency of fetal lung haemorrhage found in this study adds complexity to the issue of adult and fetal lung sensitivity to ultrasound and to the question of the pathophysiological role of cavitation in the presence of air. In addition, our result in 21-22 day fetuses does not support the hypothesis that fetal haemorrhage is associated with developing bone.

The results in this study were achieved using conditions commonly used in echocardiography and obstetrical ultrasound examinations. Therefore, caution is suggested in the medical use of ultrasound.

Acknowledgments

In adjustment to a shift from medical human radiology to science I was very fortunate to have the expert guidance throughout the research period and writing of this thesis. I would like to express my sincere appreciation to my main supervisor Assoc. Prof. A. S. Davies and co-supervisor Prof. D. J. Mellor for this and their encouragement.

Histological methods were dominant in this research and without guidance received from Mr M. J. Birtles and Mr G. R. Hessel I would have achieved little. I am grateful to them and also to pathologist Assoc. Prof. M. R. Alley who confirmed some of the important pathological findings.

An understanding of the physics of ultrasound was a crucial part of this study and consultations with physicist Dr. G. R. G. Barnes were very much appreciated.

I am grateful to Mr R. N. Ward for his technical guidance and to Ms J. D. Neale and Mr J. E. Ormsby for their assistance during experimental procedures.

The assistance of Mrs D. A. Chesterfield and Mr J. E. Ormsby from the Small Animal Production Unit (Massey University) who kindly supplied the rats used for experiments, is acknowledged.

My apology to my sons, Neshko and Milan for enduring an ever busy, working mum and my thanks for their patience during the period of completion of my thesis.

I thank Neil for his love , moral support and helpful advice over the period of this research and the writing.

Chapter 1

INTRODUCTION

1.1 Use of ultrasound in medicine

The discovery of x-rays in 1895 by Wilhelm Roentgen (Webb, 1988; Harding, 1997) and the x-ray image of his wife Bertha's hand impressed all the world. It was the beginning of medical imaging science. It realised the longstanding dream of physicians and scientists to see inside the living human body and to use this to diagnose disease.

From 1895 to the present, medical imaging science has been developing dramatically through the improvement of diagnostic x-ray machines and techniques of x-ray examination. This trend has resulted in the discovery of new techniques other than x-ray imaging such as ultrasound in the early 1960s (Webb, 1988) and nuclear magnetic resonance (NMR) in the late 1970s (Pettergew, 1989; Andrew et al., 1990). The invention of computer x-ray tomography and its introduction in clinical medicine by Hounsfield and Ambrose in 1972 (Webb, 1988) had a prominent role in developments of all three medical imaging techniques. Each of these three imaging methods employ sources of different energy; electromagnetic radiation for x-ray, sonic spectra for ultrasound and nuclear resonance energy from a strong magnetic field and radio-frequency electromagnetic radiation for nuclear magnetic resonance.

Ultrasound is now the second most commonly requested imaging procedure after plain chest x-rays and this demand shows no sign of levelling out (Cosgrove, 1997). The addition of pulsed Doppler ultrasound and colour flow imaging has extended the use of ultrasound to vascular problems (Bude and Rubin, 1996) especially echocardiography. This is a common medical examination (Cosgrove, 1997), highly effective in the diagnosis of heart and vascular disease. The use of ultrasound in obstetrical examination has increased during the past ten years particularly since the addition of pulsed Doppler ultrasound and colour flow imaging (Tarantal et al., 1993). It has become a routine procedure (Lyons et al., 1988; Fisher at al., 1994) in the early detection of pregnancy, multiple gestation and the estimation of fetal age. Also, ultrasound is widely used in the screening of fetal development, early diagnosis of fetal malformations and other problems which would influence decisions with regard to early treatment or abortion (Boyd et al., 1998; Steinhorn , 1998).

Transrectal ultrasound scanning is the standard method of assessing the prostate and is particularly useful for biopsy guidance (Cosgrove, 1997). Musculoskeletal ultrasonography delineates soft tissue components of disease processes with high reliability. It is particularly useful for shoulder and Achilles tendon injuries and for muscle tears (Cosgrove, 1997). Also, ultrasound is a necessary tool for the screening of neonates for hip malformation (Vrdoljak, 1989).

Ultrasound is commonly used in therapeutic applications as an adjunct in the management of soft tissue dysfunctions, including joint contractures, tendinitis, bursitis, skeletal muscle spasm, and pain (Ziskin and Lewin, 1993). In addition, ultrasound has been employed in the treatment of stasis ulcers, bone fractures, and in the selective killing of cancer cells (Feigl et al., 1996). In extracorporal lithotripsy, the most powerful ultrasound produced by different types of lithotripter is used to disintegrate kidney, gall bladder and salivary stones (Cleveland et al., 1998).

1.2 Physics of ultrasound

1.2.1 Ultrasound (sound) wave

The part of the sonic spectrum outside the range of human hearing is a special form of sound called ultrasound. All sound is produced by the mechanical vibration of a source. The vibration is transfered to the surrounding medium producing displacement of particles, alternately compression (a condensation area with positive pressure) and stretching (a rarefaction area with negative pressure) of the molecular structure of the medium (Evans, 1988). This oscillatory pressure disturbance transfers sound from the source through the medium as a longitudinal sound wave such as an ultrasound wave. The wave is shown in Figure 1.1 as a sinusoidal curve, with definite amplitude, wave-length and frequency which are dependent on the sound source.

The *Cycle (Cy)* consists of the positive portion or condensation and the negative portion or rarefaction (Figure 1.1).

The *period (p)* is the time it takes for one cycle to occur and is expressed in milliseconds (ms).

The *frequency (F)* is the number of cycles of ultrasound wave per unit time expressed in kilohertz (kHz) or megahertz (MHz). The limit of human hearing is normally about 20kHz. Ultrasound ranges from 20kHz to 100MHz (Evans, 1988; Lockwood, 1996). It can be subdivided in three main regions: power ultrasound (20-100kHz) used in physiotherapy, high frequency ultrasound (100kHz-1MHz) used in lithotripsy , and diagnostic ultrasound (1-100MHz). Conventional diagnostic ultrasound machines

commonly operate over a range of 1- 10 MHz, although some new units can operate at frequencies 10 to 20 times higher. By using this high frequency, a microscopic resolution can be achieved (Lockwood, 1996).

The *wavelength (λ)* is the distance over which ultrasound waves travel during one cycle (Reef, 1998). It is equal to the distance between two adjacent maximum points of the positive or negative portion of the ultrasound wave (Sears et al., 1982).
The wavelength of diagnostic ultrasound is in the range of 0.02- 0.3mm in air , and between 0.1mm and 1.5mm in body tissues (Ball and Moore, 1997).

Frequency and wave-length are inversely related if the propagation speed of ultrasound within the medium remains constant.

The *displacement amplitude (A)* is the maximal particle displacement in the condensation or rarefaction area of the medium through which the ultrasound wave travels. It is expressed as the magnitude of the maximum value of the positive or negative portion on the ultrasound wave (Figure 1.1).

The *propagation speed (c)* is the speed at which an ultrasound wave moves through a medium. It is dependent on the density and mostly the stiffness of the medium (Reef, 1998).

The *density of a medium (d)* is expressed as a concentration or mass per unit volume. An increase in density of a medium results in a decrease in the propagation speed.

The *stiffness of a medium* is the resistance of a medium to compression. Propagation speeds are generally highest in solid tissue, lower in fluid filled structures, and lowest in air-filled structures because of decreasing stiffness (Table 1.1).
The values shown in Table 1.1 are fundamental to ultrasound imaging.

1.2.2 Acoustic pressure and pressure amplitude

An oscillatory pressure disturbance or ultrasound (sound) wave produced by transfer of vibration from an ultrasound source to its surrounding medium has an amplitude called the acoustic pressure amplitude (Figure 1.1). It is the maximum pressure variation within the condensation area (positive pressure amplitude) or within the rarefaction area (negative pressure amplitude) of the medium through which an ultrasound wave transfers.

The acoustic pressure amplitude (Ap) is directly proportional to the displacement amplitude (A) of the ultrasound wave and also depends on the wavelength. Waves of shorter wave length have greater pressure variations as well

acoustic pressure amplitude for a given displacement amplitude and the maxima and minima are squeezed together. Acoustic pressure (units of megapascal, MPa) is used as the threshold parameter for effects of ultrasound on exposed tissue (Hartman et al., 1990, Penny et al., 1993, Dalecki et al., 1997A, B).

1.2.3 Acoustic power and ultrasound (sound) intensity

Ultrasound waves carry energy. The amount of energy transported per second by an ultrasound wave is called **the acoustic power** (units of Watt, W).

The intensity (I) of a travelling ultrasound wave is defined as the acoustic power that passes perpendicularly through a surface (Figure 1.2) divided by the area of that surface. The unit of ultrasound intensity is power per unit area, or W m^{-2} (Cutnell and Johnsoon, 1998). The effect of ultrasound on the medium depends on the acoustic pressure amplitude of its waves and their intensity.

I is related to ultrasound pressure by :

$$I = p^2 c^{-1} d^{-1}$$

p: acoustic pressure amplitude
c: ultrasound propagation velocity
d: density of medium

Acoustic power output (APO) of an ultrasound source is the total power carried across a surface of a medium through which ultrasound energy propagates as an ultrasound wave. The APO equals the product of intensity at the surface and the surface area of a medium where ultrasound propagates. Intensity is a fundamental acoustic output parameter regulated by the United States Food and Drug Administration, FDA (Table 1.2) and displayed on the screen of an ultrasound machine as **SPTAd** (Spatial Peak Temporal Average) derated intensity (AIUM, 1992). SPTAd is related to a thermal bioeffect mechanism of ultrasound energy. It is derated, or adjusted for tissue attenuation, from an intensity measurement taken in water.

1.2.4 Propagation of ultrasound through a medium

As ultrasound propagates through a medium its intensity changes due to several processes. The most important of these are reflection, refraction, and absorption.

Acoustic impedance (Z) of a medium is a parameter used to differentiate between the ultrasound propagation properties of different media (Ball and Moore, 1997) and it is expressed by:

Z = density of medium (**d**) x propagation speed of ultrasound (**c**).

Some typical values of acoustic impedance are given in Table 1.3.

Reflection and refraction of ultrasound

At the interface between two different media, ultrasound is reflected or its direction is changed (refracted) (Figure 1.3) as it passes through the interface (Ball and Moore, 1997). The fraction of incoming ultrasound which is reflected at an interface depends upon the change in acoustical impedance across that interface. When the two media forming the interface have very different acoustic impedances, the original ultrasound will mostly be reflected, as between air and tissue. If there are only small differences in values of acoustic impedance (**Z**), most sound is transmitted without reflection, but it is refracted. The fraction of reflected ultrasound energy at an interface is called the **reflection coefficient** (**R**). In Table 1.4 some typical values of R are shown. The conditions under which reflection of ultrasound occurs at an interface are that the size of the interface must be large compared to a wavelength, and that the roughness of the interface must be small compared to a wavelength. The midline of the fetal brain is a good example of a biological interface with good conditions for reflection of ultrasound during obstretrical ultrasound screening. Large blood vessel walls (aorta and vena cava) and organ boundaries are also good interfaces for reflection of ultrasound. In Figure 1.4 (Cutnell and Johnson, 1998) is shown a case of sound reflection where the total sound power that passes through the surface is the sum of the direct and reflected powers. Thus, the total sound intensity at a distance from the source is greater than that of the direct sound alone.

Absorption of ultrasound energy is the conversion of a part of the ultrasound energy into heat, during propagation of ultrasound through a medium. In soft tissues it is the dominant source of ulrasound energy loss. The absorption falls off exponentially with distance. It is more convenient to define an **absorption coeficient** as a '**half-value thickness**' for each tissue (Table 1.5).

Attenuation of ultrasound energy

The overall loss of ultrasound energy during travel from an ultrasound source through tissue with a decrease of intensity and amplitude of the ultrasound waves is called attenuation. **The attenuation coefficient** (units of decibels, dB cm^{-1} per 1 MHz or neper, Np cm^{-1} per 1 MHz) is specific for every tissue (Table 1.6)(Breyer and Andreic, 1989). Inflated lung has the highest attenuation coefficient of any tissue of the body (Penney et al., 1992) because of the gas content. High frequency ultrasound such as diagnostic ultrasound is attenuated more than low-frequency ultrasound, limiting the depth of tissue to which the ultrasound beam can penetrate (Reef, 1998). Increasing the resolution of the ultrasound image by increasing the frequency used decreases its penetration through the exposed tissue.

1.2.5 Source of ultrasound (transducer)

An ultrasound transducer with an array of quartz crystals is the source of ultrasound and the main part of every ultrasound machine.

A quartz crystal becomes a vibrating sound source, because of **the piezo-electric effect**. When an electrical potential difference is applied across a crystal of quartz (Figure 1.5) its polar molecules alter their orientation slightly, causing the thickness of the crystal to change. The crystal expands or contracts according to the polarity of the potential difference applied, and produces ultrasound at the same frequency as the change in polarity. The same crystal can receive reflected sound from exposed tissue and transform it to an electrical impulse, when it is in the 'quiet' stage (no ultrasound production). The record of this electrical impulse on the screen of the ultrasound machine contributes to the formation of an ultrasound image.

Each transducer is constructed to produce a specific frequency of ultrasound. A higher-frequency transducer produces shorter wavelength ultrasound, an image with better resolution, but less depth of propagation. In ultrasound medical imaging, a high frequency transducer is used to image surface tissue structures and organs such as the thyroid and other superficial glands. A low frequency transducer is used to image deeper tissue structures and organs such as the heart, liver or kidney.

Different types of transducer produce a different shaped ultrasound beam (Figure 1.6).

Focusing an ultrasound beam (focal depth)

The resolution of fine detail of tissue structure in an ultrasound image is better when a focussed, narrow or convergent one used rather then an unfocused, divergent one [Figure 1.6 (A)]. A higher ultrasound frequency is more suitable for achieving fine focusing than a low ultrasound frequency. The best image is an image of tissue structure at the level of the focal plane.

1.2.6 Ultrasound scanning

An ultrasound image is based on the detection of reflected ultrasound waves (an echo) during wave propagation through exposed tissue. Electrical pulses are applied to the transducer to generate ultrasound pulses. A wide spectrum of frequencies is present within an ultrasound pulse. The shorter the pulse, the greater the frequency range of ultrasound that is emitted by the transducer. A short pulse of ultrasound is produced and directed as a narrow beam into the patient's body. The ultrasound beam will eventually meet an interface between different tissues and reflection will occur (Figure 1.3). If the interface is orientated at 90^0 to the beam, the reflected ultrasound waves will return to the transducer along the same path as the waves of the original pulse and may be detected as an echo. The time between the generation of the original pulse of ultrasound and the detection of the returning echo, combined

with a knowledge of the propagation speed of ultrasound through the tissues allows an estimate to be made of the total distance travelled by the pulse. Strength of a echo signal depends on the frequency of ultrasound, the depth of the interface and the values of acoustic impedance of the two tissues forming this interface.

Following transformation by a piezoelectric crystal to an electrical signal and electronic amplification, a detected echo is recorded on the screen. Echoes recorded during the ultrasound exposure of some body structure results in an ultrasound image or scan. Ultrasound scans are either A- scans or B-scans (Figure 1.7).

In an **A- scan** every echo from an interface is displayed as a peak on the graph where the distance of the interface is shown on the horizontal axis. The vertical axis shows the magnitude or strength of the echo. All displayed echoes represent the number of interfaces detected during ultrasound exposure. Measurement of the distance between some echoes can give useful information. For example, the distance between interfaces of the external and internal contours of parietal bones of the skull of a fetus (biparietal diameter) gives an indication of fetal maturity.

A **B-scan** shows an image of organs of structures in two dimensions. The image is made by bright points. Different echo signal strengths are reproduced as points of different brightness giving a so-called grey scale image. For example, an echo from an interface between soft tissue and bone is strong and is displayed as a bright point on the image but an echo from an interface between soft and fibrous tissue is less strong than the previous interface and is displayed as a less bright point.
The blackest part of a B-scan is without bright points because reflection has not occurred. This anechoic space usually represents air or liquid in a cavity such as a cyst. A B-scan can be a scan plane (Figure 1.8) of a transverse section, or a longitudinal or oblique section of a body region depending on the position of the transducer during imaging . A series of these scans recorded on videotape creates an anatomical map of a body region in three dimensions.

1.2.7 Operating mode in ultrasound imaging

There are three possible operating modes obtained by using the same transducer. **2D- mode** is used for B-scans. **Doppler mode** is for Doppler imaging and **colour flow mode** for a special Doppler imaging technique which shows different colours for blood vessels according to their blood flow. The use of **duplex mode** is common. For example, a machine with two screens can display a B-scan along with Doppler, which is routine in echocardiography.

1.2.8 Doppler ultrasound

The *Doppler shift*

When a source of sound, or a receiver (listener), or both, are in **motion** relative to each other, the pitch of the sound, as heard by the listener, is not the same as when source and receiver are at rest. The most common example is the sudden drop in pitch of the sound from a car horn as one meets and passes a car proceeding in the opposite direction. This phenomenon is called the Doppler effect and it was defined by Christian Johann Doppler (1803- 1853) in 1842 .

A listener (receiver) moving toward a source of sound hears a larger frequency and higher pitch than a stationary listener. Similarly, a listener moving away from the source hears a lower pitch with smaller frequency. These changes of frequency are the Doppler shift (Weill, 1996).

Doppler ultrasound imaging (pulsed Doppler)

The type of ultrasound imaging commonly called Doppler ultrasonography relies on the ability to detect a Doppler shift as sound is reflected off moving red blood cells. If red blood cells are moving toward the source (transducer), the ultrasound is reflected back to the transducer at an increased frequency. If they are moving away, the ultrasound is reflected back at a decreased frequency. The magnitude of that frequency or Doppler shift is determined by the velocity of blood flow which can be calculated.

Most ultrasound images including Doppler ultrasonography, are obtained using pulses of ultrasound (**pulsed Doppler**), rather than continuous ultrasound waves (**continuous-wave Doppler**). A pulse from the transducer in pulsed Doppler ultra sonography is sent out into tissues, and echoes reflected from tissue interfaces at predetermined depths and received before the next ultrasound pulse is sent. Continuous-wave Doppler continuously sends out sound and continuously receives sound. The frequency shifts are detected all along the ultrasound beam with no frequency range resolution because a two dimensional image is not provided and there is no way of detecting a depth of the reflected signal (Boon, 1998).

The *pulse repetition frequency (PRF)* is the number of pulses occurring per second and is expressed in kilohertz (kHz). High pulse repetition frequency Doppler is usually used to measure high red blood cell velocity in blood vessels at shallow depths of tissue because the echoes return quickly. However, at greater depths, a slower pulse rate is needed to wait for returning echoes (Reef, 1998).

1.2.9 Mechanical Index, MI

Mechanical Index is defined as the derated peak rarefactional acoustic pressure of an ultrasound beam in MPa divided by the square root of the ultrasonic frequency (MHz) from the central part of the ultrasound beam.

$$MI = p\, F^{-0.5}$$

p: acoustic pressure

F: frequency

The use of mechanical index for on-screen labelling of an ultrasound machine has been proposed so that the potential for harmful effects on exposed tissue can be indicated. The use of mechanical index is intended to provide a real-time display that will allow the operator to adjust acoustic output, thereby minimizing patient exposure and employing the 'as low as reasonably achievable', ALARA principle.

1. 3 Risk of using of ultrasound in medicine

1.3.1 General opinions

X-rays were used for medical imaging some time before their harmful effect on tissue was suspected (Harding, 1997). Eventually, following research into the effects of x-rays on biological material, techniques and exposure limits have been developed to minimise their harmful effects. But because of the continuing technological improvement of x-ray imaging machines with a potential increase in the risk of harm, research on safety must continue (Ziskin & Lewin, 1993).

Ultrasound has been used extensively for 30 years, without an appreciation of its potential harmful effects on exposed tissue (Haar, 1990; Fisher et al., 1994; Jochle et al., 1996). This also possibly applies to nuclear magnetic resonance imaging (Andrew et al., 1990). The number of both pre- and postnatal humans and other animals exposed to ultrasound each year continues to rise. There is a widely held view that diagnostic ultrasound, as currently used, is safe and presents no measurable hazard to the patient (Wagai and Fukuda, 1988; Ball and Moore, 1997). This view is supported by the published literature (Brent et al., 1991) in which adverse effects have not been convincingly demonstrated in repeatable studies. However, individual reports of effects arising from diagnostic levels of ultrasound warrant further consideration, especially since there is good evidence that the power from diagnostic machines continues to rise. The mean total power levels in pulsed Doppler mode have increased considerably (Haar, 1996).

There have been some recent indications from animal research that biological changes, especially in the lung (Baggs et al., 1996) can arise from ultrasound

exposure. Evidence for ultrasonically induced lung haemorrhage in experimental animals continues to accumulate (O'Brien and Zachary, 1996; Dalecki et al., 1997b). Although lungs are rarely examined directly their close physical relationship with the heart means that they are frequently exposed during echocardiography (Baggs et al., 1996). Damage is all the more possible since echocardiography today usually uses pulsed Doppler ultrasound.

The widespread use of diagnostic ultrasound in pregnancy reflects a concensus among clinicians that the technique is safe as well as beneficial, and this view is generally supported by the epidemiological literature (Brent et al., 1991). Dalecki et al. (1997A) produced lung and other fetal haemorrhage with a lithotripter in mice, but since pregnancy is a contraindication for lithotripsy, fetuses are not in danger clinically. Significant damage of fetuses using diagnostic ultrasound in appropriate diagnostic conditions has not previously been demonstrated for any species. Further studies on fetuses are needed because exposure to pulsed Doppler ultrasound is common during pregnancy.

1.3.2 Previous studies on the possible risk of ultrasound in adult lung

Child et al., (1990) used a lithotripter to produce lung haemorrhage in 7 week old mice and determined the threshold for it at the acoustic pressure of 1MPa. This level is very much less than the 10MPa levels commonly used to fragment kidney stones. Hartman et al. (1990) exposed adult and fetal mice of 18 days gestation with a lithotripter. This produced significant damage to the adult mouse lung, but no significant haemorrhage to fetal lung using the same intensity of ultrasound energy for both. The threshold for lung haemorrhage in adult mice was less than 2MPa. The presence of air in adult lung and its absence in fetal lung was considered by these researchers to be the main reason for this result. However, the presence of gas in *Drosophilia* larvae was considered by Carstensen et al., 1990 to be the reason for their death following ultrasound exposure. Penny et al. (1993) demonstrated lung haemorrhage in adult mice exposed to an isolated source of pulsed Doppler ultrasound (not a clinical ultrasound machine) and determined a threshold of 1.6 MPa for this harmful effect.

Tarantal and Canfield (1994) induced lung haemorrhage in monkeys, using a commercial clinical ultrasound machine placed in "triple mode"(two-dimensional imaging + color and pulsed Doppler) as the source of ultrasound. They did not determine a threshold level because they used only one level of exposure. It was the maximum limit of mechanical index (1.8) that it was possible to achieve with this ultrasound machine.

O'Brien and Zachary (1994) also produced lung haemorrhage in mice and rabbits from exposure to pulsed Doppler ultrasound but they did not find this effect in juvenile swine, even at levels greater than a mechanical index of 2. The same researchers in

1996 used continuous (nonpulsed) 30-kHz ultrasound induced lung haemorrhage in 10-12 week old crossbred pigs, rabbits and mice. There was a significant inter-species difference in sensitivity to ultrasound. The sensitivity ratio pig:rabbit:mouse was 1: 3.7:14, supporting a conclusion that ultrasound sensitivity is inversely related to body size. However, Baggs et al.(1996) induced lung haemorrhage in neonatal swine using pulsed Doppler ultrasound and determined threshold levels between 0.6 and 1.0 MPa , or a mechanical index of 0.6, values which
are similar to those previously reported for adult mice.

1.3.3 Previous studies in fetuses

There are two types of studies of possible harmful effect on exposed fetuses in different animal models. These are morphological studies which look at changes recorded in exposed fetuses soon after exposure, and teratologic studies on long term effects on prenataly exposed fetuses.

Acute morphological studies

Hartman et al. (1990) exposed 50 18 day mouse fetuses to a lithotripter. In only 2% was lung haemorrhage seen as a sign of lung damage. This effect was produced using ten times higher intensity of ultrasound (20MPa) than the threshold ultrasound exposure intensity for adult mouse lung damage. Atkinson et al. (1990) studied effects of ultrasound exposure on placental transfer during the last third of gestation in the rat (days 15 to 22). They concluded that the finding of placental vasostasis could be an effect of ultrasound exposure.

Dalecki et al., (1996) exposed 43 18 day mouse fetuses to a lithotripter over the abdominal wall of their dams. At 10 MPa of exposure intensity, all exposed dams but only 2 per cents of exposed fetuses suffered intestinal haemorrhage. The same researchers repeated this study in 1997. This time they found that in a significant number of fetuses with haemorrhage occurred in tissue near developing bone of the head, limbs, ribs. The threshold for the haemorrhage was determined as 1 MPa.

Teratologic studies

Experimental efforts to implicate ultrasound in an effect on in utero development have been inconclusive (Brent et al., 1991; Brown et al., 1991). Some studies have reported increased malformation rates (Shojy et al., 1975), while others have found no such effects (Kimmel et al., 1989). Effects of ultrasound exposure on fetal body weight have also been reported in some studies (Tarantal and Hendrickx, 1993; Hande and Devi, 1993), but not in others (Kimmel et al., 1989). Fisher et al. (1994) after their study in prenatally exposed rats using diagnostic pulsed ultrasound, concluded that there were no changes in fetal weight and no increase in skeletal or visceral malformations. The results of an *in vitro* experiment on rat embryos (Angles

et al., 1990) suggest that if pulsed ultrasound caused significant hyperthermia, it could affect development during early organogenesis of the neural plate and in particular they suggest that the embryo is at greater risk of damage during hyperthermic conditions. Carnes and Dunn (1995) have shown that ultrasound exposure in utero is capable of disrupting fetal development of the fetal mouse testis and having of potential for subsequent effects on fertility in the adult male.

Wilson and Waterhouse (1984) made a cancer epidemiology study of children which were exposed in utero, or not, to diagnostic ultrasound. They found that exposure was not correlated with the incidence of cancer.

1.4 Aim of the present study

This study attempts to answer the following questions as an approach to determine pathomechanisms of any harmful effect of ultrasound on biological material.

(i) Can pulsed Doppler ultrasound as produced by a clinically current ultrasound machine damage adult lung?

(ii) What is the threshold for this damage?

(iii) Can diagnostic pulsed Doppler ultrasound produce fetal damage in the last third of the gestation period?

(iv) Is fetal lung less sensitive than adult lung to damage from pulsed Doppler ultrasound?

(v) Can histological or physiological differences in adult and fetal lung tissue halp to explain the apparent difference in lung sensitivity to pulsed Doppler ultrasound?

Table 1.1 **Values of compressibility, density and speed of sound in biological material.**

Material	**Compressibility** (10^9 m s^2 kg^1)	**Density** (10^3 kg m^{-3})	**Speed of sound** (m s^{-1})
Bone (skull)	0.08- 0.05	1.38- 1.81	3050-3500
Liver	0.38	1.06	1570
Kidney	0.40	1.04	1560
Blood	0.38	1.06	1570
Fat	0.51	0.92	1460
Lung	5.92	0.40	650

Data from Lerski (1988).

Table 1.2 **Current FDA limits for SPTAd** (from Ultramark 9 HDI reference manual, 1994).

Clinical application	**FDA limit** (mW cm^{-2})	**SPTAd display**
Fetal imaging & other	94	94
Cardiac	430	430
Peripheral vascular	720	720

Table 1.3 **Values of acoustic impedance (Z) for biological materials.**

Material	Acoustic impedance
Bone	7.80
Liver	1.65
Kidney	1.62
Blood	1.61
Fat	1.38
Lung	0.26

Data from Lerski (1988).

Table 1.4 **Values of intensity reflection coefficient (R) for biological interfaces.**

Reflecting interface	Intensity reflection coefficient (R)
Muscle/blood	0.0009
Fat/kidney	0.006
Fat/muscle	0.01
Bone/muscle	0.41
Bone/fat	0.48
Soft tissue/air	0.99

Data from Lerski (1988).

Table 1.5 **Thickness of various materials required to reduce the intensity by half (half value thickness).**

Material	Half value thickness(cm) for 2 MHz	Half value thickness(cm) for 5 MHz
Air	0.06	0.01
Bone	0.1	0.04
Liver	1.5	0.5
Blood	8.5	3.0
Water	340	54

Data from Lerski (1988).

Table 1.6 **Values of attenuation coefficient for ultrasound for biological material**

Material	Attenuation coefficient (Nepers cm^{-1} MHz^{-1})
Brain	0.029
Liver	0.023
Muscle	0.11
Lung	2.0

Data from Breyer and Andreic (1989) and Penney et al.(1992).

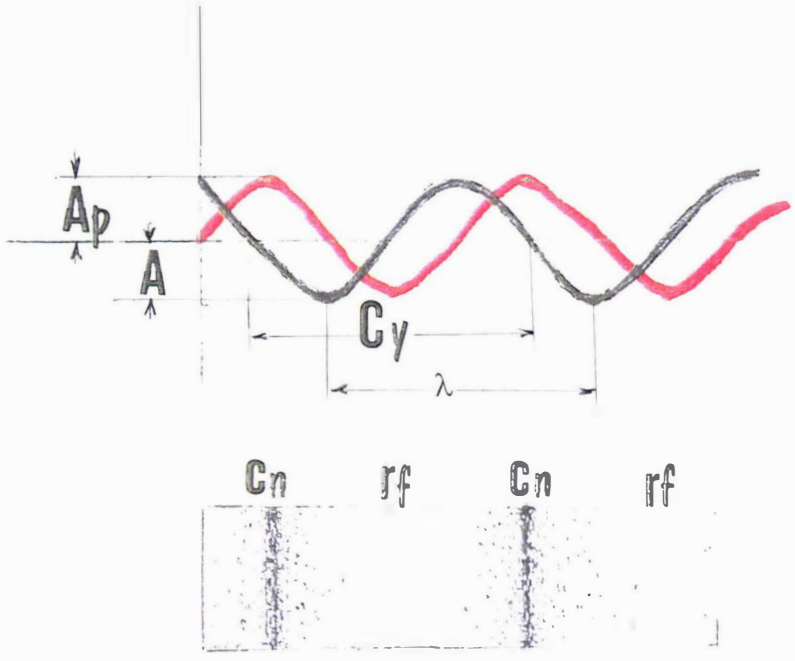

Figure 1.1 **Ultrasound (sound wave).** **A**: displacement amplitude; **Cy**: cycle; λ: wavelength; **Cn**: condensation area and **Rf**: rarefaction area of the medium through which ultrasound travels; **Ap**: acoustic pressure amplitude.
(Modified from Sears et al.,1982)

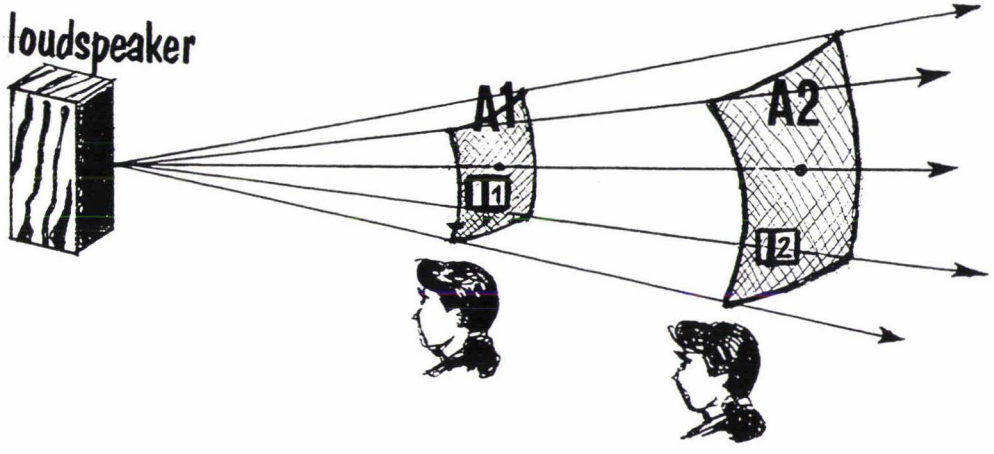

Figure 1.2 **Intensity (power per unit area) of sound (ultrasound) waves as the acoustic power that passes perpendicularly through an area. A1:** area 1 ; **I1:** intensity of sound at the area 1; **A2:** Area 2; **I2:** intensity of sound wave at the area 2. (Modified from Cutnell and Johnson, 1997).

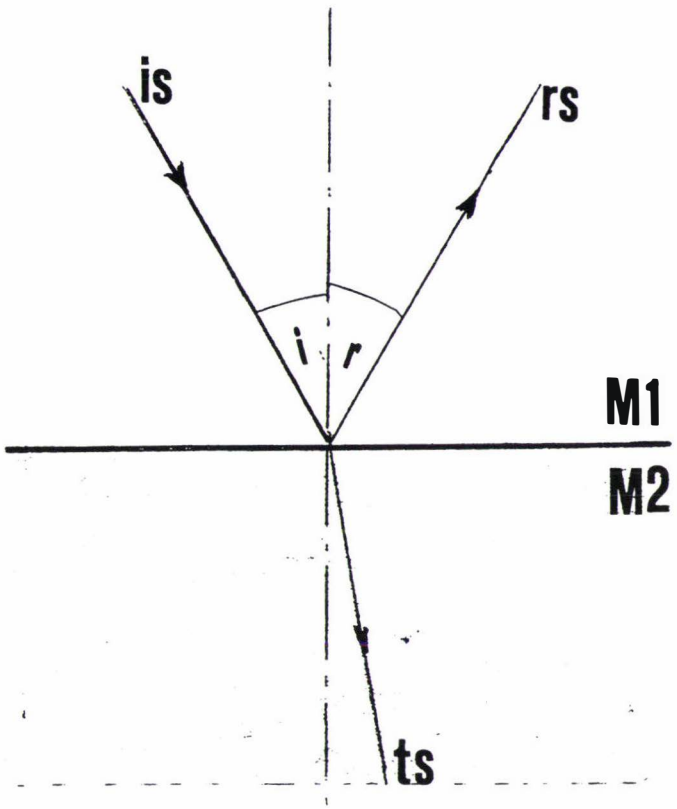

Figure 1.3 **Reflection and refraction of sound (ultrasound) at an interface between two media. M1**: medium 1 ; **M2**: medium 2; **is**: incident sound; **ts**: transmitted (refracted) sound; **rs**: reflected sound; **i**: angle of incidence; **r**: angle of reflection. (Modified from Ball and Moore, 1997.)

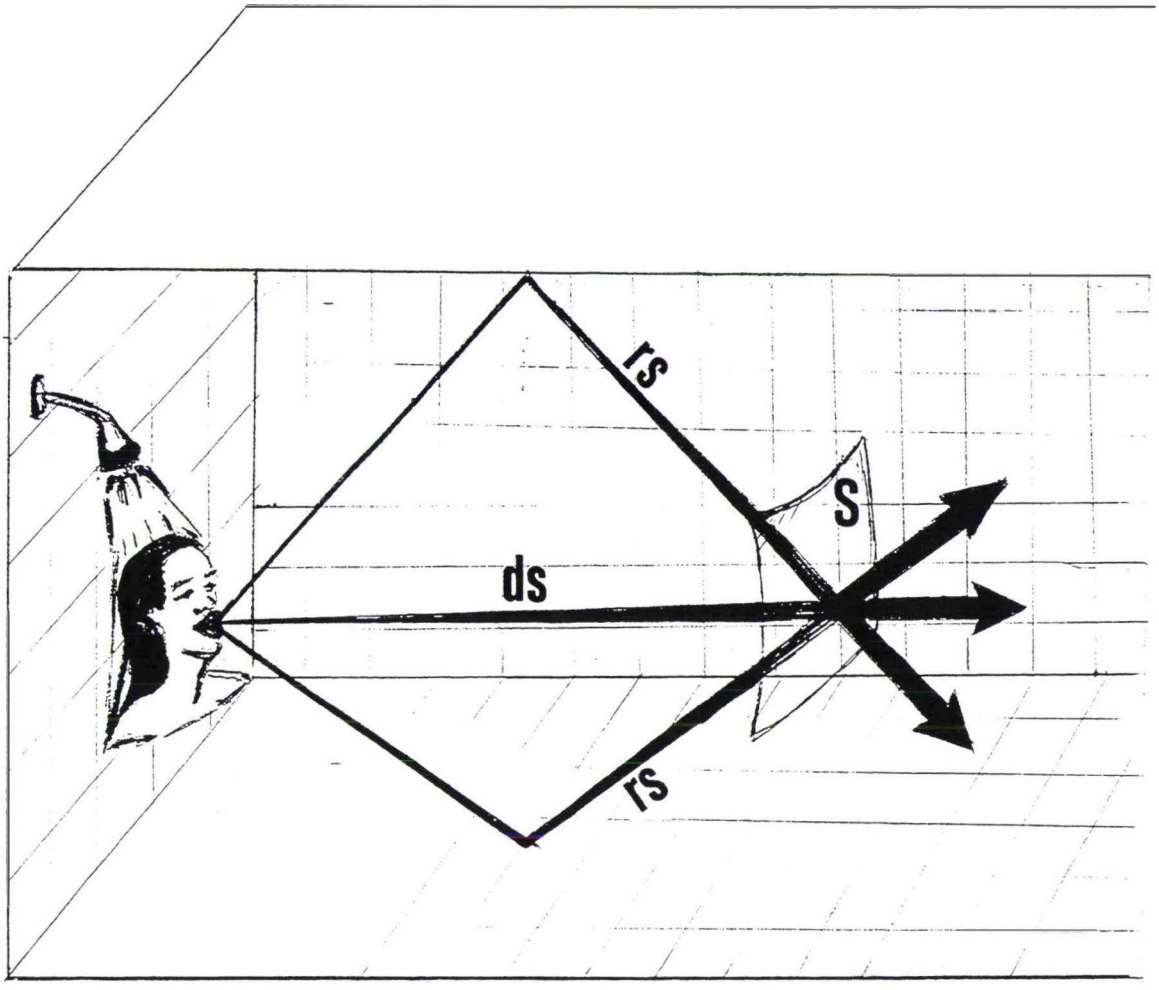

Figure 1.4 **A case of sound reflection (singing in the shower) where the total sound power that passes through the surface is the sum of the power of direct and reflected sound. ds**: direct sound; **rs**: reflected sound; **S**: the imaginary spherical surface. (Modified from Cutnell and Johnson, 1998).

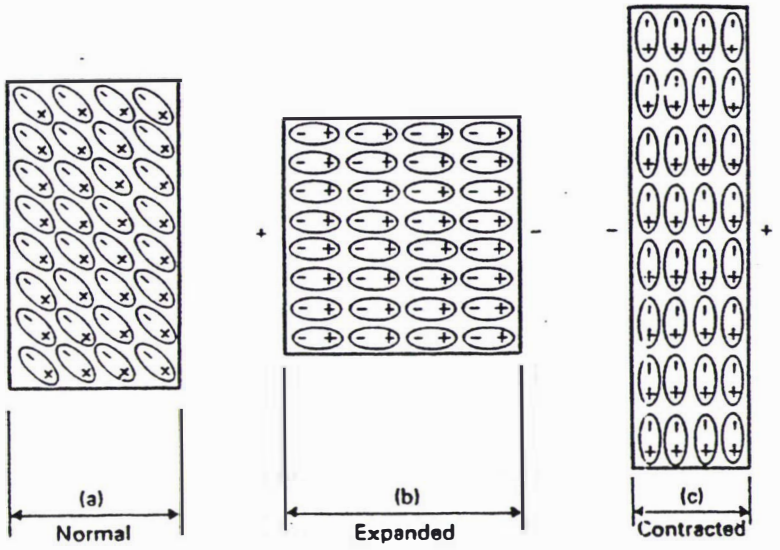

Figure 1.5 **The piezo-electric effect.** Piezo-electric crystals whose molecules posses polar properties are shown in the three different states: **(a)**- normal; **(b)**- expanded after applying a potential difference ; **(c)**- contracted as the result of reversing the applied potential (modified from Ball and Moore, 1997).

A

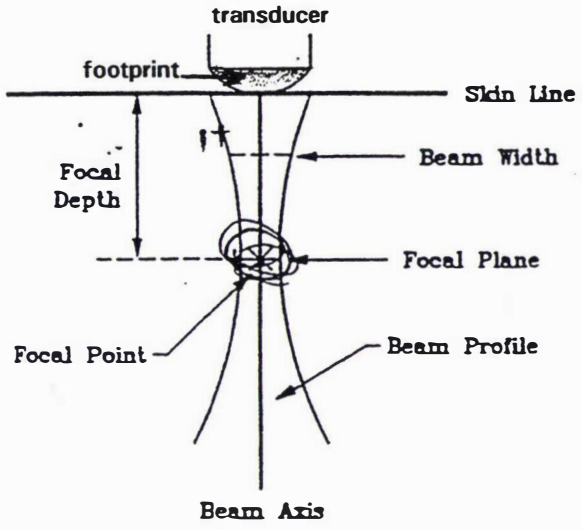

B

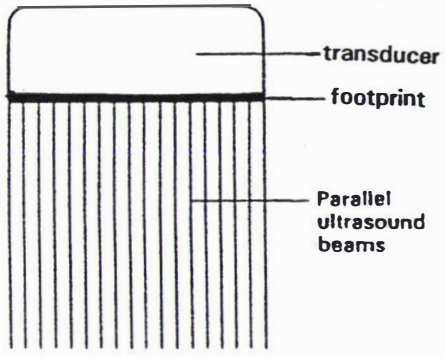

C

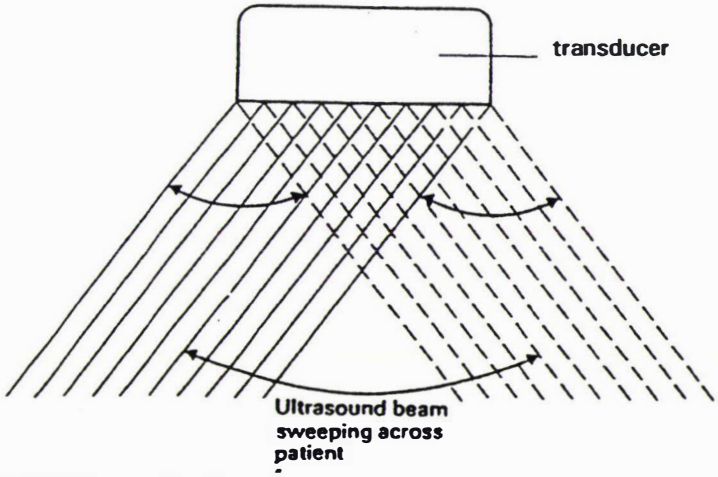

Figure 1.6 **Different types of transducer.** **(A)** focused transducer with focused ultrasound beam ; **(B)** unfocused transducer with parallel ultrasound beam; **(C)** unfocused transducer with divergent ultrasound beam.
(Modified from Ultramark 9 HDI reference manual, 1994 and Ball and Moore, 1997)

A

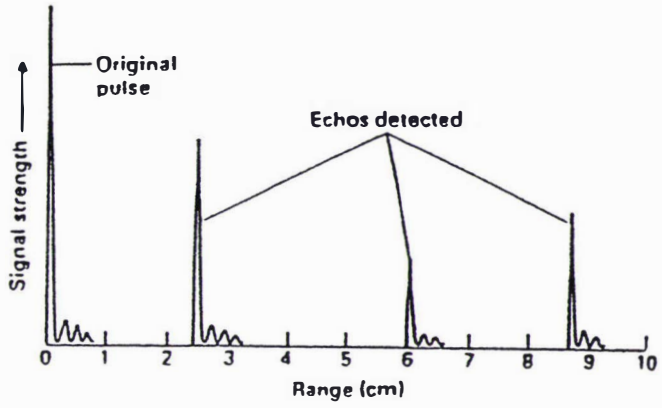

B

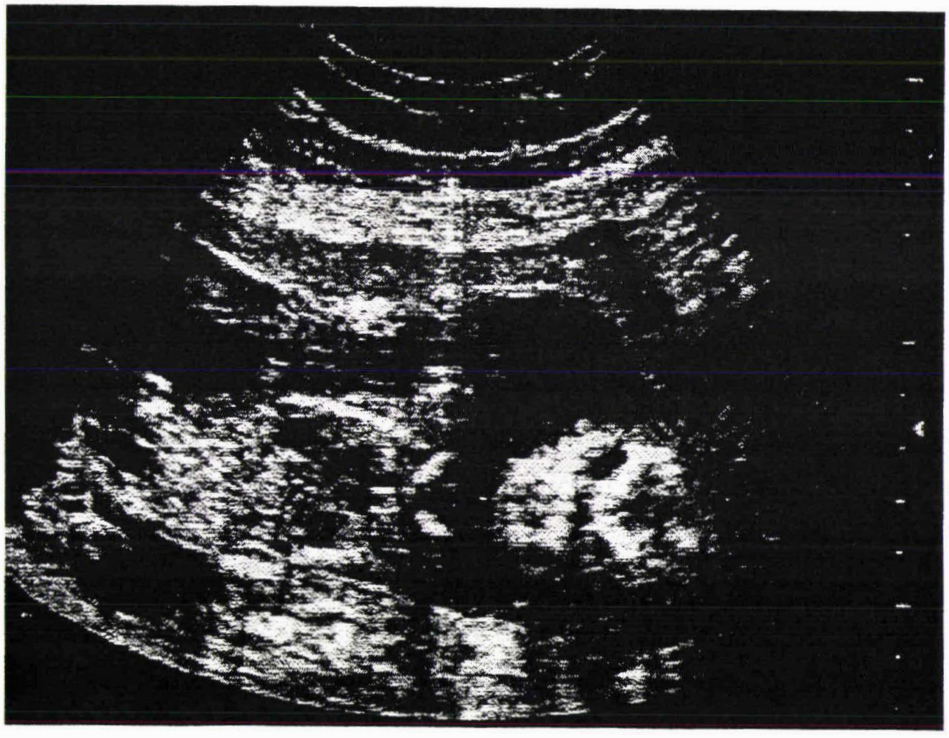

Figure 1.7 **Ultrasound scans. (A)** A-scan (Modified from Ball and Moore, 1997) **(B)** B-scan (human fetus).

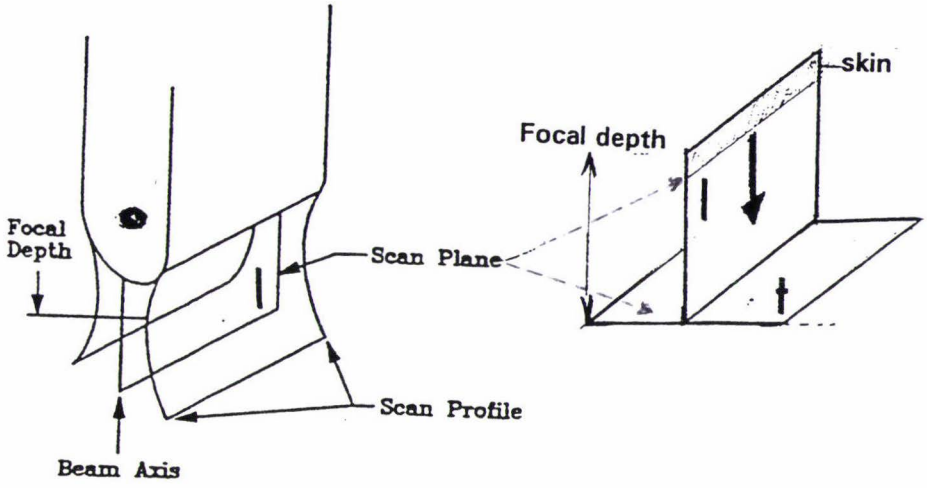

Figure 1.8 **Scan plane.** Scan plane of a longitudinal section of a body region (l); scan plane of a transverse section of a body region (t).
(Modification from Ultramark 9 HDI reference manual, 1994).

Chapter 2

MATERIALS AND METHODS

2.1 Experimental animals

All animal procedures employed in this study were approved by the Massey University Animal Ethics Committee. Forty-one white Sprague Dawley rats aged from 10 to 26 weeks (32 ultrasound exposed and 9 controls) were used [Table 3.1 Chapter 3)]. The animals were kept in an air conditioned room (22+-2^{0}C, 60% relative humidity) illuminated 12/24 hours and supplied with food and water *ad libitum*.

Thirty-four rats were pregnant (27 exposed and 7 controls) in the last third of gestation and 188 of their fetuses were also used in this study (147 ultrasound exposed and 41 controls) [Table 4.1 (Chapter 4)]. Females were caged with males of the same strain at 6.00 p.m. The occurrence of copulation was established the following morning at 9.00 a.m by checking for vaginal plugs. The day on which a vaginal plug was found was called day 0 of gestation (Schneider and Norton, 1979). Seven rats were intentionally not pregnant (5 exposed & 2 controls).

For 20 of the pregnant rats used, 5-6 fetuses in the left uterine horn were indirectly exposed by placing the transducer over the left ventral abdominal wall. After lung exposure, the abdominal wall of 6 pregnant rats was opened and the fetuses were exposed directly through the uterine wall. Eighteen fetuses of another 3 pregnant rats which had laparatomy were control fetuses unexposed to ultrasound.

In total, 112 fetuses were indirectly and 35 directly exposed. Twenty fetuses were controls for the indirectly exposed fetal group and 18 for the directly exposed group.

2.2 Ultrasound machine

2.2.1 General information

The ultrasound machine used in this study was an Ultramark 9 HDI (Figure 2.1) produced in 1994 by ATL (Advanced Technology Laboratories, Inc.; Bothell, WA, USA). This is a commercial ultrasound system similar to many scanners currently in clinical use.

All ultrasound exposures were performed with two convex focused transducers, P5-3 and P7-4, also produced by ATL. P5-3 is the most commonly used transducer in echocardiography and P7-4 in obstetrical ultrasound examination. Table 2.1 shows the main technical characteristics of the transducers.

2.2.2 Adjustment of focal depth

The focal depth of each transducer in this study was adjusted by using specially made perspex boxes (Figure 2.2) filled with LA5 HRS acoustic standoff (a medium with an attenuation of ultrasound energy of zero) produced by ATL Professional Medical Supply (USA).

The small body size of the experimental animals required this adjustment to achieve exposure of the adult and fetal lung at particular focal depth and known MI. As explained in Chapter 1, the values of MI on the screen, for every type of transducer and modality of operation, is measured at the focal depth. For example, the ultrasound exposure of adult rat lung at MI 1.0, using the P5-3 transducer in Doppler mode, can be achieved only at a focal depth of between 3 to 5 cm. The depth of a rat lung from the surface of the thorax is 3-5 mm. Therefore an additional depth of 3cm was made using standoff between the transducer and the animal.

The perspex standoff holder was firmly clamped to the transducer and closely applied to the body surface of each rat (Figure 2.2).

2.3 Experimental procedures

2.3.1 Anaesthesia

Before ultrasound exposure, all experimental animals were anaesthetized using Sodium Pentobarbitol (Nembutal; Virbac Laboratories Ltd ; Auckland, New Zealand) administered intraperitoneally at 60 mg/kg of body weight.

2.3.2 Shaving and depilation

Hair was removed from the areas on the surface of the dorsal right thoracic wall and left lateral abdominal wall of anaesthetized rats. This was accomplished by clippers followed by application of depilation paste (Veet- creme depilatoire; Reckett & Colman Ltd; Auckland, New Zealand) to avoid the loss of ultrasound energy from the presence of air on the surface of hairs, which would attenuate ultrasound energy.

2.3.3 Ultrasound exposure

The general features of exposure

All experimental rats, excluding the controls, were exposed to 6 minutes of pulsed Doppler ultrasound over the right lung and 6 minutes over the fetuses.

In this study there were four groups for the adult rat lungs and the rat fetuses (three exposed groups and one control group) with different intensity as set by four values of mechanical index. These values were 0.0 (controls), 0.5, 0.6 and 1.0.

MI 0.6 was the first chosen value for ultrasound exposure as this is the predicted threshold value based on previous research data for mouse lung haemorrhage (Hartman et al., 1990 , Dalecki et al.,1997A). MI 1.0 was chosen for this study as a value over 0.6 but much less than the maximal 1.8. It is also a common value during clinical ultrasound examination. MI 0.5 was chosen as a value under 0.6 and also a frequent value in ordinary clinical situations. Other parameters of ultrasound exposure for each of the four groups are shown in Table 2.2.

All ultrasound exposures were performed at maximum output in pulsed Doppler mode, which is commonly used in echocardiogaphy and obstetric ultrasound examinations.

Ultrasound gel(Vibragel) manufactured by Polyganic Enterprises Ltd. (Christchurch, New Zealand) was spread over the exposed region. The gel minimised the loss of ultrasound energy between the transducer and the exposed body region.

Specific features of exposure of adult rat lungs

The right lungs of all adult rats, excluding the controls, were exposed dorsally. The transducer was placed on the surface of the right side of the chest about 3mm from the vertebrae and over a transverse line between the vertebrae and the end of the sternum (Figure 2.3). The position of the transducer during exposure provided a transverse direction of the ultrasound beam as would be used to produce a transverse sectional image (scan) of the examined region [Figure 1.8 (Chapter 1)].

The specific features of exposure of fetuses

112 fetuses, each within a left uterine horn, were exposed indirectly for 6 minutes. The transducer was placed over the dam's left abdominal wall. The position of the transducer provided an ultrasound beam such that it produced a sagital sectional image (scan) of the examined region [Figure 1.8 (Chapter 1)].

Thirty-five fetuses were exposed directly after laparotomy of the dam (Figure 2.4). Every second fetus from both uterine horns was exposed separately for 6 minutes. Anaesthesia, and exposure of the whole dam, was therefore prolonged in animals treated in this way.

2.3.4 Euthanasia

All experimental animals were anaesthesied throughout ultrasound exposure and were subsequently killed with an overdose (400mg/kg of body weight) of sodium pentobarbitol injected intraperitoneally, or intrarenally for rats on which laparatomy had been performed. Because this drug crosses the placenta (Plumb, 1999) this dose also killed the fetuses.

2.4 Light microscopy

2.4.1 The adult lung

Within the first 25 minutes after death the adult rats' lungs and heart were removed as a whole and macroscopically investigated. The lungs were inflated by filling them with 1.5 to 2.5 ml of formol saline through the trachea. They were fixed

in formol saline, for at least 24 hours. The lungs were separated into lobes and dehydrated progressively to absolute alcohol, cleared using chloroform and xylene, and paraffin embedded. The samples were sectioned at a thickness of 7 nm, parallel to the costal surface at a depth of 1mm to 3mm. The sections were de-waxed with xylene, hydrated progressively and stained with haematoxylin and eosin.

Transversely sectioned lobes

The lobes of 8 rats' lungs (7 exposed and one control) with a previous finding of haemorrhage (on sections parallel to the pleural surface) were sectioned transversely to the pleural surface to determine depth of the haemorrhagic areas.

2.4.2 Fetuses

Within the first 30 minutes after death, all exposed fetuses and controls were removed from the uterine horn, separated from the placenta and other layers, measured for body length and macroscopically investigated. Before fixing in Bouin's fluid for 24 hours, they were incised 2-3 mm to the right of the sternum to ensure that the pleural cavity was filled with fixative and that the lungs were well perfused. For 24 hours of fixation, the fetuses older then 15 days were decalcified by immersion in Goodings & Stewart decalcifer (Culling et al., 1985). Whole fetuses were progressively dehydrated to absolute alcohol, paraffin wax processed and sectioned from the dorsal body surface to a depth of 3-4 mm (Figure 2.5). The sections were cut at 7 nm thickness. They were de-waxed with xylene, hydrated progressively and stained with haematoxylin and eosin.

Serially sectioned fetuses

Following examination of these fetal sections, six fetuses were selected to include three (aged 18-19 days) in which lung haemorrhage had been identified, and three in which lung haemorrhage was not apparent (aged 21-22 days). These blocks were serially sectioned, giving sections at approximately 1mm spacing, through to the ventral body surface.

2.5 Statistics

2.5.1 Scoring of microscopical findings

The presence of haemorrhage as a pathological finding was recorded as + (present), - (not present) or +- (doubtful) [Table 3.1 (Chapter 3) and Table 4.1 (Chapter 4). Each slide was assessed also by an independent histologist who scored each slide blindly (Birks et al., 1997).

2.5.2 Statistical method

Mantel-Haenszel method

This method was chosen for this study as a basic statistical method for binary data (presence or absence of haemorrhage)(McNeil, 1996).

Odds ratio and relative ratio were calculated as risk parameters for each experimental group (Figure 2.6). 'Odds' means the ratio of the probability of an event-disease occurring to the probability of it not occurring. A disease (haemorrhage in this study) odds ratio is estimated; this is the ratio of the odds of disease in exposed individuals to the odds in those unexposed (controls) (Thrusfield, 1995). If the odds ratio is close to 1, the exposure to the suspected risk factor (ultrasound exposure in this study) is unlikely to be associated with the risk of disease (haemorrhage in this study) (Pfeiffer, 1996).

Relative ratio (RR) is a prevalence ratio for a disease or events resulting from exposure to a risk factor. The disease (haemorrhage) is RR times more likely to occur among those exposed to the suspected risk factor (in this study it is an ultrasound exposure) than among those with no such exposure. If RR is greater or smaller than 1, the exposure is likely to be associated with the risk of disease, and the greater the departure from 1 the stronger the association.

The relative risk is the preferred parameter in a cohort study because, when the relative risk is greater than 1, the odds ratio will always overestimate it, particularly when disease not rare (Thrusfield, 1995). If the disease is rare (less than 10%), odds ratio can be used to estimate relative ratio (Pfeiffer, 1996).

Logistic regression analysis

This method is used in this study (SPSS program; SPSS Inc. Chicago, USA) to predict a binary dependent variable (haemorrhage) from a set of independent variables (mechanical index, fetal age and method of ultrasound exposure) (McNeil, 1996), calculating a logistic odds ratio as a parameter for risk. The method is especially useful to handle covariates (fetal age and way of exposure) for each mechanical index group.

Table 2.1 **The main technical parameters of the transducers used in this study.** Footprint (Figure 1.6); MI, mechanical index. The value of MI shown is the maximal value possible at the indicated focal depth for each transducer.
Values are taken from the Ultramark 9HDI reference manual, 1988.

Transducer	**Operating frequency (size)** (MHz)	**Doppler frequency (size)** (MHz)	**Footprint** (mm)	**Focal depth** (cm)	**MI**	**Intensity Max.** (W/cm)
P5-3	3.5	3.0	16	1.7	1.4	314
P7-4	5.0	4.0	11	3.0	1.0	661

Table 2.2 **Parameters of ultrasound exposure for each of the three exposure groups as displayed on the screen of the ultrasound machine. PRF**, pulse repetition frequency (Chapter 1); **SPTAd**, parameter for thermal effect of ultrasound exposure (Chapter 1).

MI	**Transducer**	**Standoff height** (cm)	**Focal depth** (cm)	**PRF**	**SPTAd**
1.0	P5-3	3	3.25	3704	92
0.6	P7-4	4	4.5	3704	78
0.5	P7-4	12	12.5	3704	75

	HAEMORRHAGE	NO HAEMORRHAGE	TOTAL
EXPOSED	a	b	a + b
NON-EXPOSED	c	d	c + d
TOTAL	a + c	b + d	N

$$RR = (a/\{a+b\})/(c/\{c+d\})$$

$$OR = (a/b)/(c/d) = (axd)/(cxb)$$

Figure 2.6 **Calculation of the relative risk (RR) and the odds ratio (OR) for comparing risk factors** (Modification from Pfeiffer, 1996)

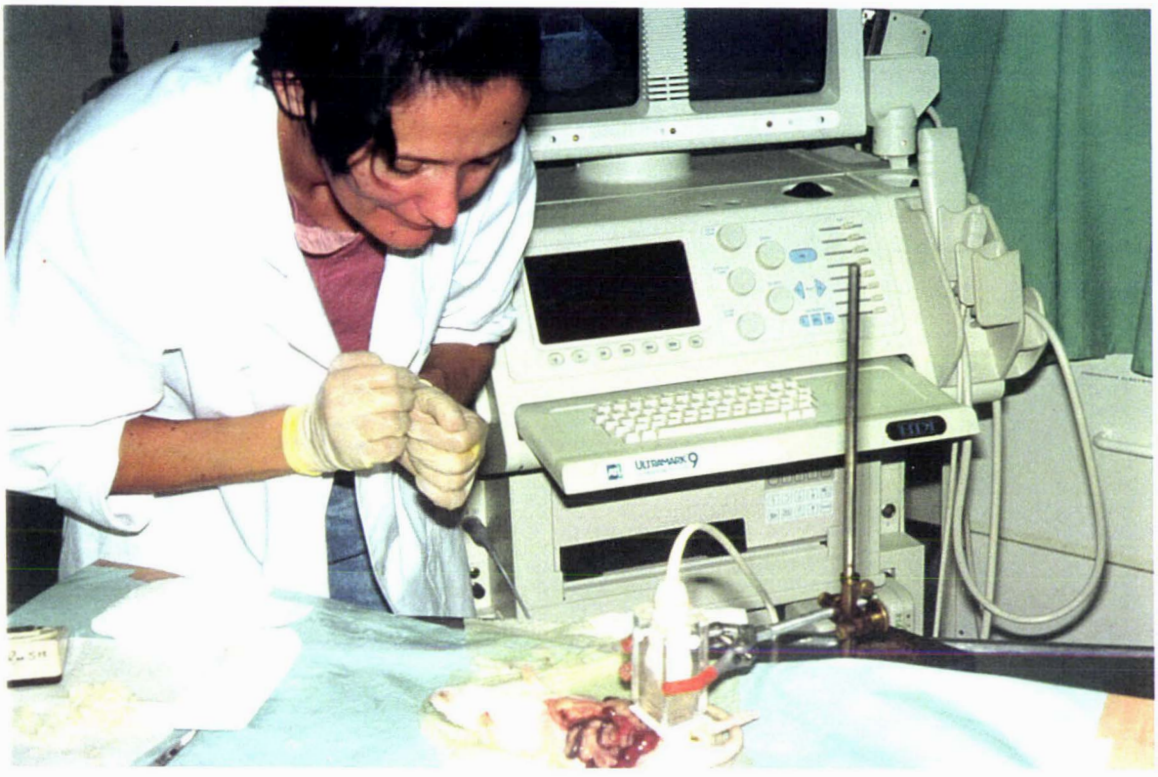

Figure 2.1 **Ultramark 9 HDI, ultrasound machine used in this study.**

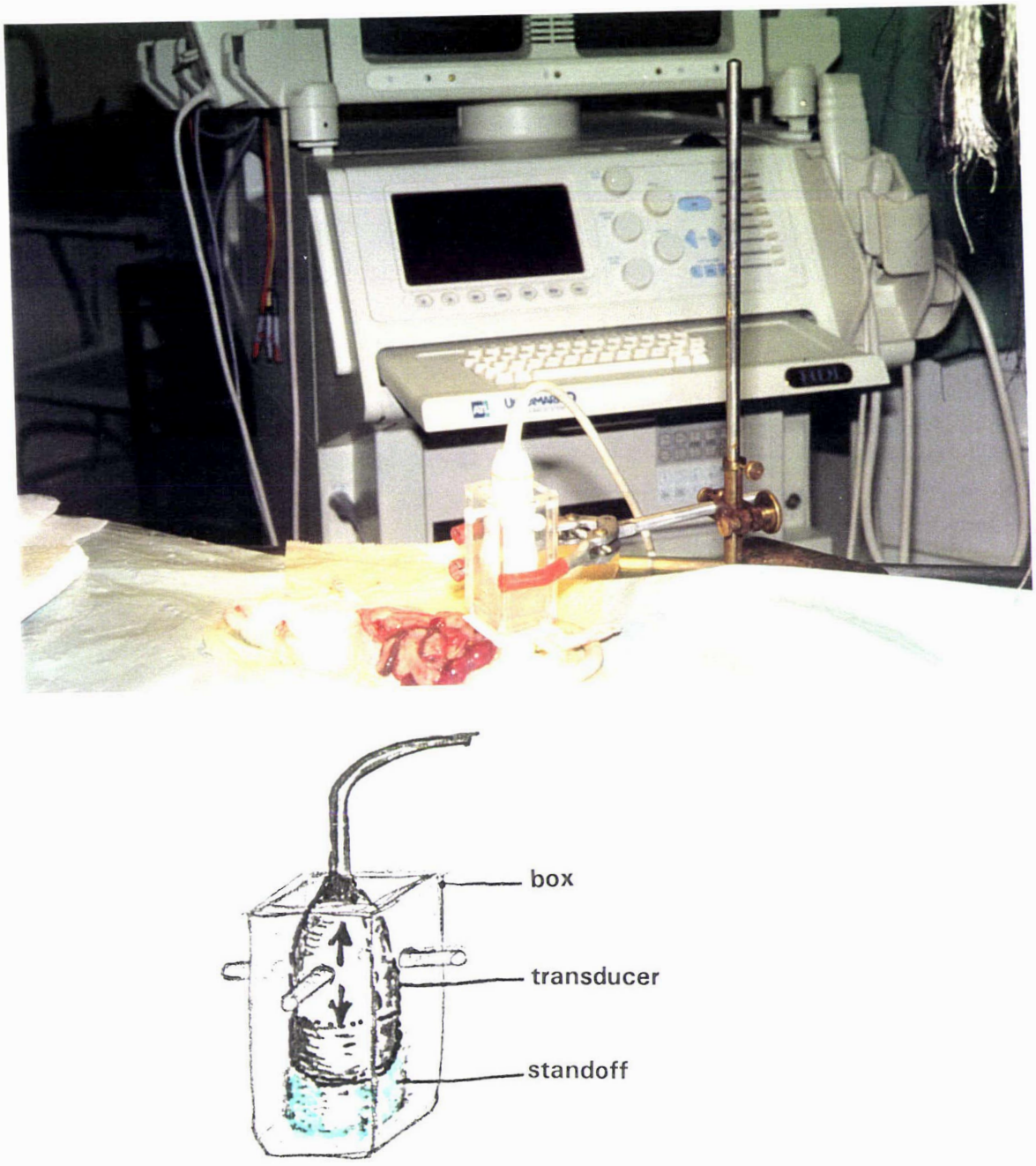

Figure 2.2 **Perspex box for the transducer filled with standoff for adjustment of focal depth.**

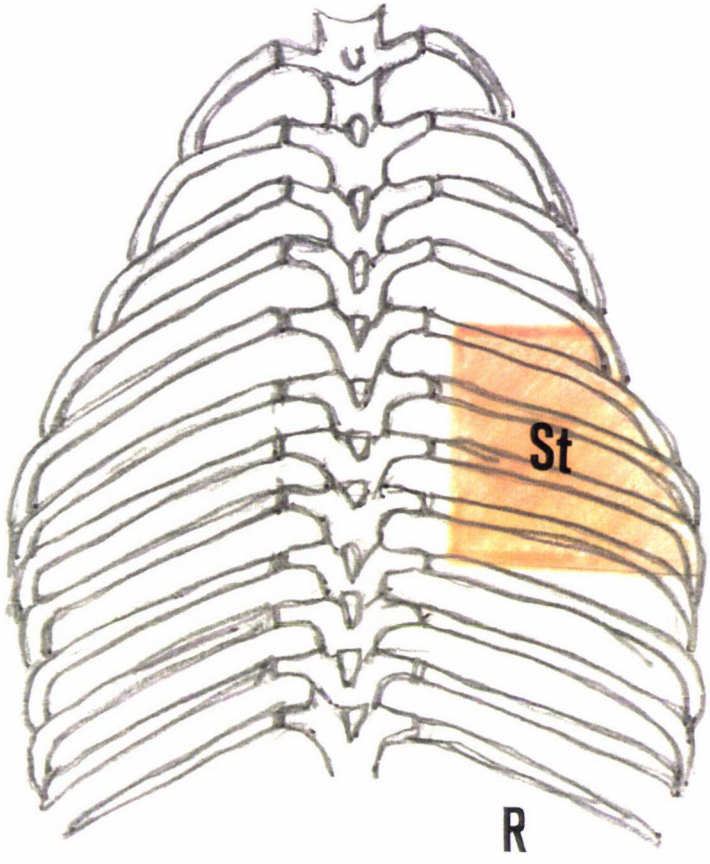

Figure 2.3 **Position of the transducer over the right dorsal chest wall during exposure of the lungs in adult rat** (Diagram). Right side of chest (**R**). Surface where the transducer is placed (**St**).

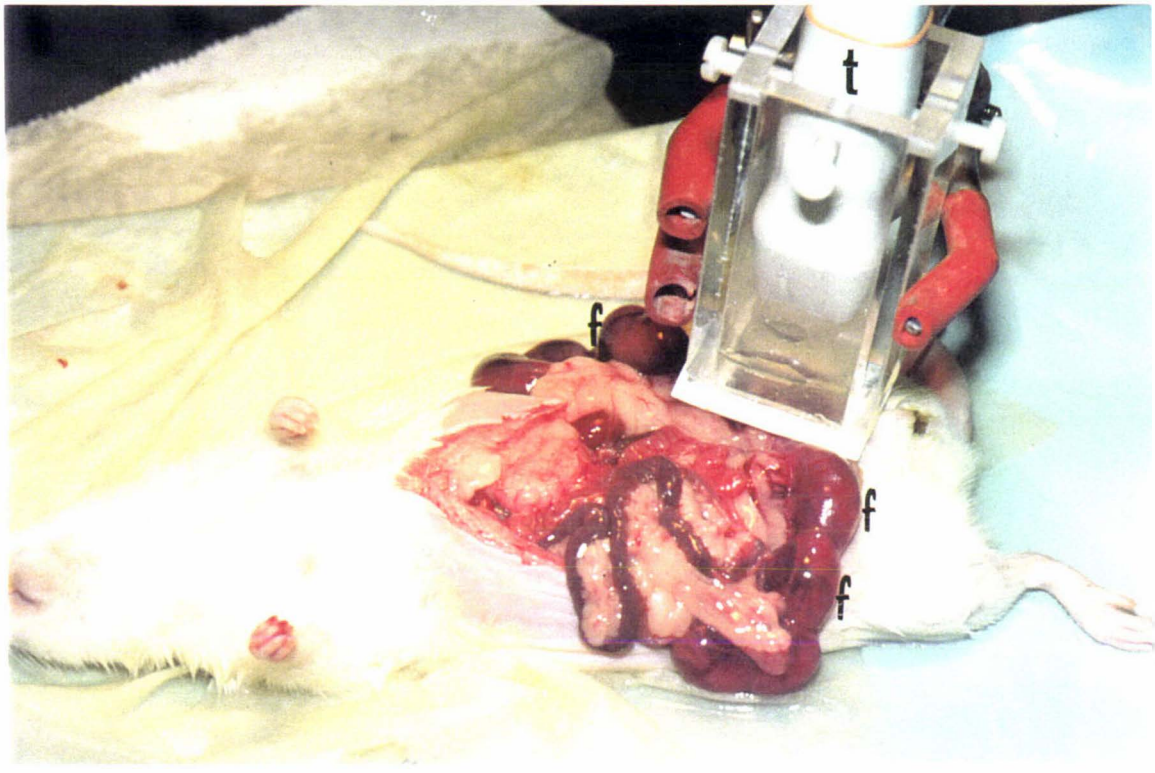

Figure 2.4 **Direct exposure of fetuses after laparotomy of the dam.** Fetus (**f**); transducer (**t**). Magnification: x 0.75.

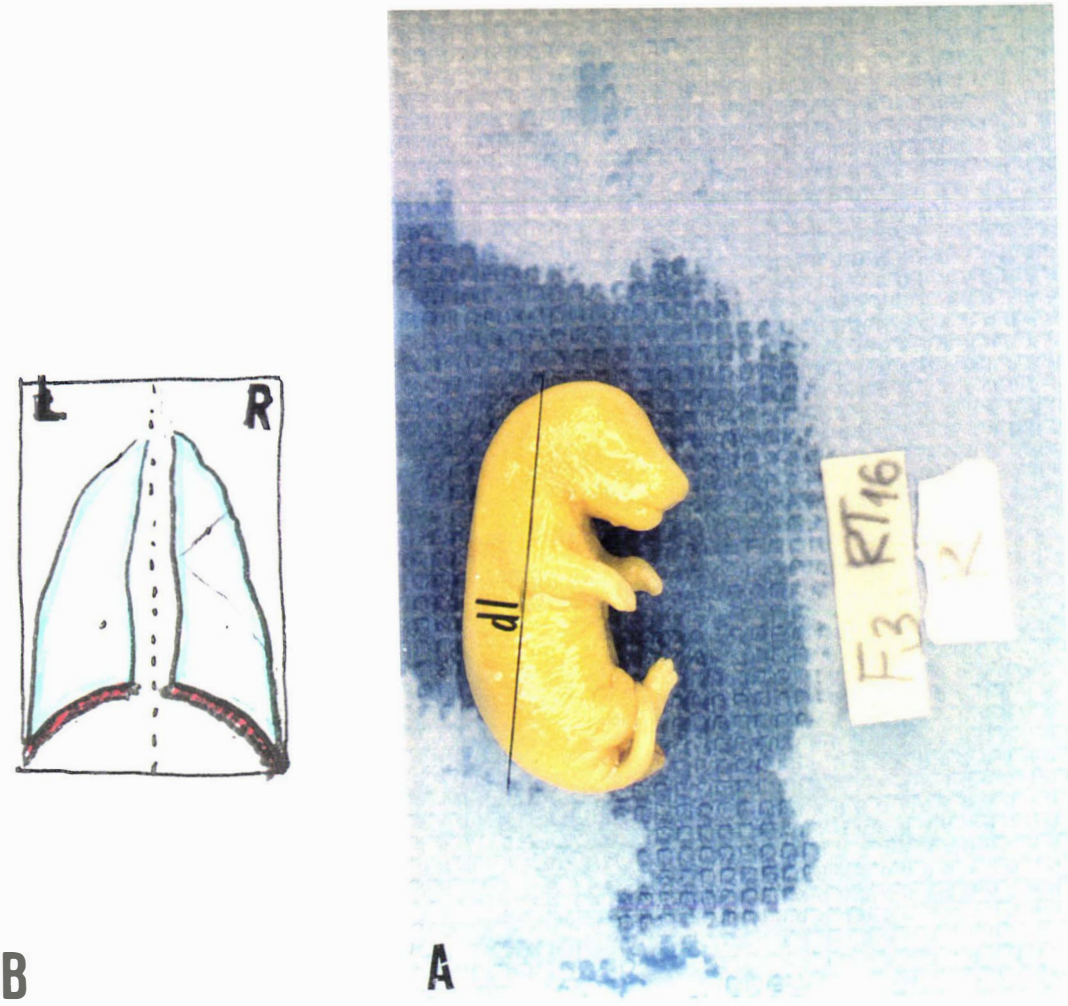

Figure 2.5 **Depth of dorsal fetal tissue section.**
(**A**) Right lateral view of fetus; depth line (**dl**). Magnification: x 2.7. (**B**) Diagrammatic view of fetal lung section taken at the line **dl**. The extent of lung visible at this depth is maximal.

Chapter 3

RESULTS FOR ADULT RAT LUNGS

Introduction

The effect of pulsed Doppler ultrasound on the lungs of rats was limited to varying degrees of lung haemorrhage. It was necessary to examine the normal lung structure of the rat closely in order to interpret changes due to ultrasound exposure. These results therefore include anatomical observations on the rats studied, with reference to the literature as necessery.

3.1 Normal rat lungs

The lower respiratory system of the rats, like that of all mammals, consists of paired lungs and a series of air passages that lead to and from the lungs.

3.1.1 Anatomy

The right and left lungs lie within the thorax (Figure 3.1) on each side of the mediastinum which contains the heart, great vessels, trachea, right and left bronchi, esophagus, lymph vessels and nerves. Together the lungs are described as a cone with an apex, a base, and costal surface. The apex is rounded and lies cranially in the thorax associated with the first rib and the blood vessels and nerves entering the neck. The base is concave and is associated with the thoracic surface of the diaphragm.

The costal surface is convex and is closely associated with the costal cartilages, the ribs and the intercostal muscles. The middle part of the mediastinal surface, where the principal bronchus and the pulmonary artery and vein enter the lung, is the hilus.

The lungs are covered by a thin layer of visceral pleura. Costal pleura covers the inner surface of the thoracic wall and together with the mediastinal pleura, and visceral pleura of the lung, build a closed flattened sac containing and lubricated by a small amount of serosal fluid.

3.1.2 Structure

The lungs are composed of bronchi and smaller air passages, alveoli, connective tissue, blood vessels, lymph vessels and nerves. Conforming to the ramification of the bronchial tree (Hebel and Stromberg, 1986) the right lung is divided (Figure 3.2) into four distinct lobes: cranial, middle, caudal and accessory. The smaller left lung is not separable into lobes. Each lobe is made up of many lobules, composed of terminal bronchioles, rudimental respiratory bronchioles, alveolar ducts and alveoli [Figure 3.3 (A)].

The part of lung distal to a terminal bronchiole which includes the short respiratory bronchioles with only occasional alveolar outpockets (alveolar ducts and alveoli) is called the **acinus** (Mercer and Crapo, 1991).It contains the gas exchange surfaces of the lung.

A ventilatory unit of an acinus includes a respiratory bronchiole and may have a distal alveolar outpocket. In Figure 3.3 (**A**) are shown two types of ventilatory unit. The Type I ventilatory unit includes a rudimentary respiratory bronchiole distal to the terminal bronchiole. The terminal bronchiole has smooth muscle within its walls, and is lined by ciliated respiratory epithelium, easily visible only at high magnification. There is an alveolar duct with only a few alveoli. The Type II ventilatory unit has a longer respiratory bronchiole, and each alveolar duct leads to more alveoli with branching alveolar outpockets (Mercer and Crapo, 1991).

Blood supply

The lung has both a pulmonary and a bronchial circulation. The **pulmonary circulation** is provided by the left and right branches of the pulmonary artery to each lung. Within the lung, each artery divides into many branches. From segmental arteries branches arise at acute or right angles (Hebel and Stromberg, 1986). Branch arteries arising at acute angles are conduits carrying blood to distant parts of the lung while right angle branches distribute blood locally to a dense **alveolar capillary network** around the walls of the alveoli (Figure 3.4). The pulmonary capillaries join up, eventually becoming the pulmonary veins which open into the left atrium of the heat. In distinction from the human lung, smooth muscle is present in much smaller pulmonary arterial vessels or arterioles and the pulmonary veins of the rat have a thicker muscular wall (Kay, 1991).

The **bronchial circulation** in the rat arises from bronchial arteries from the aorta, and supplies the walls of the bronchi and bronchioles but not pleura as in humans (Kay, 1991).

3.1.3 Ultrastructure

Internally, alveoli appear as irregular cavities. The structure of the alveolar walls is similar to that of other mammals (Hebel and Stromberg, 1986). Alveoli are surrounded and separated from one another by a thin connective tissue layer that contains numerous blood capillaries called an **alveolar septum** [Figure 3.3 (B)]. The alveolar septum is the site of the air-blood barrier. Respiratory gases are exchanged across capillary, endothelial and alveolar epithelial cell layers.

The epithelium consists of flat Type I cells (Type I pneumocytes), and also Type II cells (Type II pneumocytes) that secrete surfactant, a detergent-like substance that helps prevent collapse of the alveoli due to surface forces (Widdicombe at al., 1991A).

3.2 Lung haemorrhage

3.2.1 General features of the haemorrhages

Usually the haemorrhages found in this study were multifocal. Two or more circular foci with varying diameters were grouped together (Figure 3.5). Adjacent foci were often fused. This general feature of haemorrhage was more noticeable by microscopy than by gross inspection of the lung.

In each haemorrhagic focus, free blood cells and plasma effusions were located in the alveolar spaces (Figure 3.6 & 3.7). Blood cells were densest in the central part and least dense at the periphery of a focus. An area with haemorrhage was well demarcated from unaffected lung tissue (Figure 3.8).

3.2.2 Types of haemorrhage

Frank haemorrhage

Frank hemorrhage when viewed macroscopically was usually located within a single lobe as a dark red colored area, containing a few circular dark foci (Figure 3.5) with diameters ranging from 3 to 5 mm. Frank haemorrhage was microscopicaly observed and is described below.

Within the central part of each focus (Figure 3.6) and (Figure 3.9), the alveolar spaces were filled with dense aggregations of blood cells. Peripherally to the foci, the density of blood cells within alveolar spaces was less and it was possible to see some free blood cells separated from each other. In a few cases, intensive haemorrhage was manifest by blood cells within bronchi (Figure 3.9 & 3.10).

Microscopically detected haemorrhage

Microscopic haemorrhage was also seen without macroscopic change although in a few cases there was macroscopically a slight change in colour.
Multifocal or unifocal (single) haemorrhages were seen. Alveolar spaces within these haemorrhagic areas contained loosely aggregated or separated red blood cells, denser at the centres of the foci (Figure 3.7).

Doubtful haemorrhage

Extensive alveolar capillary vasocongestion in a region of insufficiently inflated lung made haemorrhage difficult to identity (Figure 3.11). Compare this with normal rat lungs which were well inflated and without vasocongestion (Figure 3.3).
This type of haemorrhage was scored as +- (Table 3.1)

Artifactual haemorrhage

In sectioning lung tissue for microscopy, red blood cells become placed outside blood vessels. Three different expressions of artifactual haemorrhage [Figure 3.12 (B)] were seen:
i) A layer of blood cells collected close to some blood vessels.
This layer overrides alveolar walls and alveolar spaces like a blood smear [Figure 3.12 (A)].
ii) A few free blood cells within alveolar spaces seen in different areas of the lung.
iii) Free blood cells located outside the tissue section.

Haemorrhage in the control lung

A solitary haemorrhagic focus was seen in only one of the control rats [Figure 3.13 (A)]. A lack of vasocongestion about the haemorrhagic area distinguished this haemorrhage from the focal haemorrhage seen in exposed lung, evidence that this damage was not acute.

Severe vasocongestion seen in some of control lungs [Figure 3.13 (B) was not seen to this intensity as a result of exposure to ultrasound.

3.2.3 Location of haemorrhage within a lung

Regions of the lung with haemorrhage are shown in Table 3.1. Of all the 32 exposed rats 12 lungs had gross or focal haemorrhage, 8 of which had haemorrhage in the caudal lobe of the exposed right lung. Three other rats had haemorrhage in the cranial and two other rats in the middle lobe of the right lung. In two cases, the exposed lungs had haemorrhage in both caudal and middle lobes. Of the 9 control rats, only one had haemorrhage. This was in the middle lobe. All haemorrhages were

located superficially beneath costal visceral pleura on the costal surface. From serial transverse sections (Chapter 2) it was found that haemorrhage extended into the lung to a depth of about 1mm (Figure 3.9).

In two exposed (*Rp6, *Rpd29) rats and one control *Rpdc8 rat, diffuse multifocal haemorrages occurred in the entire left lung and cranial lobe of the left lung. These pathological changes, because of their extent and intensity were not considered
to be the result of acute damage that could be attributable to ultrasound. These lungs were excluded from the analysis.

Of four doubtful haemorrhages, three were found within the caudal lobe and one in the cranial lobe. One of these rats had doubtful haemorrhage in both the cranial and middle lobe of the lung.

3.2.4 Threshold study

Mechanical index (MI), as displayed on the screen of the ultrasound machine, was used to determine the threshold value for lung haemorrhage. The three different intensities of pulsed Doppler ultrasound exposure MI 0.5, 0.6 and 1.0 resulted in different proportions of lung haemorrhage for each groups (Table 3.1).

The highest incidence of haemorrhage (64.2 per cent) was in the group exposed at the highest MI (1.0). Also, 7.1 per cent of doubtful haemorrhage was found in the same exposure group.This result compares with 12.5 per cent of haemorrhage in the sham exposed group at MI 0.0. The significance of this is indicated by a high value of the risk ratio of 4.5, and the odds ratio of 10.4 (Thrusfield, 1995) and a logistic odds ratio of 8.6 (Figure 3.14). In the group exposed at MI 0.5, 12.5 per cent of the exposed lungs had doubtful haemorrhage. Therefore this level of exposure appears to be less associated with risk than the controls which had 12.5 per cent of obvious haemorrhage. A calculated value of the odds ratio of 1 also confirmed that the risk of lung haemorrhage at MI 0.5 is negligible. The risk of haemorrhage increases at MI 0.6.

The threshold value for the lung haemorrhage appears to be between MI 0.5 and 0.6 (Figure 3.15).

Table 3.1 **Effects on adult rat lung exposed to 6 minutes of pulsed Doppler ultrasound.**

Effect of varying mechanical index (MI) on the presence of haemorrhage (+), doubtful haemorrage (+-) and on the absence of haemorrhage (-) in different regions of the lungs [right lung (Caudal lobe, Cd; Middle lobe, Md ; Cranial lobe, Cr] and left lung, LL] and the percentage of lung haemorrhage. Risk ratios and odds ratios indicate the incidence of lung haemorrhage for all lungs at each MI of ultrasound exposure. Rats marked with an asterisk "*R" are excluded from the analysis (Chapter 3.2.3). Rats marked "Rd" had their fetuses exteriorised and exposed directly (Chapter 2).

MI	Rat	Age (weeks)	Body weight (g)	Pregnant	Lung haemorrhage	Region of haemorrhage	% lung haemorrhage	Risk ratio	Odd ratio
	Re1	10	350	+	+	Cd			
	R1	12	307	-	-				
	R2	12	327	+	+	Cd			
	R3	12	377	+	+	Cd			
	Re4	13	408	+	+	Cd			
1.0	R4	12	400	+	+	Cr	64.2(+)	4.5	10.4
	R8	13	382	+	+	Cd	7.1(+-)		
	R9	12	335	+	-				
	R16	18	384	+	-				
	R17	17	443	-	+	Cd, Md			
	R18	18	464	-	+-	Cd			
	R19	18	401	-	+	Cd			
	R20	26	451	+	-				
	Rd26	26	412	+	+	Cd			
	Re3	10	342	+	+	Md			
	R5	12	408	+	-				
	R6	12	343	+	+	Cr, LL			
	R7	12	367	+	-		22.2(+)		
0.6	R21	26	413	+	+ -	Cr	33.3(+-)	1.7	2
	Rd22	28	464	+	+ -	Cd, Md			
	Rd27	24	346	+	-				
	Rd28	32	462	+	+ -	Cd, Md			
	Rd25	32	465	+	-				
	R10	16	391	+	-				
	R11	16	383	+	-				
	R12	16	404	+	-				
	R13	16	410	+	-				
0.5	R14	16	374	+	+ -	Cd	12.5(+-)	1	1
	R15	16	442	-	-				
	R23	28	418	+	-				
	Rd24	24	398	+	-				
	*Rd29	24	386	+	+	All lungs			
	Rce1	10	318	+	-				
	Rc1	12	343	+	-				
	Rc2	13	335	+	-				
0.0	Rc3	16	343	+	+	Md	12.5 (+)		
	Rc4	16	332	-	-				
	Rc5	18	335	-	-				
	Rcd6	28	400	+	-				
	Rcd7	32	443	+	-				
	*Rcd8	24	364	+	+ -	All lungs			

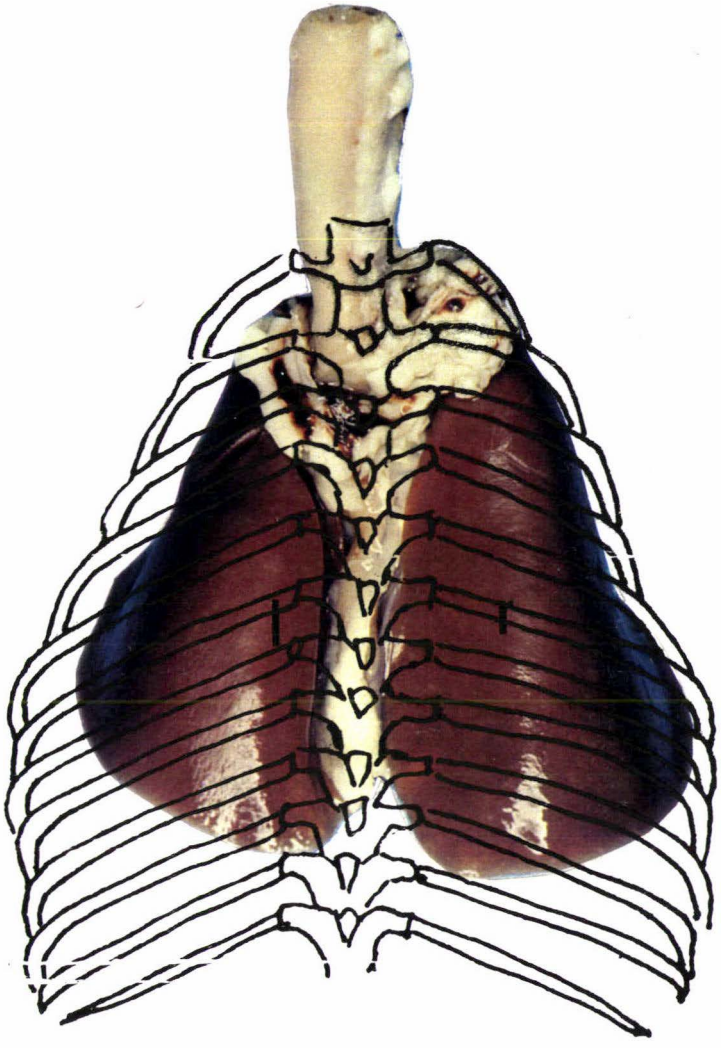

Figure 3.1 **Normal rat lungs (dorsal view) and relationship with the ribs.**
Rat Rc1: right lung (r) ; left lung (l).
Magnification: x1.7

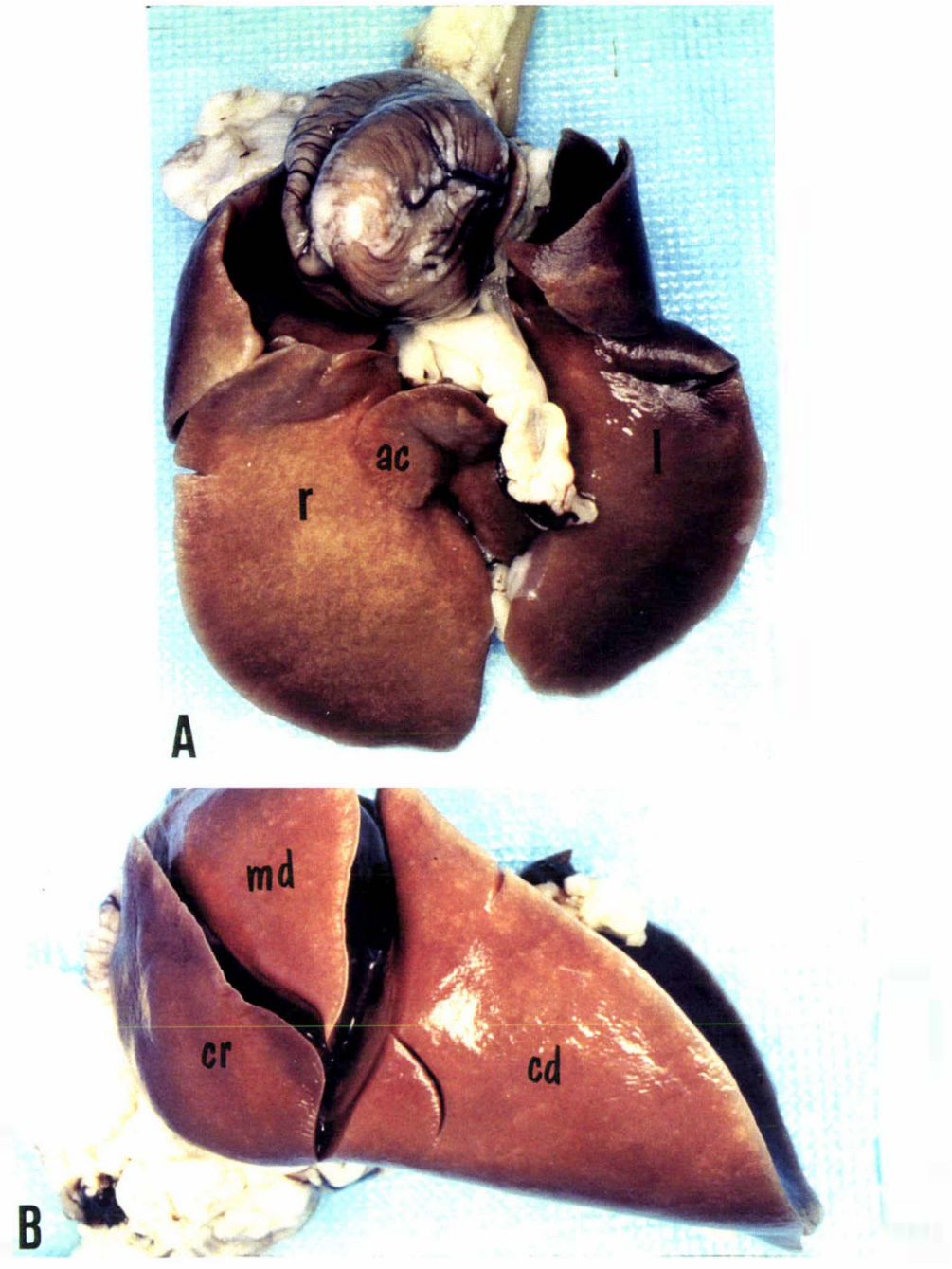

Figure 3.2 **Division of the right lung in normal rat lungs.** Rat Rc1: **(A)** ventral view; right lung **(r)** ; left lung (l) ; accessory lobe (ac). **(B)** lateral view ; caudal lobe (**cd**); middle lobe **(md)** ; cranial lobe (**cr**).
(Haematoxylin/Eosin staining). Magnification: x1.7

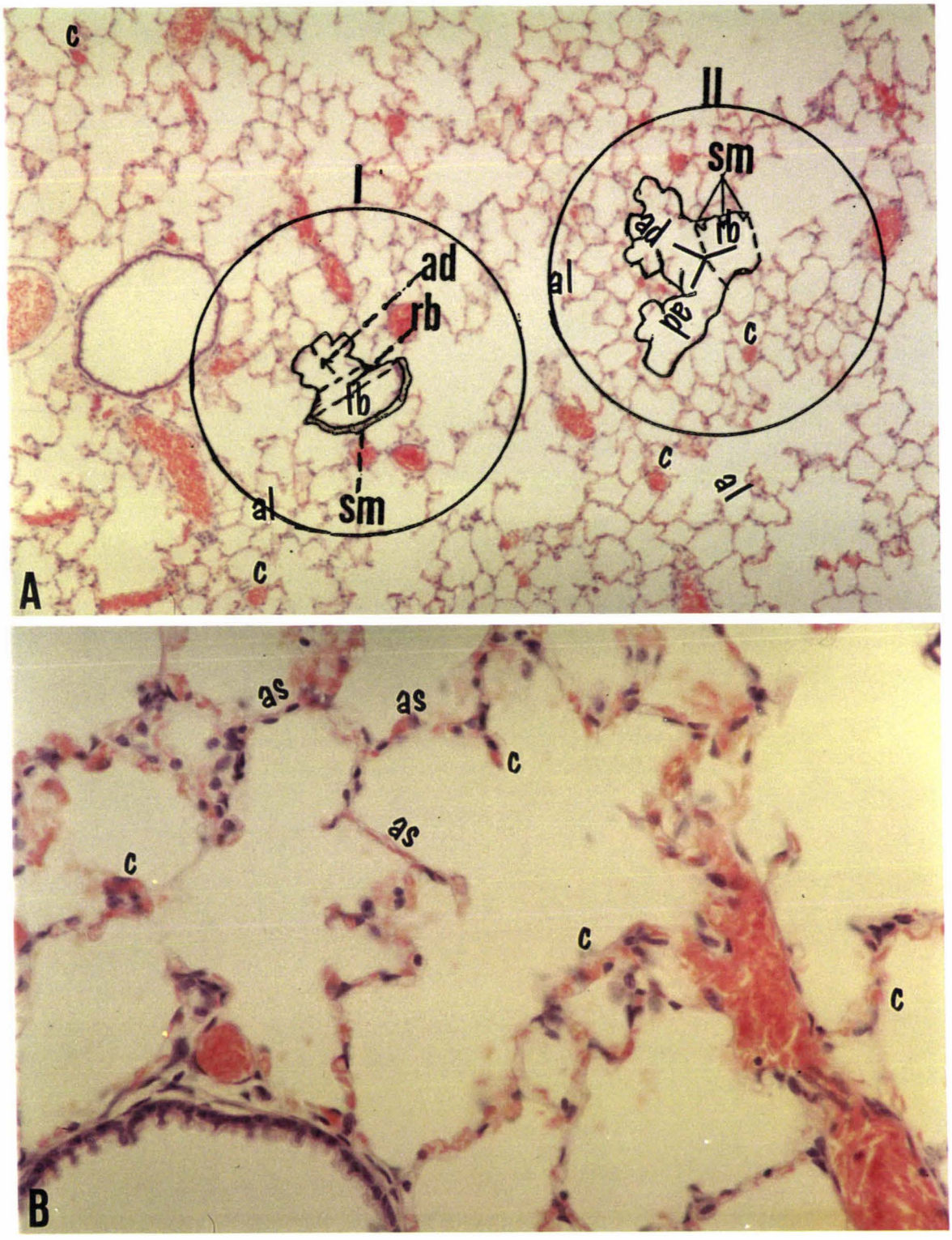

Figure 3.3 **Terminal air passages and alveoli.** Rat Rc6: **(A)** - terminal bronchiole **(tb)**; smooth muscle **(sm)** ; respiratory bronchiole **(rb)** ; alveolar duct(ad) ; alveolus **(al)**. capillary within alveolar septa **(c)**. Ventilatory unit type I, and type II. (Haematoxylin/Eosin staining). Magnification: x108.

(B)- alveolar septum **(as)**. Capillary **(c)**. (Haematoxylin/Eosin staining). Magnification x430.

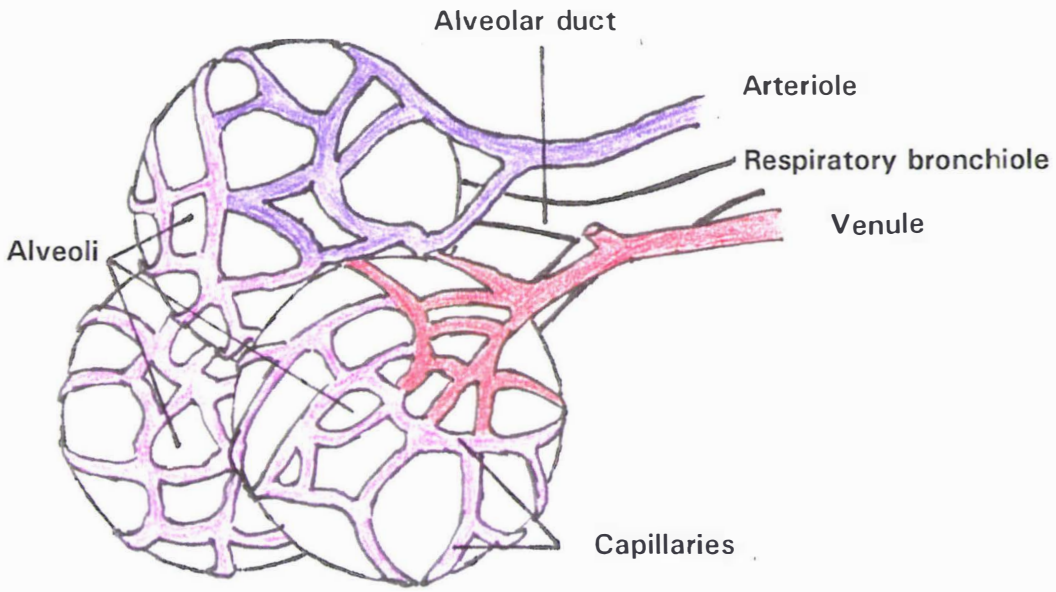

Figure 3.4 **Diagram of the capillary network surrounding the alveoli** - (adapted from Wilson, 1990).

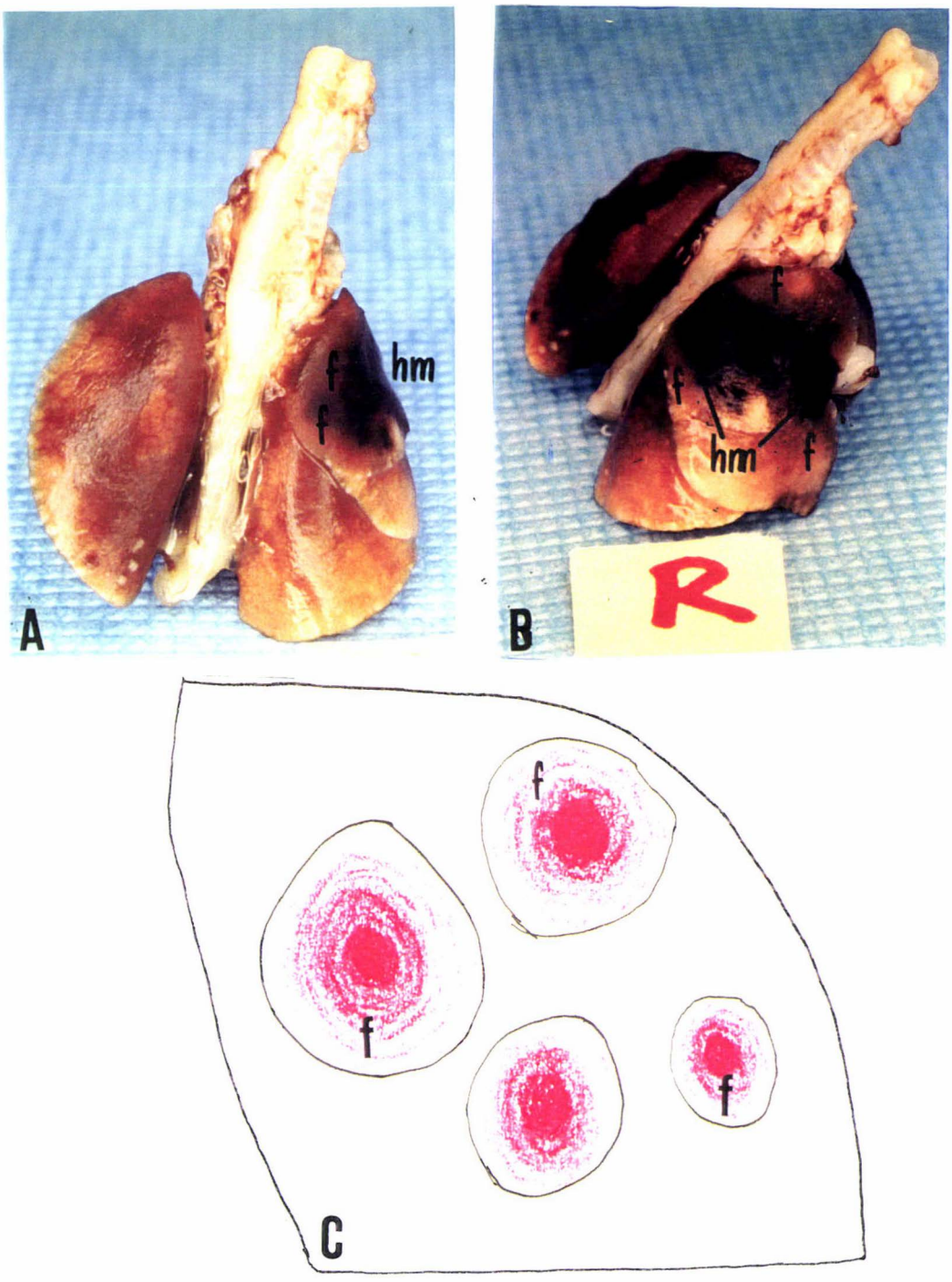

Figure 3.5 **Multifocal lung haemorrhage in adult rat lung (gross).** Rat R4: **(A)** -Dorsal view of the lungs. Magnification: x1.6. (B)- right lateral view of the lungs with haemorrhage (**hm**) in the cranial lobe of the right lung.
Haemorrhagic foci (**f**) within the haemorrhagic area. Magnification: x1.6.
(C) diagram of a lobe with the haemorrhagic foci.

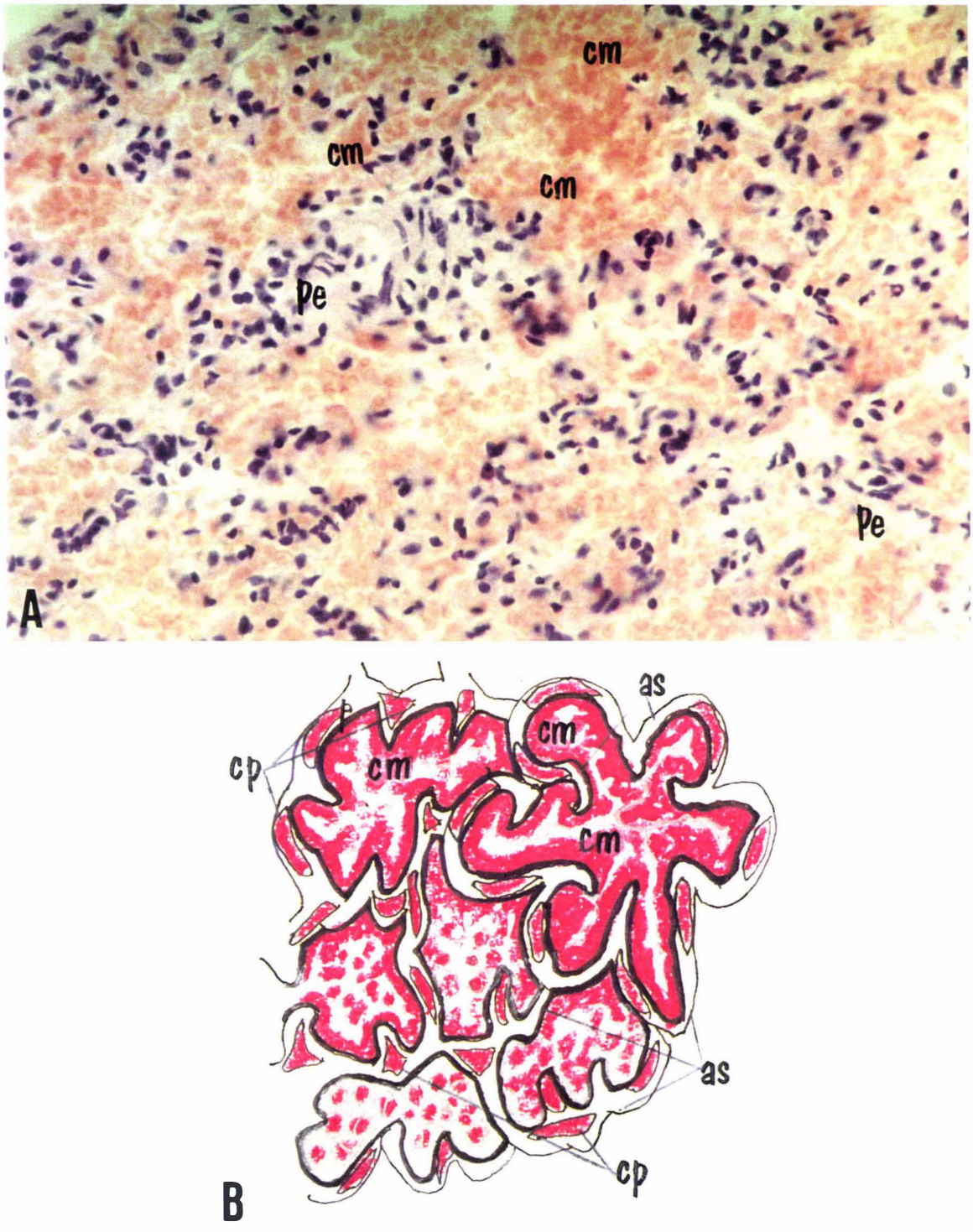

Figure 3.6 **Gross haemorrhage (haemorrhagic focus).** Rat R19: (A)- Magnification : x430. (Haematoxylin/Eosin staining). **(B)**- Diagram of microscopic appearance of a haemorrhagic focus in gross haemorrhage. Alveolar septa **(as)** ; capillary **(cp)**; conglomerates of blood cells(**cm**) ; plasma effusion (**pe**).

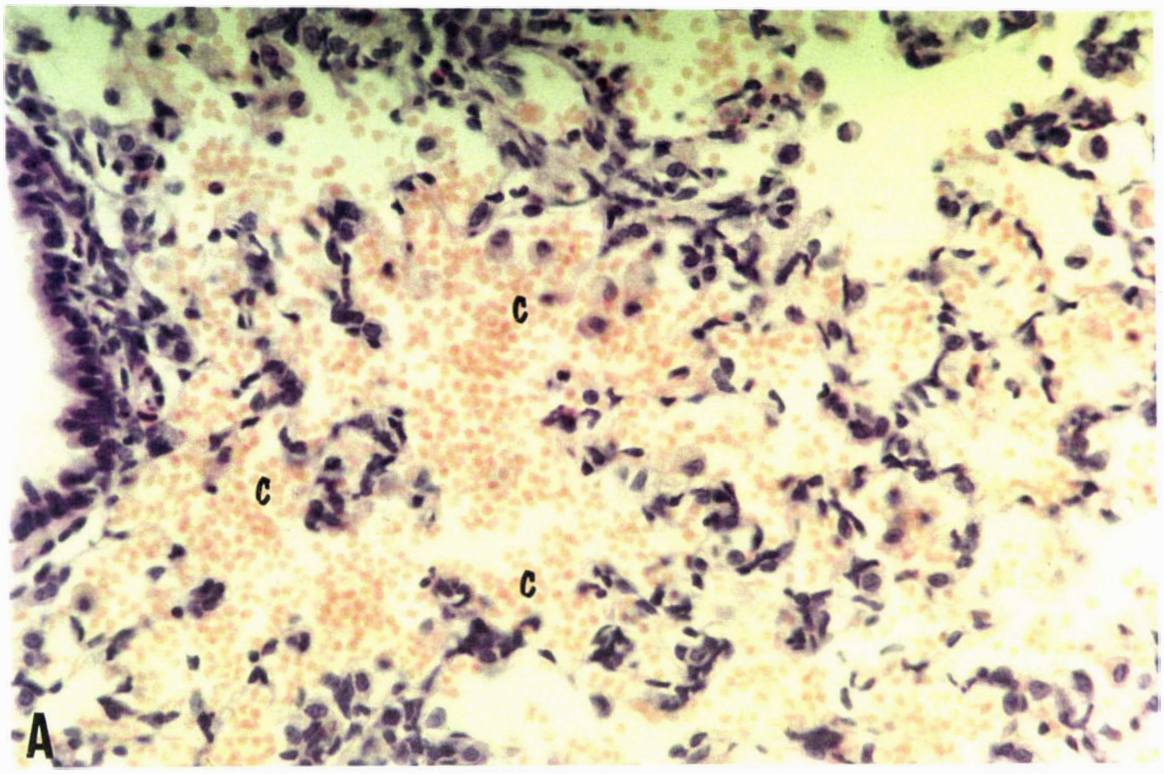

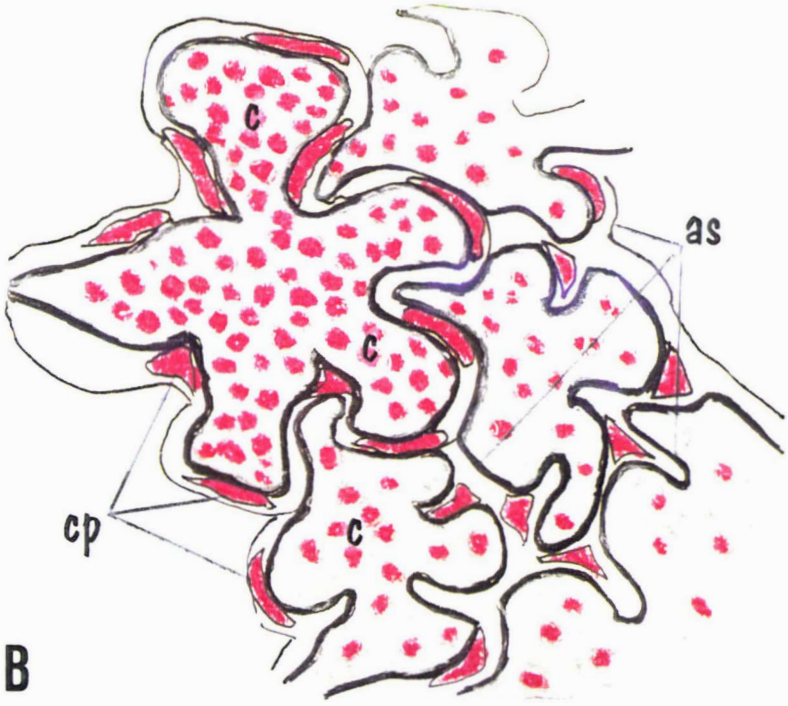

Figure 3.7 **Focal haemorrhage (haemorrhagic focus).** Rat R6: **(A)**- Magnification: x430. (Haematoxylin/Eosin staining). **(B)**- Diagram of microscopic appearance of a haemorrhagic focus in focal haemorrhage. Alveolar septa (**as**) ; capillary (**cp**) ; separated blood cells (**c**) within alveolus.

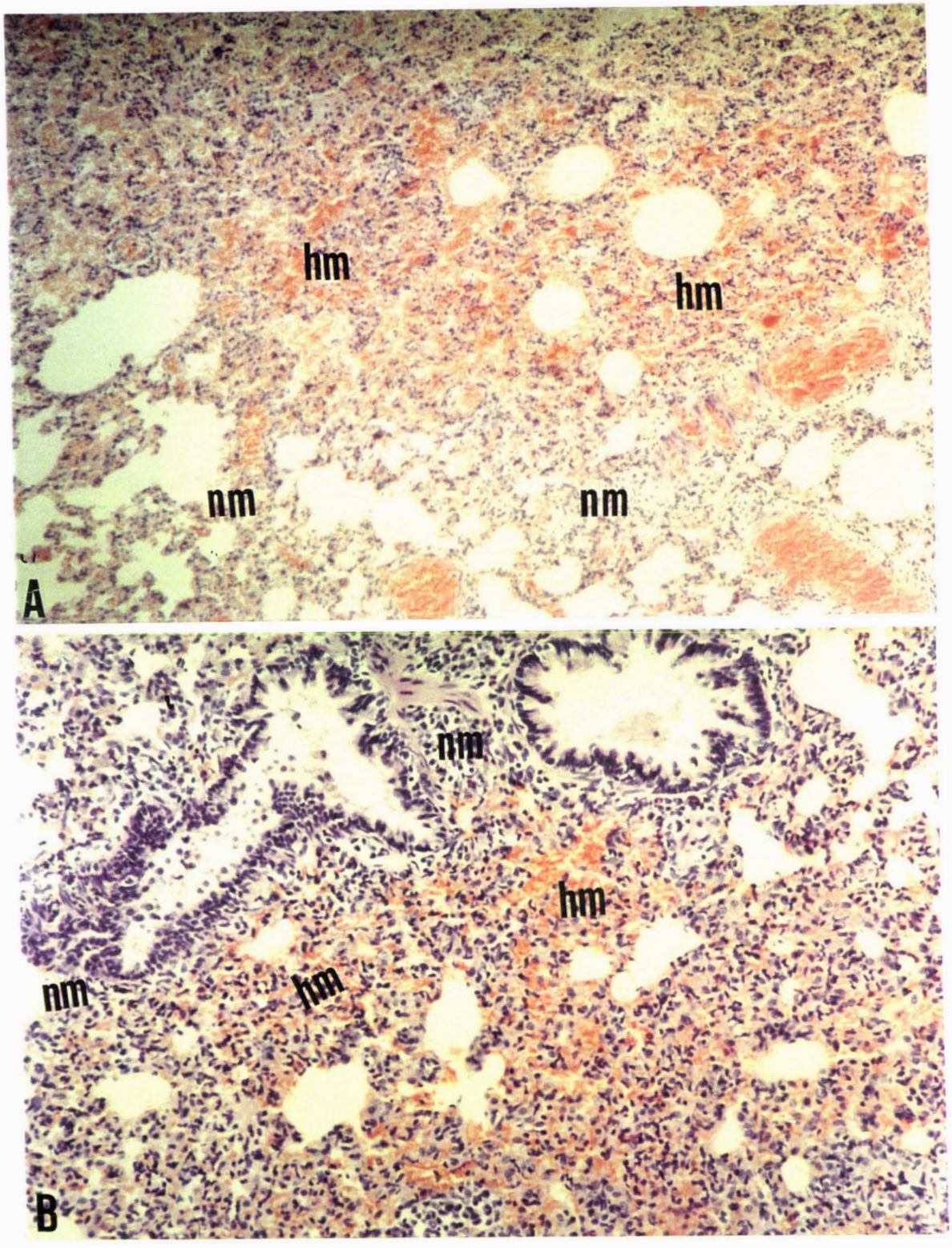

Figure 3.8 **Demarcation of haemorrhagic area from normal lung tissue.**
Rat R19: **(A)**- Magnification: x108 ; **(B)**- Magnification: x430. (Haematoxylin/Eosin staining). Haemorrhage (**hm**) ; normal (**nm**) lung without haemorrhage.

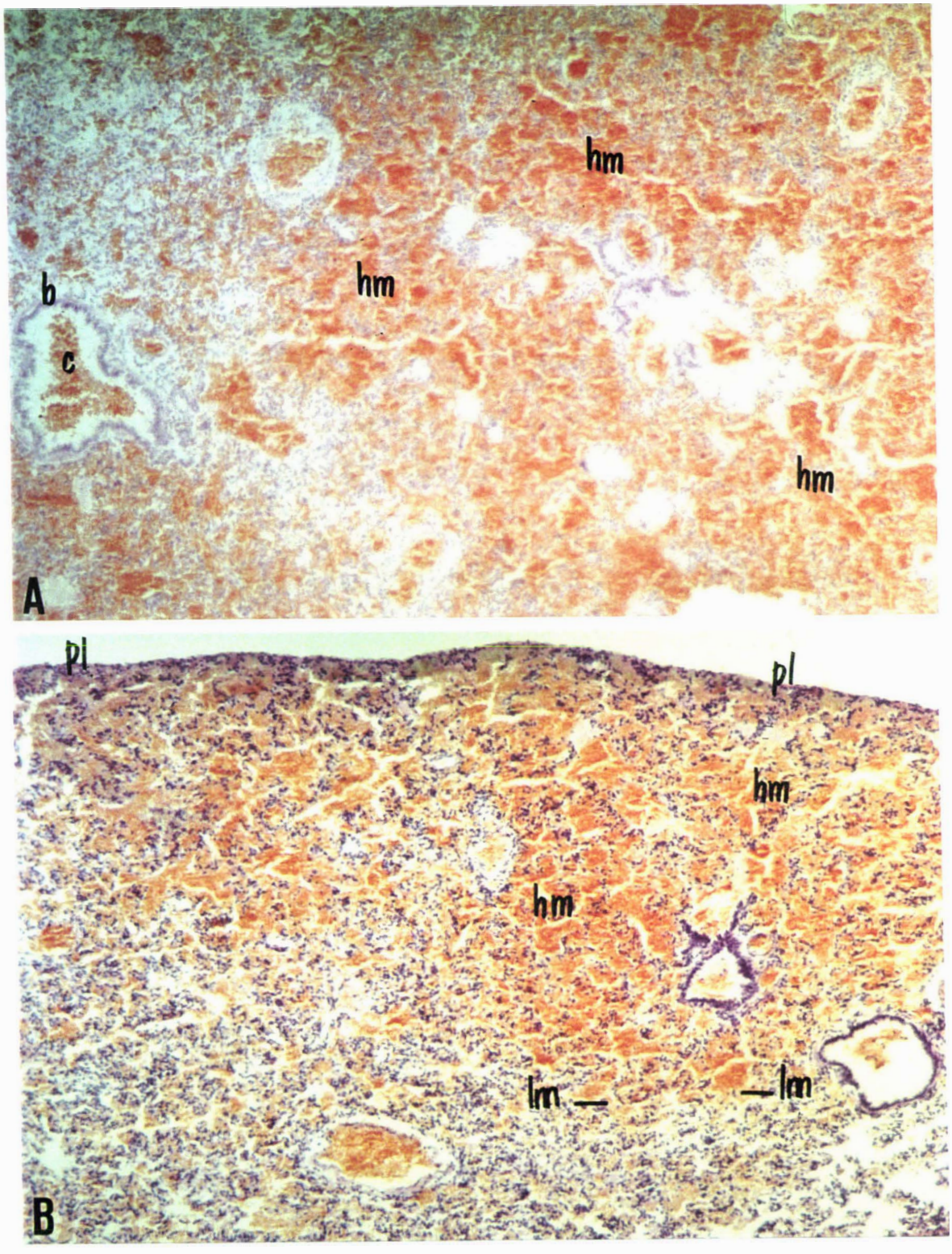

Figure 3.9 **Depth of the lung haemorrhages.** Rat Re4: (**A**)- Section cut parallel to the pleural surface and (**B**)- transverse section to the pleural surface of the caudal lobe at the haemorrhagic region with gross multifocal haemorrhage. Magnification: x108. (Haematoxylin/Eosin staining). Pleura (**pl**); haemorrhage (**hm**); limit of haemorrhage (**lm**); bronchiole (**b**); intrabronchiolar haemorrhage (**c**) .

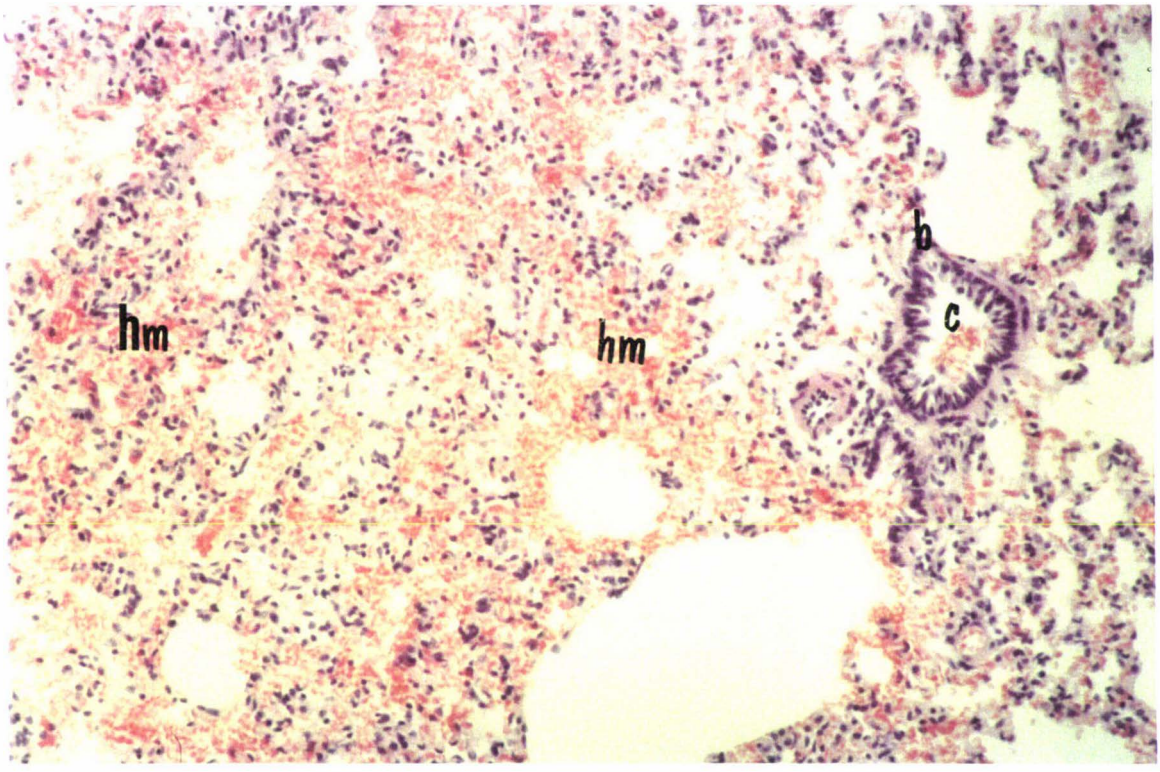

Figure 3.10 **Gross haemorrhage with present of blood cells within a bronchus.** Rat R3: Magnification: x215. (Haematoxylin/Eosin staining). Blood cells (**c**) within bronchus (**b**). Haemorrhagic region (**hm**).

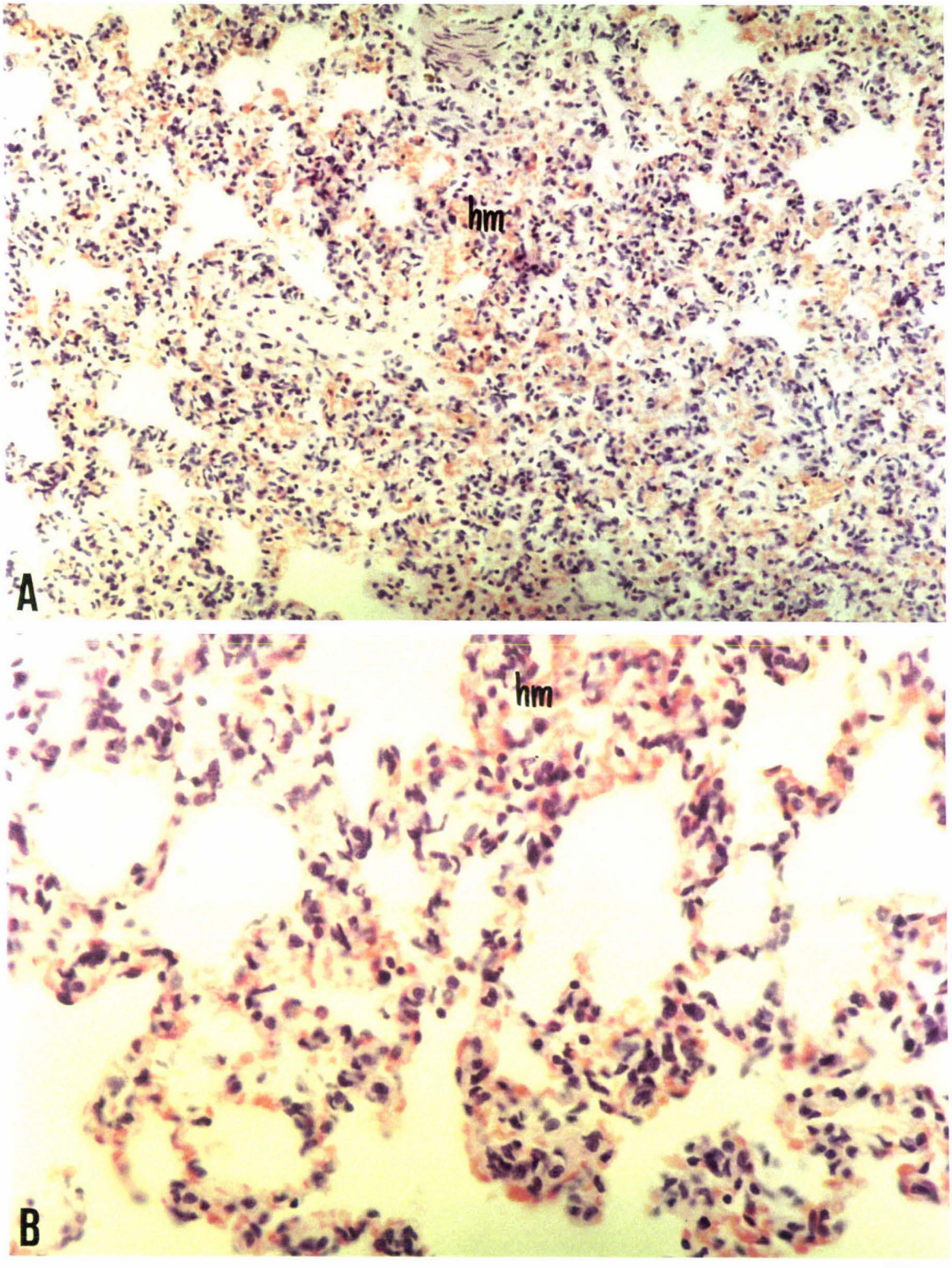

Figure 3.11 **Doubtful haemorrhage**. Rat R14 : **(A)**- poorly inflated lung. Magnification: x215. (Haematoxylin/Eosin staining). Rat Re4: **(B)**- vasocongestion in poorly inflated lung. Magnification: x430. (Haematoxylin/Eosin staining). Doubtful haemorrhagic (**hm**) region.

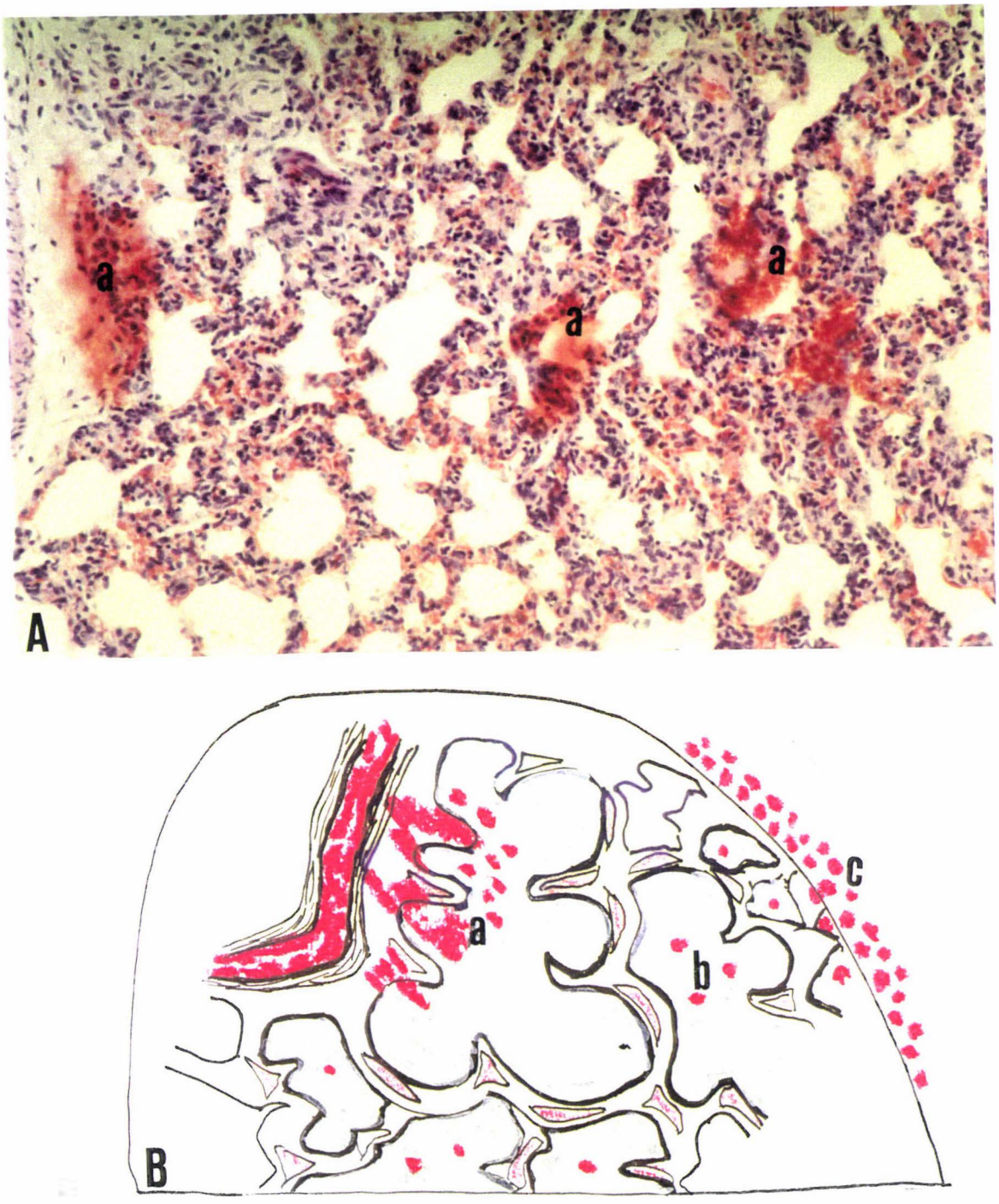

Figure 3.12 **Artifactual haemorrhage**. Rat Rc4: **(A)**- Magnification: x215. (Haematoxylin/Eosin staining). **(B)**- Diagram of different types of artifactual haemorrhage. Blood smear (**a**) ; a few blood cells within alveolar spaces (**b**); free blood cells outside of the lung section (**c**).

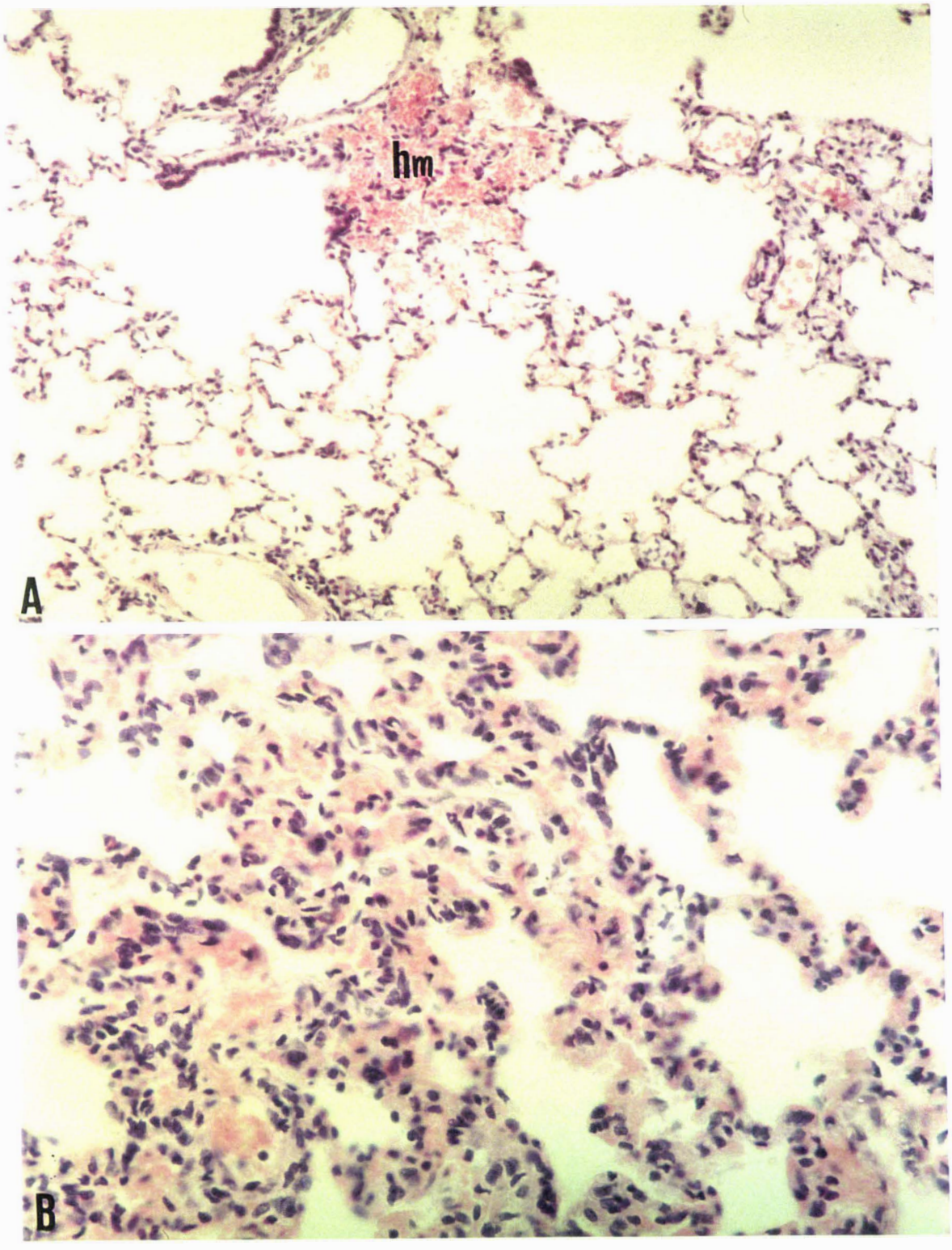

Figure 3.13 **Control lungs.** Rat Rc3: **(A)**- Solitary haemorrhage (hm). Magnification: x215. (Haematoxylin/Eosin staining). Rat Rc4: **(B)**- Severe vasocongestion. Magnification: x430. (Haematoxylin/Eosin staining).

14 Oct 98 SPSS for MS WINDOWS Release 6.1

Classification Table for LUNG_HM

Observed		Predicted .00 (0)	Predicted 1.00 (1)	Percent Correct
.00	0	17	4	80.95%
1.00	1	3	9	75.00%
			Overall	78.79%

---------- Variables in the Equation --------

Variable	B	S.E.	Wald	df	Sig	R	Exp(B)
MI			2.7412	3	.4333	0000	
MI(1)	1.3558	**9.3156**	.0212	1	.8843	0000	**3.8800**
MI(2)	-6.9174	**27.7913**	.0620	1	.8034	.0000	.0010
MI(3)	2.1612	9.2979	.0540	1	.8162	.0000	**8.6820**
PREGNANT(1)	-.1909	.6720	.0807	1	.776	.0000	.8262
WEEKS	-.1062	.1075	.9746	1	.3235	.0000	.8993
B_WEIGHT	.0204	.0169	1.4501	1	.2285	.0000	1.0206
Constant	-8.7876	10.6415	.6819	1	.4089		

Correlation Matrix:

	Constant	MI(1)	MI(2)	MI(3)	PREGNANT(1)
Constant	1.00000	-.88918	.87708	-.86208	-.00163
MI(1)	-.88918	1.00000	-.99536	.98577	.00652
MI(2)	.87708	-.99536	1.00000	-.99616	-.00611
MI(3)	-.86208	.98577	-.99616	1.00000	.02215
PREGNANT(1)	-.00163	.00652	-.00611	.02215	1.00000
WEEKS	.29127	-.04707	.01182	.00358	-.05302
B_WEIGHT	-.47646	.05503	-.01602	-.00603	.08813

	WEEKS	B_WEIGHT
Constant	.29127	-.47646
MI(1)	-.04707	.05503
MI(2)	.01182	-.01602
MI(3)	.00358	-.00603
PREGNANT(1)	-.05302	.08813
WEEKS	1.00000	-.76207
B_WEIGHT	-.76207	1.00000

Figure 3.14 **Logistic regression of the results for adult rat lung haemorrhage.**
This statistical model provides an overall fit for the data classification of 78.79%. Of the variables, Exp (B) is a logistic odds ratio (parameter for risk). MI (1) is 0.5; MI (2) is 0.6 and MI (3) is 1.0.

S.E. is standard error which is the highest for MI, 0.6. This affects Exp. (B) which showed no risk (its value is less than 0.5) for lung haemorrhage at this intensity of ultrasound exposure.

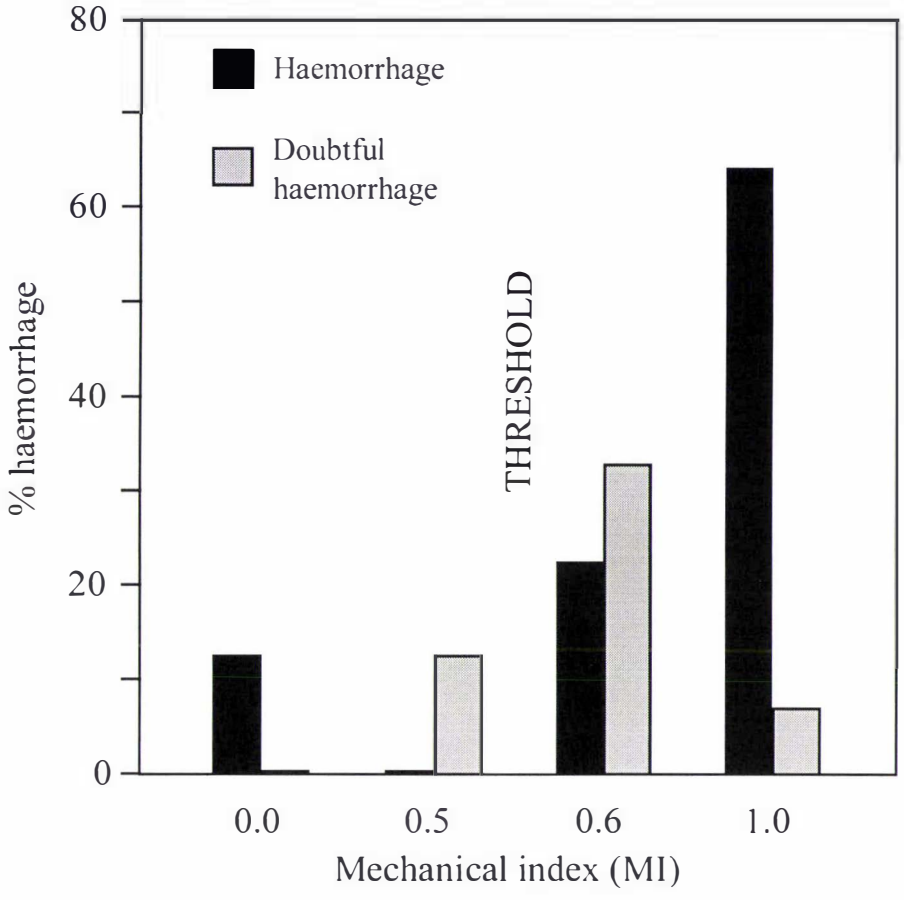

Figure 3.15 **Threshold range of pulsed Doppler ultrasound exposure for adult rat lung haemorrhage**

Chapter 4

RESULT FOR FETUSES

Introduction

The effect of pulsed Doppler ultrasound exposure on rat fetuses in the last third of gestation was limited to varying degrees of haemorrhage in the lungs and other tissues, particularly in the head.

The observations on all fetuses studied (Table 4.1) were made from a single dorsal histological section in the dorsal plane one third of trunk depth from the dorsal surface [Figure 2.5 (Chapter 2)]. Additionally, serial sections of six selected embryos were made through the remaining two-thirds of the trunk.

4.1 Results in fetal rat lung

The interpretation of pathological findings in the fetal lung were based on observations of normal fetal lungs at different stages of development in the last third of gestation assisted by published descriptions of rat lung embryology.

4.1.1 Normal lung in the last third of gestation

The lungs form by a gland-like budding process controlled by a epithelial-mesenchymal interaction (Farrel, 1982). In the rat two lung buds appear after 12 days of gestation as an outgrowth of the foregut (Hebel and Stromberg, 1986). The lung buds subsequently branch within the enclosing mesenchyme to form the gas-conducting portion of the lung (Figure 4.1).

There are three stages of lung development in rat, as in other laboratory animals as well as humans. These are the **glandular, canalicular,** and **saccular** stages (Farrell, 1982). Striking differences in morphology are especially evident in the rat. Because of the short gestation period of 22 days, advances from one stage to the next can occur in a period as short as 24 hours. All three stages of rat lung development were seen in this study and they are shown in Figure 4.2.

During the **glandular** stage (16, 17 days) loose mesenchymal tissue surrounds lung buds of endodermal cells. Vascularisation of the mesenchyme is becoming apparent. The airway pattern has been formed. Respiratory epithelium is characterised by a nearly homogenous population of high columnar epithelial cells which are transparent to light.

In the **canalicular** stage (18-19 days) the acinar region of the lung is first recognized and increasing vascularization occurs; the terminal ends of endodermal lung buds branch and grow to form the future air sacs. High columnar epithelial cells differentiate (Figure 4.3) into two cell types: prospective flattened lining cells (Type I pneumocytes) and cuboidal secretory cells (Type II pneumocytes).

The final intrauterine phase was formerly termed the alveolar stage but is now known as the terminal sac period or **saccular** stage (21, 22 days). It is characterized by further differentiation of the respiratory region. Saccules with thin septa become prominent. In respiratory epithelium, type I pneumocytes become progressively thinner and they form broad cytoplasmic extensions over capillary endothelial cells minimizing the barrier to gas exchange (Farrel, 1982). This leads to a marked increase in the internal surface area of the lung. By morphometric assessment , it may be determined that the relative dimensions of tissue space and potential air space are reversed during the saccular stage of development. During the saccular stage, the potential air spaces are filled with a liquid, "fetal pulmonary fluid", which begins to be secreted during the glandular stage.
(Farrell, 1982).

4.1.2 Fetal lung haemorrhage

The haemorrhage found occurs unifocally (Figure 4.4) or multifocally (Figure 4.5 and 4.6). In multifocal haemorrhage, foci are either separated or grouped (Figure 4.7). The haemorrhagic foci differ in shape from triangular to elliptical and a range from about 0.03 to 0.14 mm in diameter. All are well demarcated from normal lung tissue. Each haemorrhagic focus contains evenly distributed aggregations of blood cells within loose mesenchymal tissue. Free blood cells are not seen within the respiratory passages. Fetal lung haemorrhages are located beneath the costal surface of the visceral pleura in the caudal half of usually one lung (Figure 4.8).

Severe vasocongestion is seen in some fetal lungs (Figure 4.9).

4.2 Non-lung fetal haemorrhage

Haemorrhages in tissues other than lung were found in the liver and soft tissues of the head, neck, parascapular region of the shoulder, axilla and parasacral

region (Table 4.2) in dermis, subcutaneous tissue and muscle adjacent to bone. All haemorrhages were seen only microscopically, with the exception of one fetus (F6, Rt11) which had frank haemorrhage on the head [Figure 4.10 (B)].

The haemorrhage was usually a solitary, dense, irregularly shaped collection of blood cells, well distinguished from the surrounding less dense loose connective tissue of the dermis, subcutaneous tissue and within developing bone (Figure 4.11 and 4.12), and less distinguished in muscle (Figure 4.13) and liver (Figure 4.14). Haemorrhagic regions ranged from about 0.1 to 0.25 mm in diameter. Only in the fetus with gross haemorrhage on the head were multifocal haemorrhages located in the dermis and subcutaneous tissues of the head [Figure 4.10 (A)], neck and parasacral region.

4.3 Effect of varying mechanical index (MI) on the incidence of fetal haemorrhage

The proportions of fetuses with any haemorrhage, and specifically haemorrhage in lungs or tissues other than lung (non-lung) relative to the total number of fetuses (both indirectly and directly exposed) for each exposure group and in the controls are shown in Table 4.3 (shaded areas) and Figure 4.15.

4.3.1 Fetuses with lung haemorrhage

No lung haemorrhage was found in the controls. For fetuses exposed to ultrasound, the proportion of fetuses with lung haemorrhage is not related to the level of exposure.

4.3.2 Fetuses with non-lung haemorrhage

Some haemorrhage was seen in unexposed fetuses, less than the incidence in exposed fetuses, with a slight increase as the mechanical index increased.

4.3.3 Fetuses with haemorrhage in any tissue

Nine of 38 exposed fetuses with haemorrhage were affected in both lung and non-lung tissues. 76 per cents had haemorrhage in one or the other, but not both. At any level of exposure, there was over twice the incidence of haemorrhage than in the controls at 10.3%. The proportion of fetuses with any haemorrhage (either in the lung only, in tissues other than lung, or in both lung and non-lung tissues) did not increase with mechanical index (Figure 4.15), as shown by the risk and odds ratios (Table 4.1) that were less for MI 1.0 than for MI 0.5 and 0.6.

For the proportion of fetuses with any haemorrhage, regression values were negative [Figure 4.16(B)]. There was greater risk of haemorrhage in exposed fetuses than was in controls {the logistic odds ratio for MI [Exp (B)] was greater than 0.5) but the effect was not dependent on the intensity of ultrasound.

4.4 Effect of method of exposure on the incidence of fetal haemorrhage

Each experimental group had fetuses exposed indirectly or directly. Table 4.3 and Figure 4.16 show the distribution of lung, non-lung and any haemorrhage for each method and level of exposure.

The results for both the direct and indirect methods were widely divergent at different levels of exposure (Figure 4.17). Particularly consistent is the finding of no hemorrhage in directly exposed fetuses at MI 0.6. Directly exposed fetuses at this level were all aged 21 days after conception (Table 4.1) suggesting that the age of the fetus may have affected these results. The applied multiple regression method does not show that method of exposure significantly influenced results for each exposure group [Figure 4.16 (A)].

4. 5 The effect of fetal age on haemorrhage

Because fetuses were not selected for treatment based on daily age, the distribution of age through the various treatments is very uneven, from 0 to 62 per cent (Table 4.4). There are therefore values missing from the histogram in Figure 4.18 and Table 4.5. No fetuses at 20 days were used. Lung haemorrhage was not seen in fetuses of 16, 21 and 22 days. In only one fetus of 21 or 22 days was haemorrhage seen, and this was not in the lung. Multiple regression shows that fetal age significantly influenced the results for each exposure group [Figure 4.16 (B)]. The negative regression coeficient (R) shows that the risk of any fetal haemorrhage is higher in younger than in older fetuses.

4.6 Results for serially sectioned fetuses

In order to investigate the distribution of haemorrhage throughout entire lungs, three fetuses in which lung haemorrhage was found in a single section were studied in serial sections through the remainder of the body. Several new haemorrhagic foci were found at a depth of 4 to 9 mm in both lungs in two of these fetuses and in only one lung of the third fetus (Figure 4.19). All haemorrhagic foci are seen subpleurally in the caudal half of the lungs with diameters ranging from about 0.03 to 0.14 mm.

In one of these fetuses, additional haemorrhage was also seen in the skin (Figure 4.20), face and liver at depth of 5-6 mm from dorsal surface of body.

In the three fetuses in which no haemorrhage had been previously found in any tissue, only one haemorrhagic focus became evident. This was at a depth of 5mm in the lung of the 22 day old fetus.

Table 4.1 **Effects on rat fetuses in the last third of gestation exposed indirectly or directly to 6 minutes of pulsed Doppler ultrasound.**
Effect of varying mechanical index (MI) including control (MI 0.0) according to the presence of haemorrhage in lung or non-lung tissue. A fetus with haemorrhage in lung tissue, non-lung tissue, or in both lung and non-lung tissues are counted as a fetus with any haemorrhage. The risk ratio and odds ratio are shown for fetuses at each MI of ultrasound exposure, to identify the risk of any fetal haemorrhage produced at different levels of exposure. Fetuses marked with an asterisk "*R" are excluded from the analysis (see Chapter 4). Rats marked "Rd" had their fetuses exteriorised and exposed directly.

MI	Rat	No. of fetuses	Fetal age (days)	Fetal length (mm)	No. of fetuses with lung haemorrhage	No. of fetuses with non-lung haemorrhage	No. of fetuses with any haemorrhage	Risk ratio	Odds ratio
	Re1	5	16.0	15.0	0	3	3		
	R2	6	18.0	23.0	0	1	1		
	R3	6	21.0	32.0	0	0	0		
	R4	6	22.0	40.2	0	1	1		
	Re4	6	22.0	41.5	0	1	1		
1.0	R8	7	18.0	20.8	1	2	2	2.4	2.9
	R9	6	16.0	12.3	0	1	1		
	R16	6	19.0	26.8	2	0	2		
	R20	6	19.0	26.0	1	1	2		
	Rd25	5	21.0	31.5	0	0	0		
	Rd26	6	18.0	20.7	1	4	4		
	Re3	7	17.0	17.5	1	3	4		
	R5	6	19.0	26.4	1	1	2		
	R6	6	18.0	21.2	1	1	1		
0.6	R7	6	18.0	21.3	2	2	3	2.7	3.8
	R21	6	19.0	30.6	1	2	2		
	Rd22	6	21.0	34.5	0	0	0		
	Rd28	6	21.0	37.0	0	0	0		
	R10	5	18.0	20.2	2	2	2		
	R11	5	18.0	20.4	1	1	2		
0.5	R12	5	21.0	36.0	0	0	0		
	R13	6	21.0	33.8	0	0	0	2.7	3.7
	R14	6	19.0	26.6	1	1	2		
	Rd24	6	18.0	21.7	2	2	3		
	*Rpd29	6	18.0	21.0	2	4	5		
	Rce1	6	18.0	24.0	0	0	0		
	Rc1	6	18.0	23.0	0	1	1		
	Rc2	5	16.0	13.5	0	1	1		
0.0	Rdc6	6	19.0	28.7	0	0	0		
	Rdc7	6	18.0	21.7	0	1	1		
	*Rdc8	6	19.0	25.5	2	2	4		
	*Rc23	6	19.0	24.6	1	1	2		

Table 4.2 **Location of non-lung fetal haemorrhages.**

Location	No of regions with haemorrhage	% of total number of haemorrhagic regions
Head - skin	7	
Head - muscle	4	48.0
Head - developing bone	3	
Liver	6	20.6
Axilla - skin	1	6.8
Axilla - muscle	1	
Neck - muscle	1	3.4
Parascapular region - skin	2	14.6
Parascapular region - muscle	2	
Parasacral region - skin	2	6.8

Table 4.3 **Percentage of rat fetuses with lung, non-lung or any haemorrhage exposed to 6 minutes of pulsed Doppler ultrasound of varying mechanical indices (MI).**
Fetuses are exposed indirectly or directly.

MI	Lung haemorrhage by indirect exposure	Lung haemorrhage by direct exposure	Lung haemorrhage by indirect and direct exposure	Non-lung haemorrhage by indirect exposure	Non-lung haemorrhage by direct exposure	Non-lung haemorrhage by indirect and direct exposure	Fetuses with any haemorrhage by indirect exposure	Fetuses with any haemorrhage by direct exposure	Fetuses with any haemorrhage by indirect and direct exposure
1.0	7.4	9.0	7.7	18.5	36.3	22.0	24.0	36.3	26.1
No. of fetuses	54	11	65	54	11	65	54	11	65
0.6	19.3	0.0	13.9	29.0	0.0	20.8	38.7	0.0	27.9
No. of fetuses	31	12	43	31	12	43	31	12	43
0.5	14.8	33.3	18.4	14.8	33.3	18.1	22.2	50.0	27.8
No. of fetuses	27	6	33	27	6	33	27	6	33
0.0	0.0	0.0	0.0	11.7	8.3	10.3	11.7	8.3	10.3
No. of fetuses	17	12	29	17	12	29	17	12	29

Table 4.4 **Distribution of fetuses by age, as a percentage of total fetuses within each mechanical index (MI) exposure group.**

MI (No)	16 days (%)	17 days (%)	18 days (%)	19 days (%)	21 days (%)	22 days (%)
1.0 (65)	16.9	0.0	29.0	18.4	16.9	18.4
0.6 (43)	0.0	16.2	27.9	27.9	27.9	0.0
0.5 (33)	0.0	0.0	48.4	18.1	33.3	0.0
0.0 (29)	17.2	0.0	62.0	20.6	0.0	0.0

Table 4.5 **Percentages of fetuses with lung, non-lung and any haemorrage at each fetal age within each mechanical index (MI) group.**

MI	Age (days)	No of fetuses	Fetuses with lung haemorrhage (%)	Fetuses with non-lung haemorrhage (%)	Fetuses with any haemorrhage (%)
	16	11	0.0	27.2	27.2
	17	0			
1.0	18	19	10.5	36.3	36.3
	19	12	16.6	8.3	33.3
	21	11	0.0	0.0	0.0
	22	12	0.0	16.6	16.6
	16	0			
	17	7	14.2	42.0	57.1
0.6	18	12	25.0	25.0	33.3
	19	12	16.6	16.6	33.3
	21	12	0.0	0.0	0.0
	22	0			
	16	0			
	17	0			
0.5	18	16	31.2	31.2	43.7
	19	6	16.6	16.6	33.3
	21	11	0.0	0.0	0.0
	22	0			
	16	5	0.0	20.0	20.0
	17	0			
0.0	18	18	0.0	11.1	11.2
	19	6	0.0	0.0	0.0
	21	0			
	22	0			

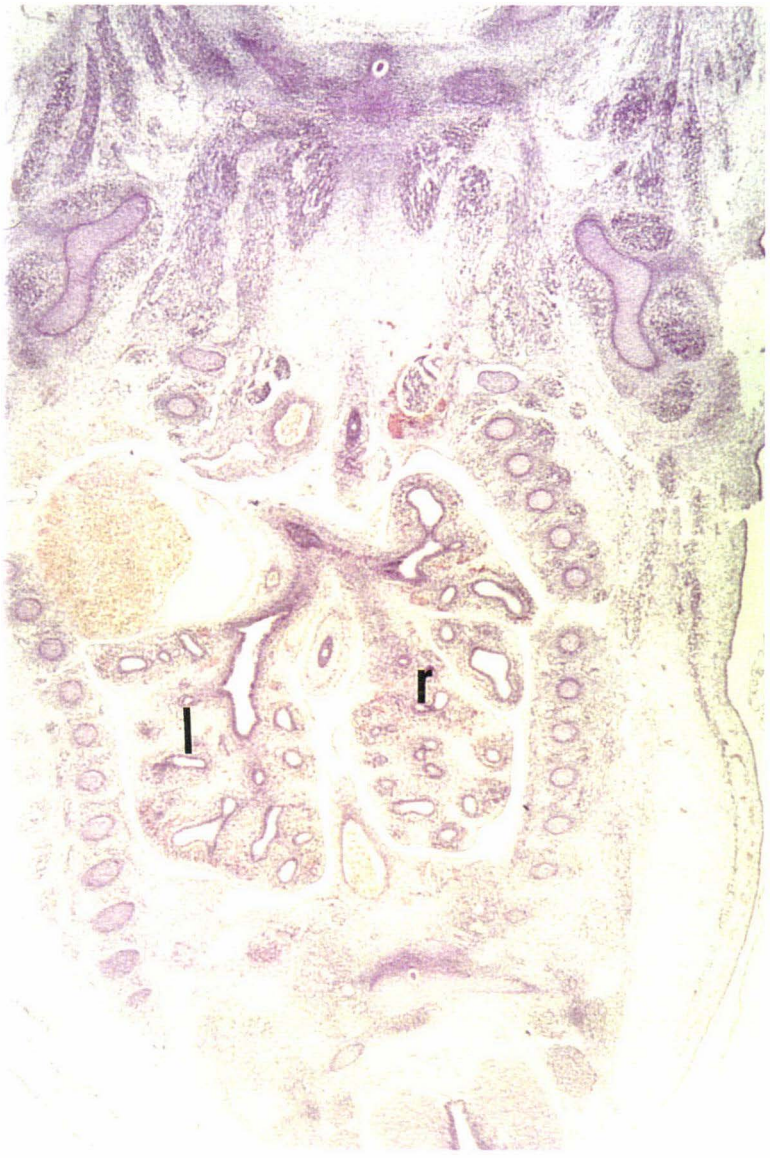

Figure 4.1 **Lung development at 16 days in a rat fetus. The future gas- conducting portion of the lung has formed by branching of the lung buds within the enclosing mesenchyme.**

Rat Rc2 (Fetus F1) : dorsal longitudinal section through the entire lung in the rat. Right lung (**r**); left lung (**l**). Magnification: x26
(Haematoxylin/Eosin staining).

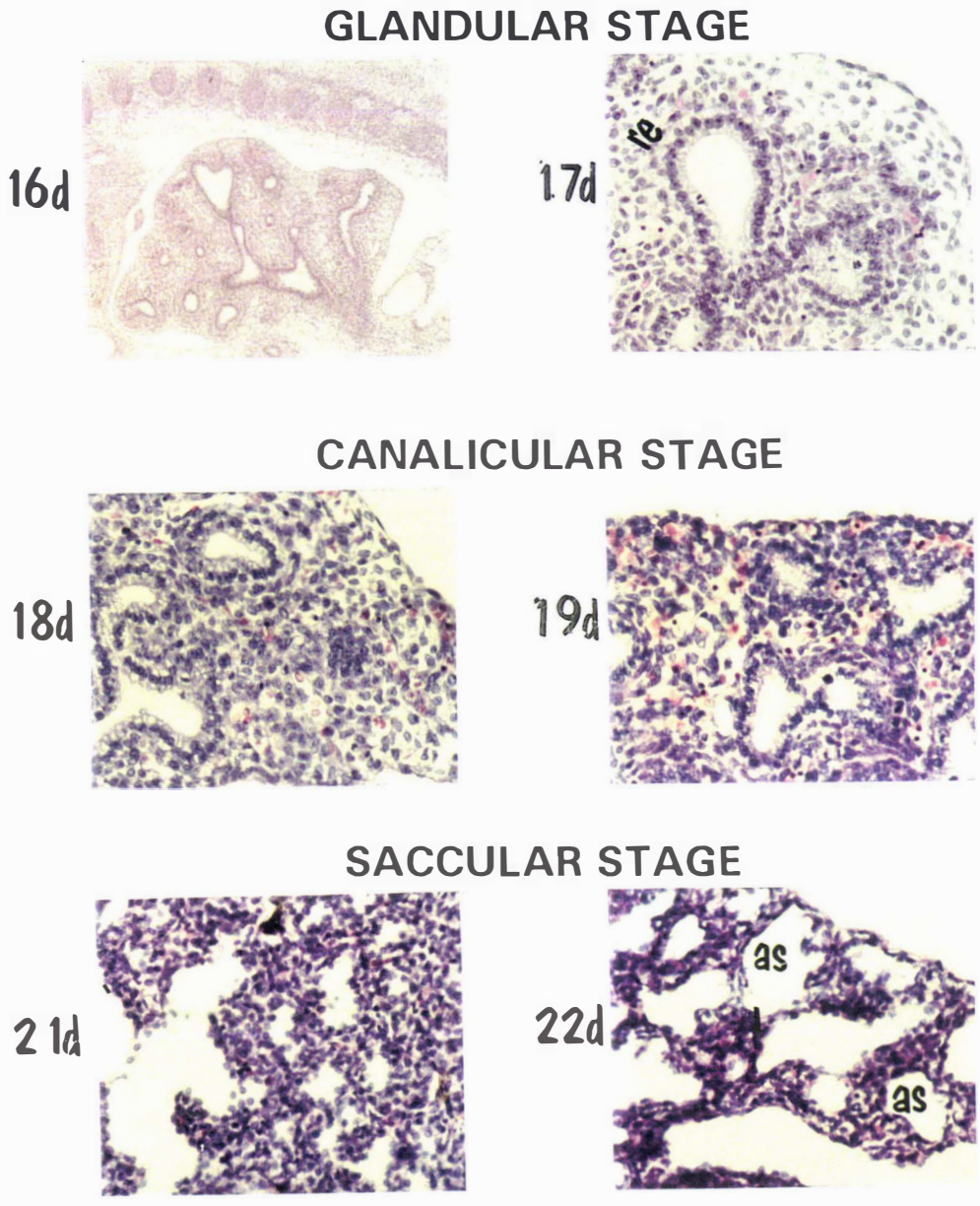

Figure 4.2 **Lung development in the last third of gestation**- Gestation age in days. (**i**) 16 days (Re1-F1): Magnification: x43. (**ii**) 17 days (Re3-F1): High columnar respiratory epithelium (**re**). Magnification: x215. (**iii**) 18 days (Rd26-F1): Magnification: x215.
(**iv**) 19 days (R5-F2): Magnification: x215. (**v**) 21 days (Rd22-F3): Magnification x215. (**vi**) 22 days (R4-F2): Air space (**as**). Magnification: x215
(Haematoxylin/Eosin staining).

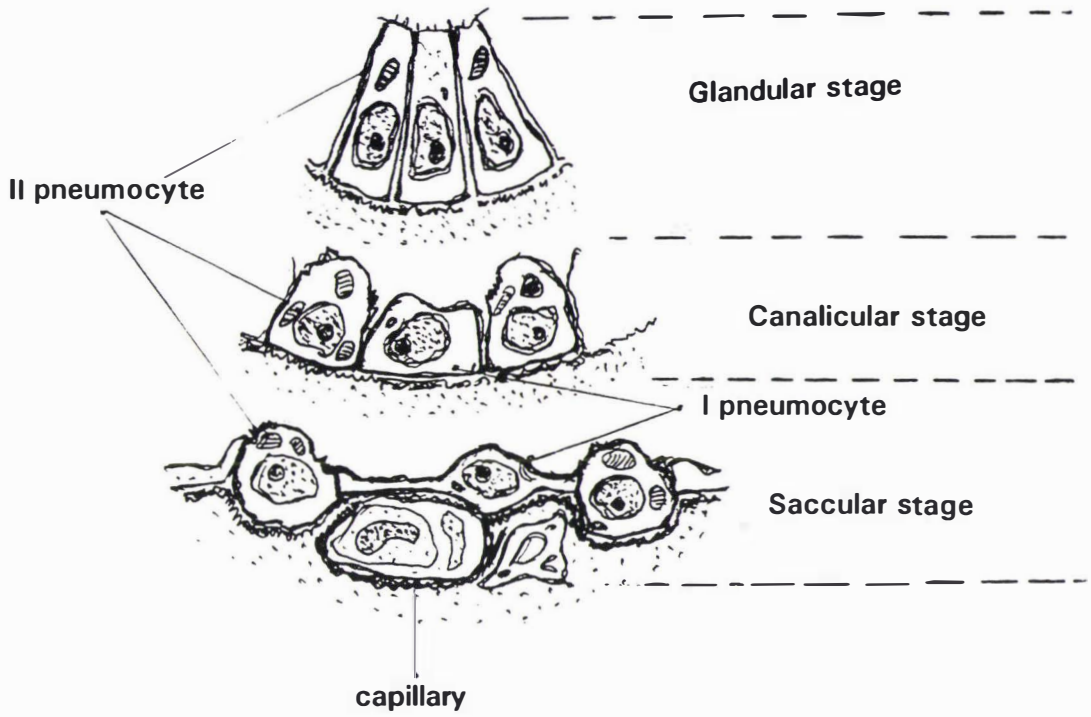

Figure 4.3 **Differentiation of the terminal respiratory epithelium in the last third of rat gestation (diagramatic view adapted from Farrell, 1982).**

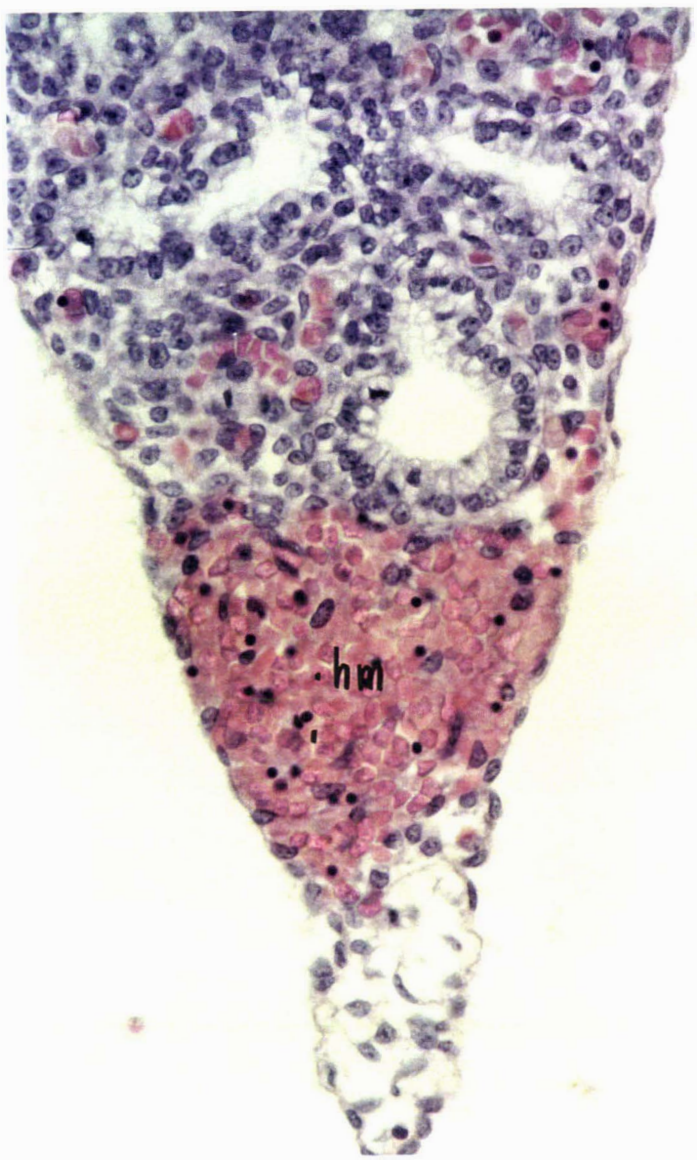

Figure 4.4 **Unifocal fetal lung haemorrhage.** Rat R16 (Fetus F3): Haemorrhagic region (**hm**). Magnification: x430. (Haematoxylin/Eosin staining).

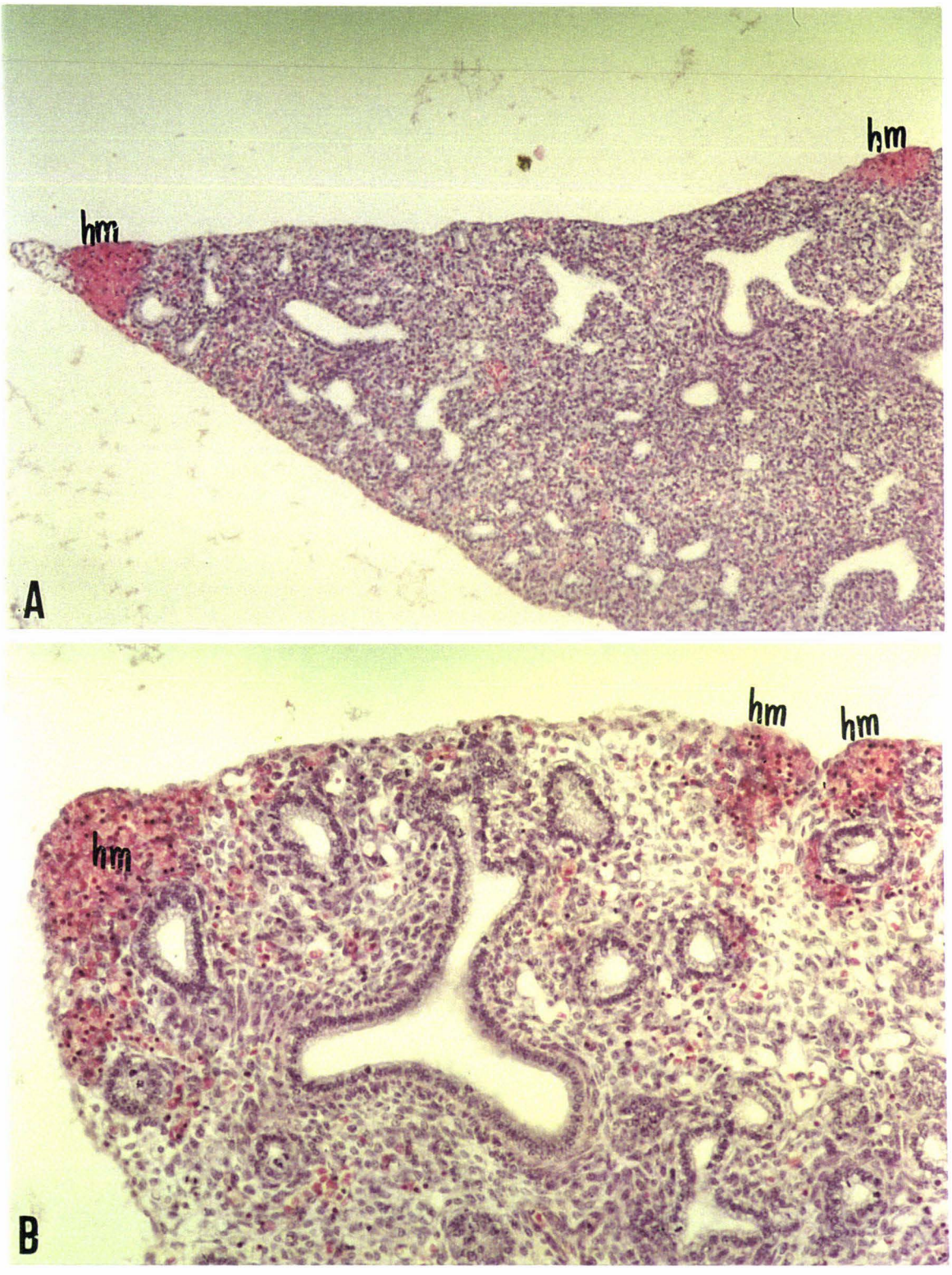

Figure 4.5 **Multifocal fetal lung haemorrhage.** Rat R5 (Fetus F5): (**A**) Magnification: x26. (Haematoxylin/Eosin staining). Rat R16 (Fetus F3): (**B**) Magnification: x108. (Haematoxylin/Eosin staining).
Haemorrhagic region (**hm**).

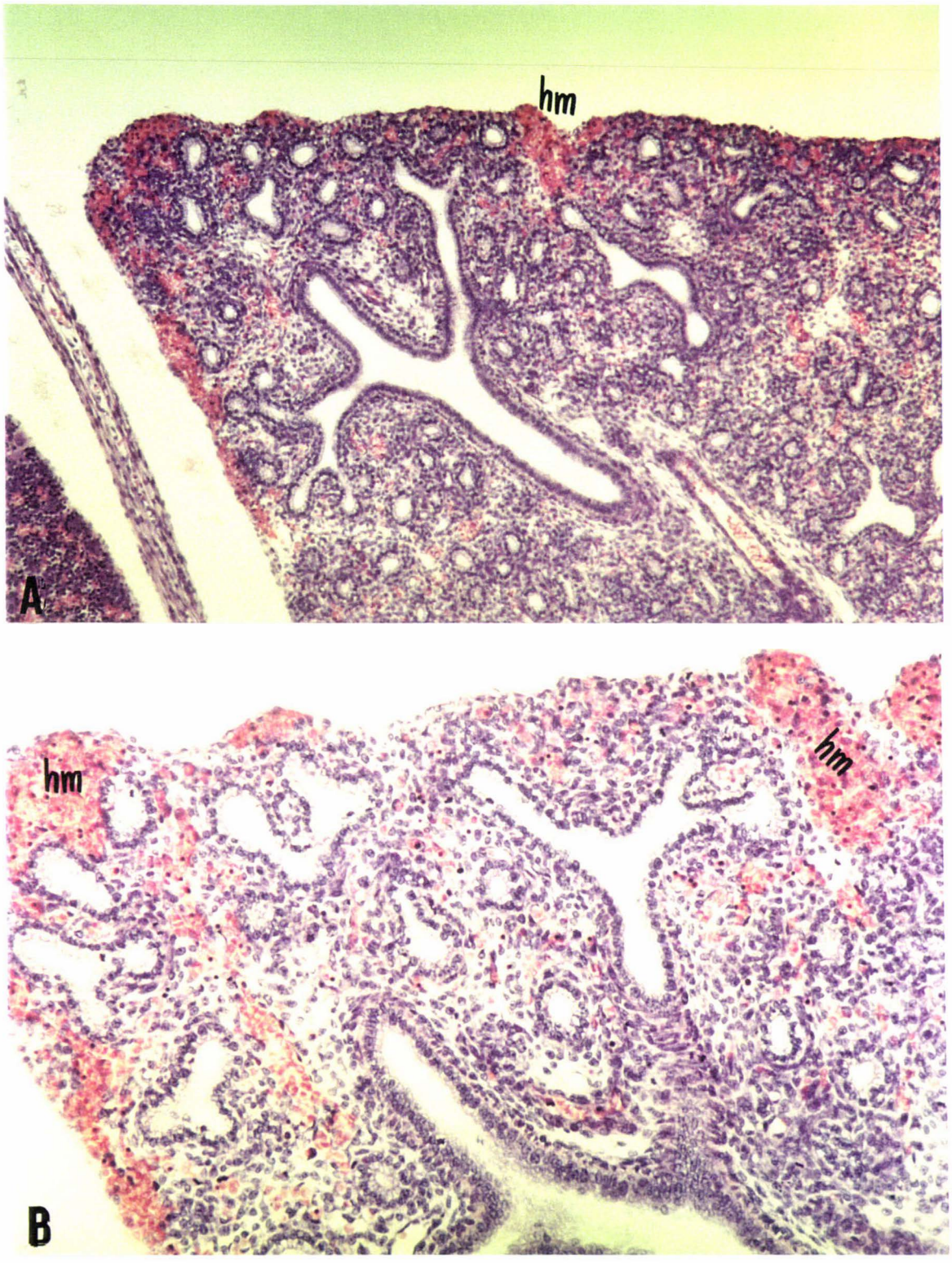

Figure 4.6 **Multifocal fetal lung haemorrhage**. Rat Rd26 (Fetus F4): (**A**) Magnification: x108 ; (**B**) deeper lung section. Magnification: x 215.
(Haematoxylin/Eosin staining).
Haemorrhagic region (**hm**).

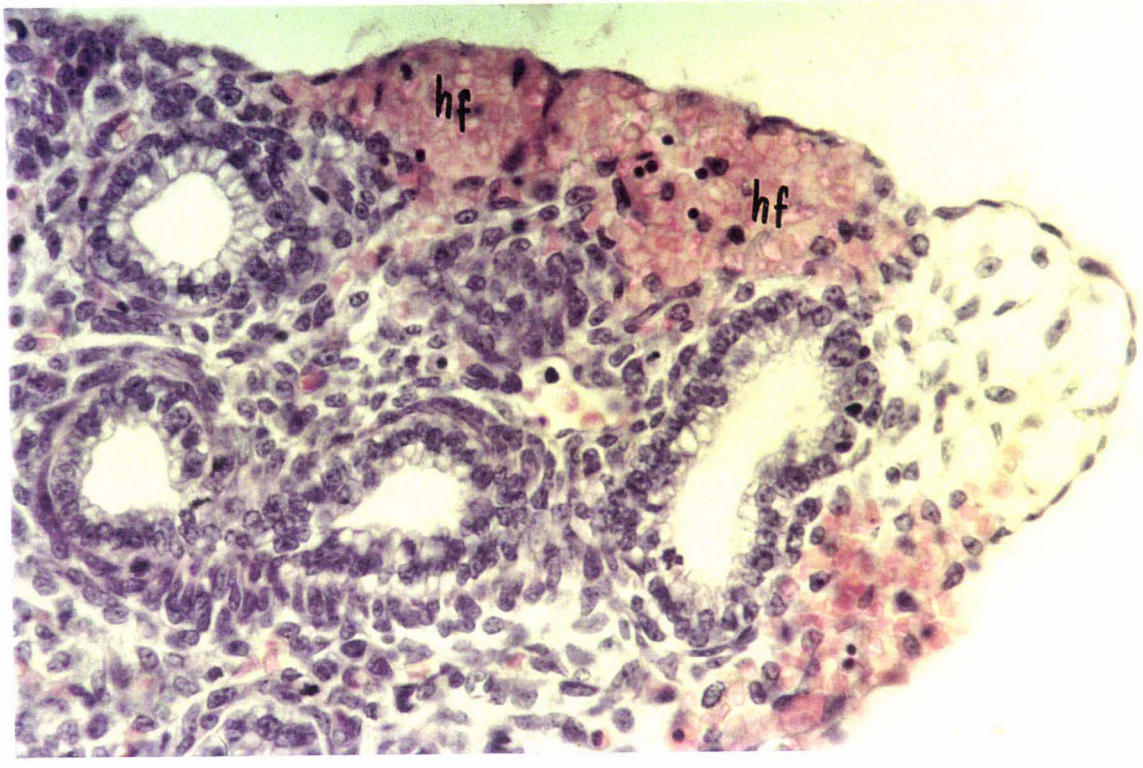

Figure 4.7 **Multifocal fetal lung haemorrhage with grouped foci**. Rat R6 (Fetus F5): Haemorrhagic focus (**hf**). Magnification: x430. (Haematoxylin/Eosin staining). .

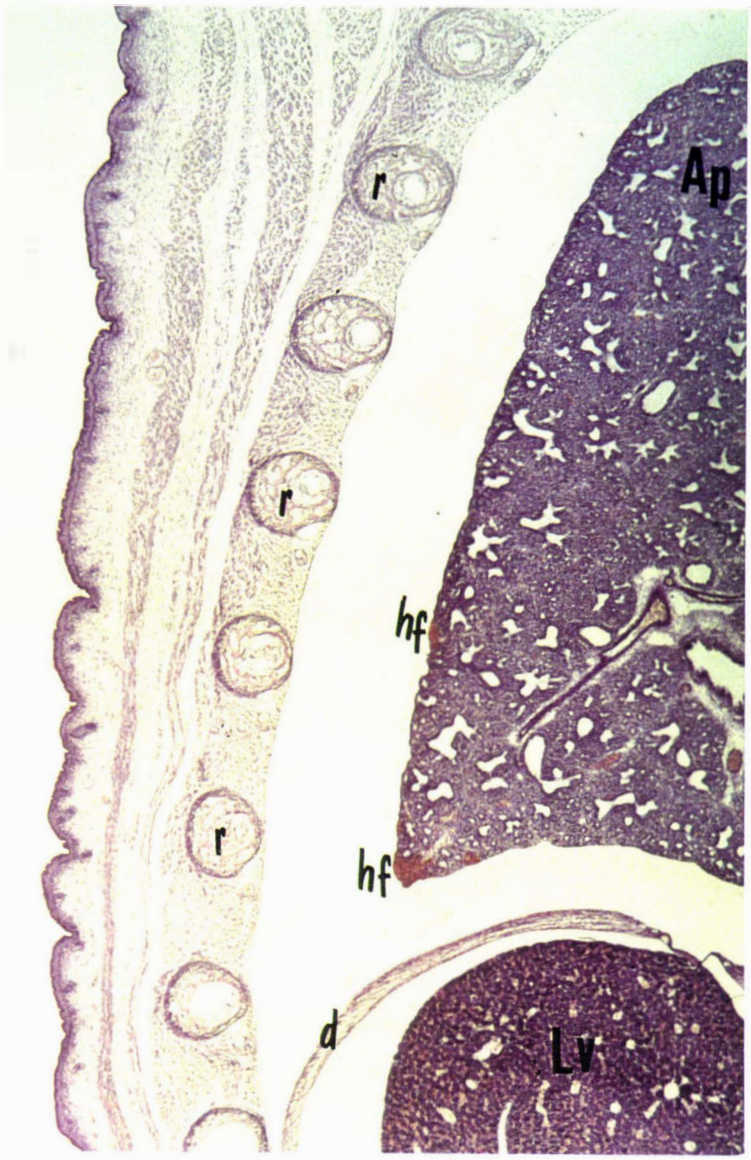

Figure 4.8 **Location of rat fetal lung haemorrhage.** Rat R5 (Fetus F5): Haemorrhagic focus (**hf**); rib (**r**) ; lung apex (**Ap**) ; liver (**Lv**) ; diaphragm (**d**). Magnification 26x. (Haematoxylin/Eosin staining).

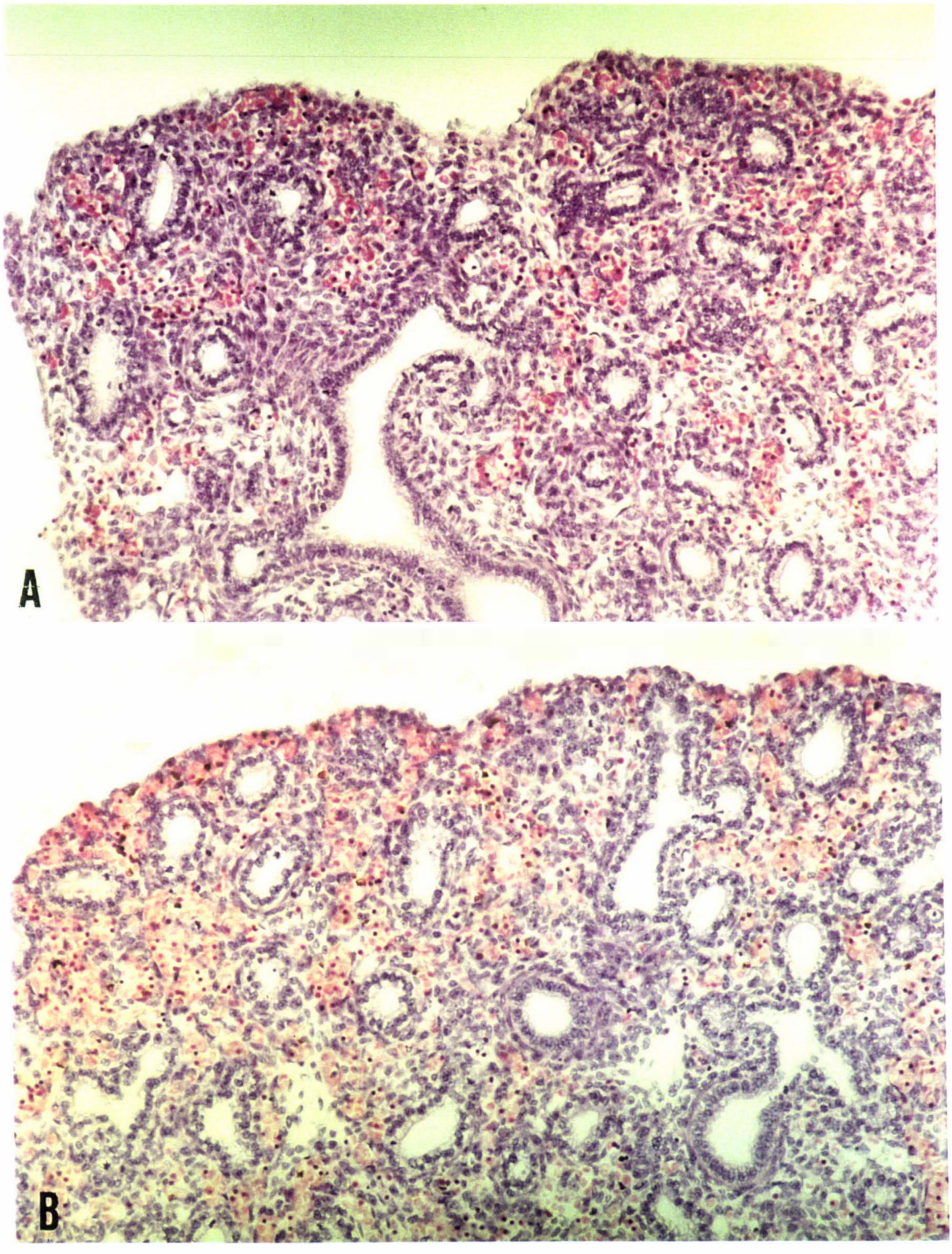

Figure 4.9 **Severe vasocongestion in fetal lungs.** Rat Rd24 (Fetus F3): (**A**) Magnification: x215. Rat Rc7 (Fetus F6) : (B) Magnification: x215. (Haematoxylin/Eosin staining).

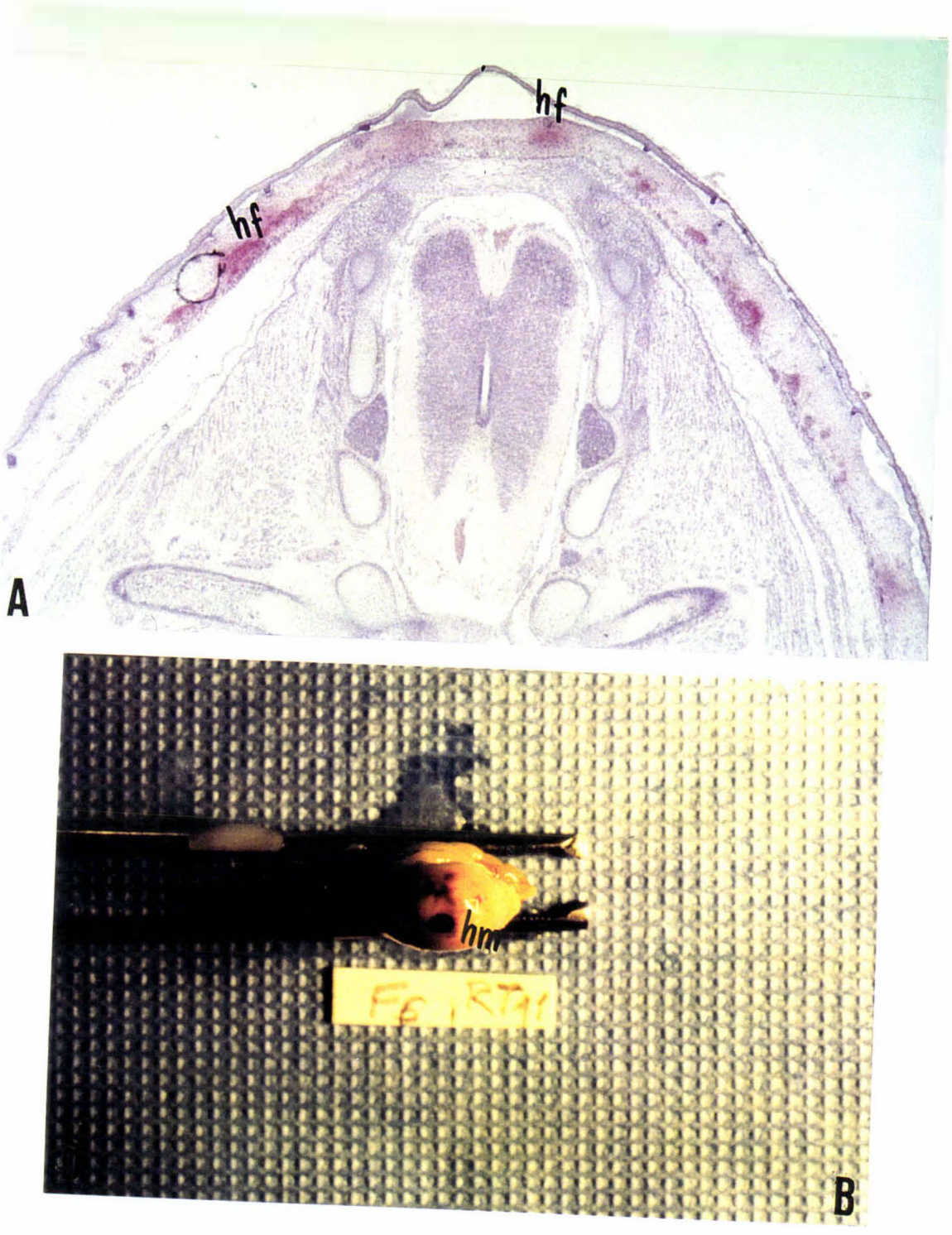

Figure 4.10 **Multifocal rat fetal haemorrhage in the head.** Rat R11 (Fetus F6): (**A**) Magnification: x25. (**B**) Magnification 2.7x. Haemorrhagic region (**hm**) ; haemorrhagic focus (**hf**).
(Haematoxylin/Eosin staining).

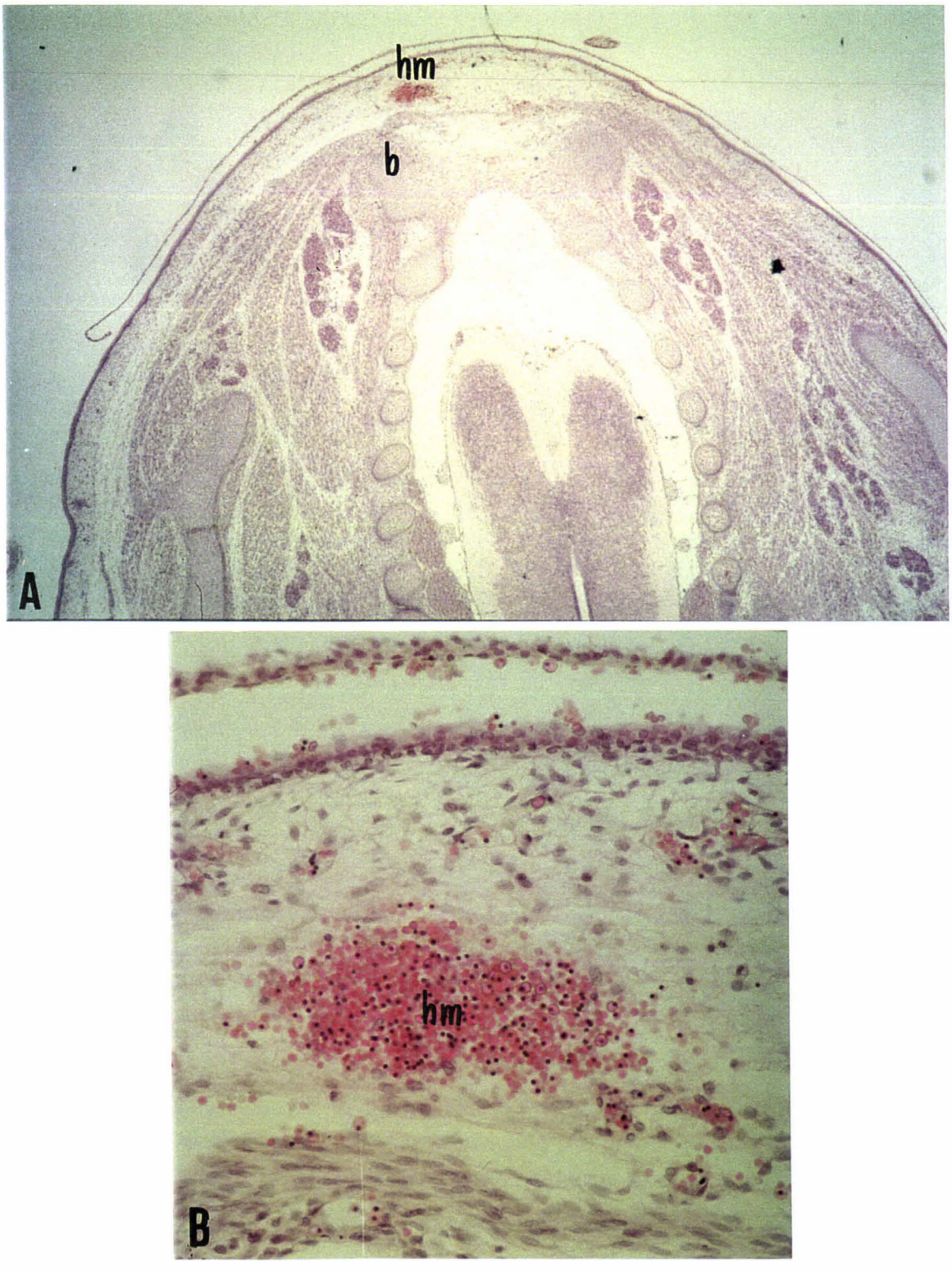

Figure 4.11 **Solitary rat fetal haemorrhage in the occipital part of head.** Rat Re3 (Fetus F2): **(A))** Magnification: x43. **(B)** Magnification: x215.
Haemorrhagic region (**hm**); bone tissue (**b**).
(Haematoxylin/Eosin staining).

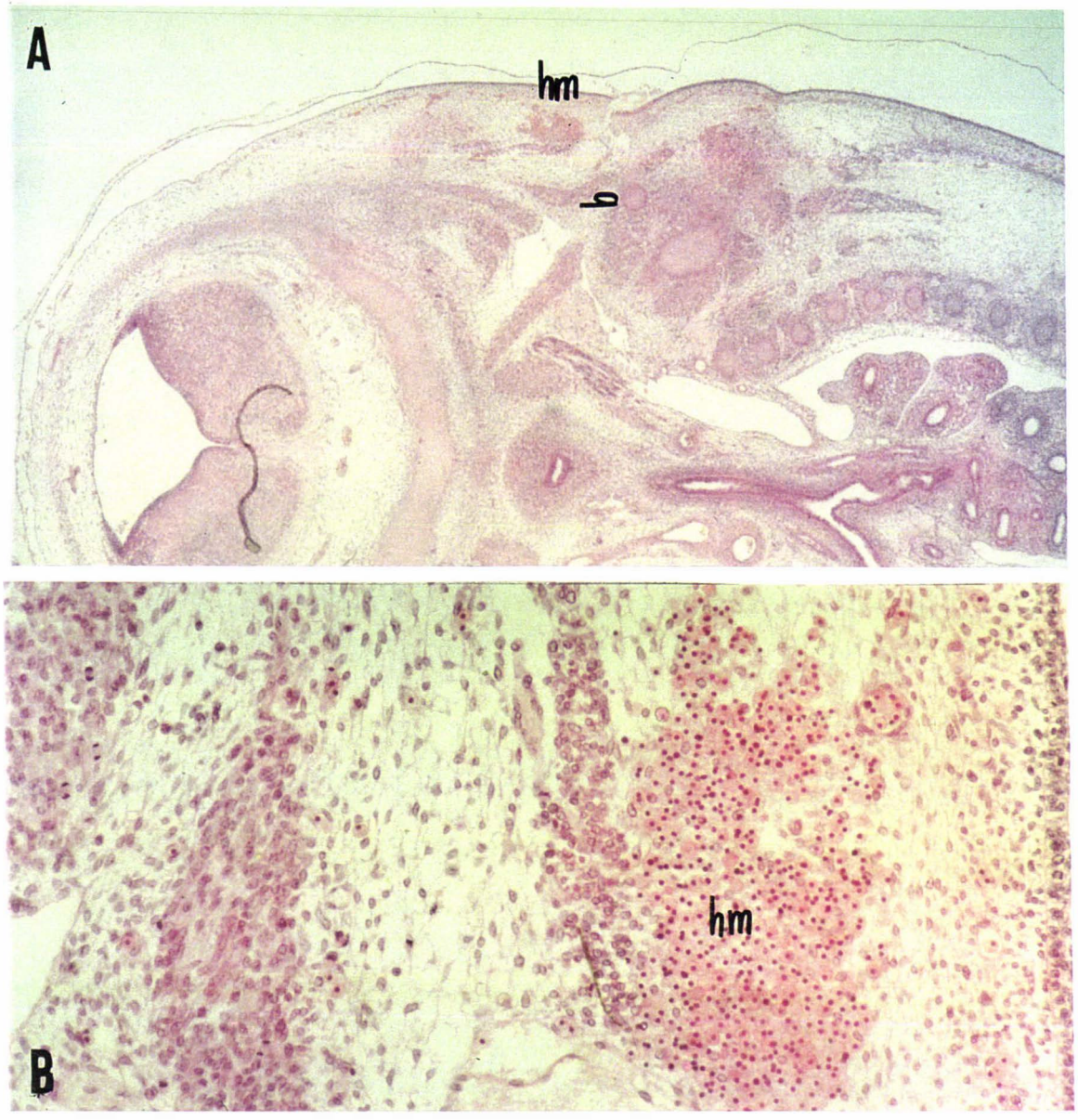

Figure 4.12 **Solitary haemorrhage in the neck**. Rat Re2 (Fetus F1): (**A**) Magnification: x26. (**B**) Magnification: x215.
Haemorrhagic region (**hm**); bone tissue (**b**).
(Haematoxylin/Eosin staining).

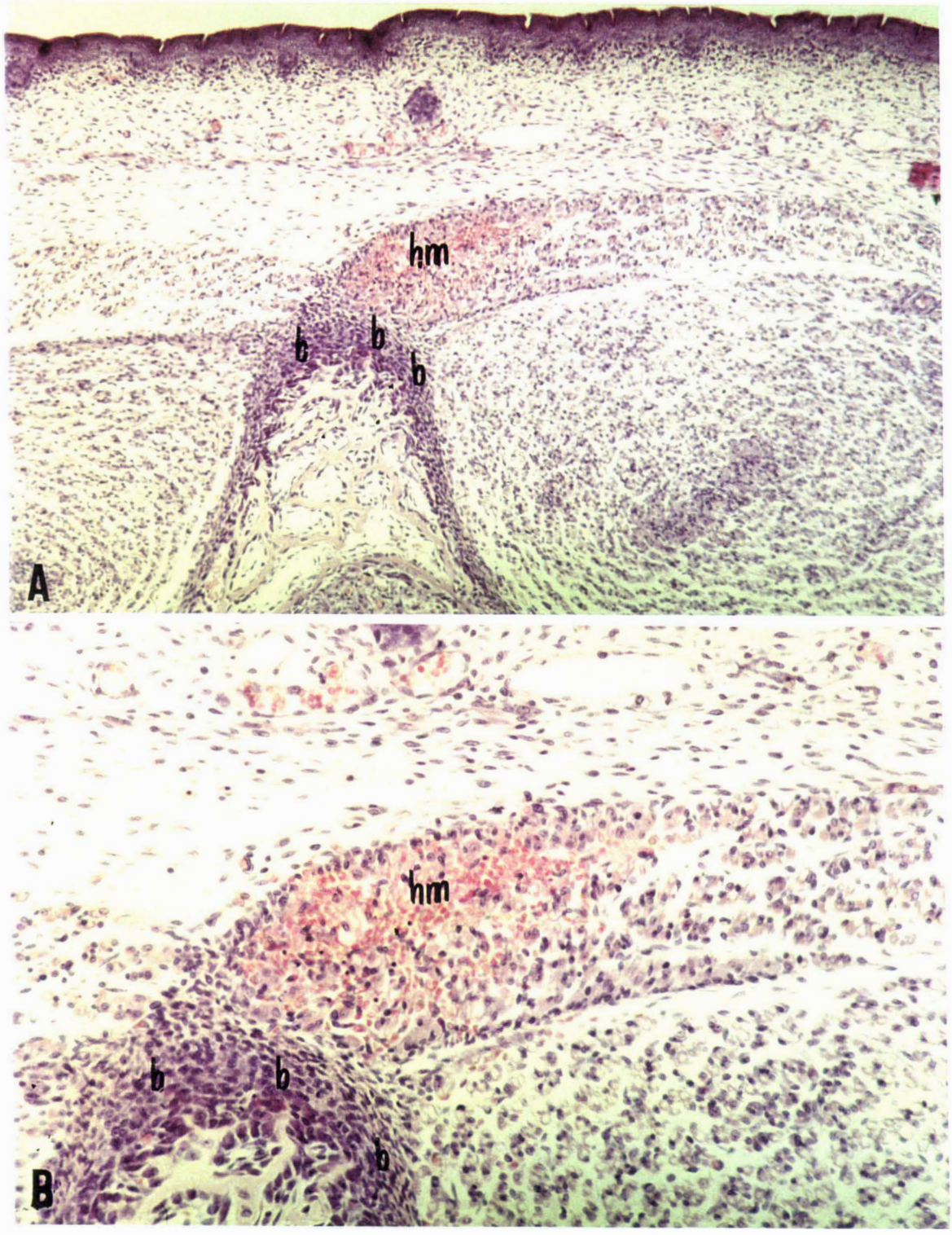

Figure 4.13 **Haemorrhage in parascapular muscle.** Rat R5 (Fetus F1): (**A**) Magnification x108. (**B**) Magnification: x215.
Haemorrhagic region (**hm**); bone tissue (**b**).
(Haematoxylin/Eosin staining).

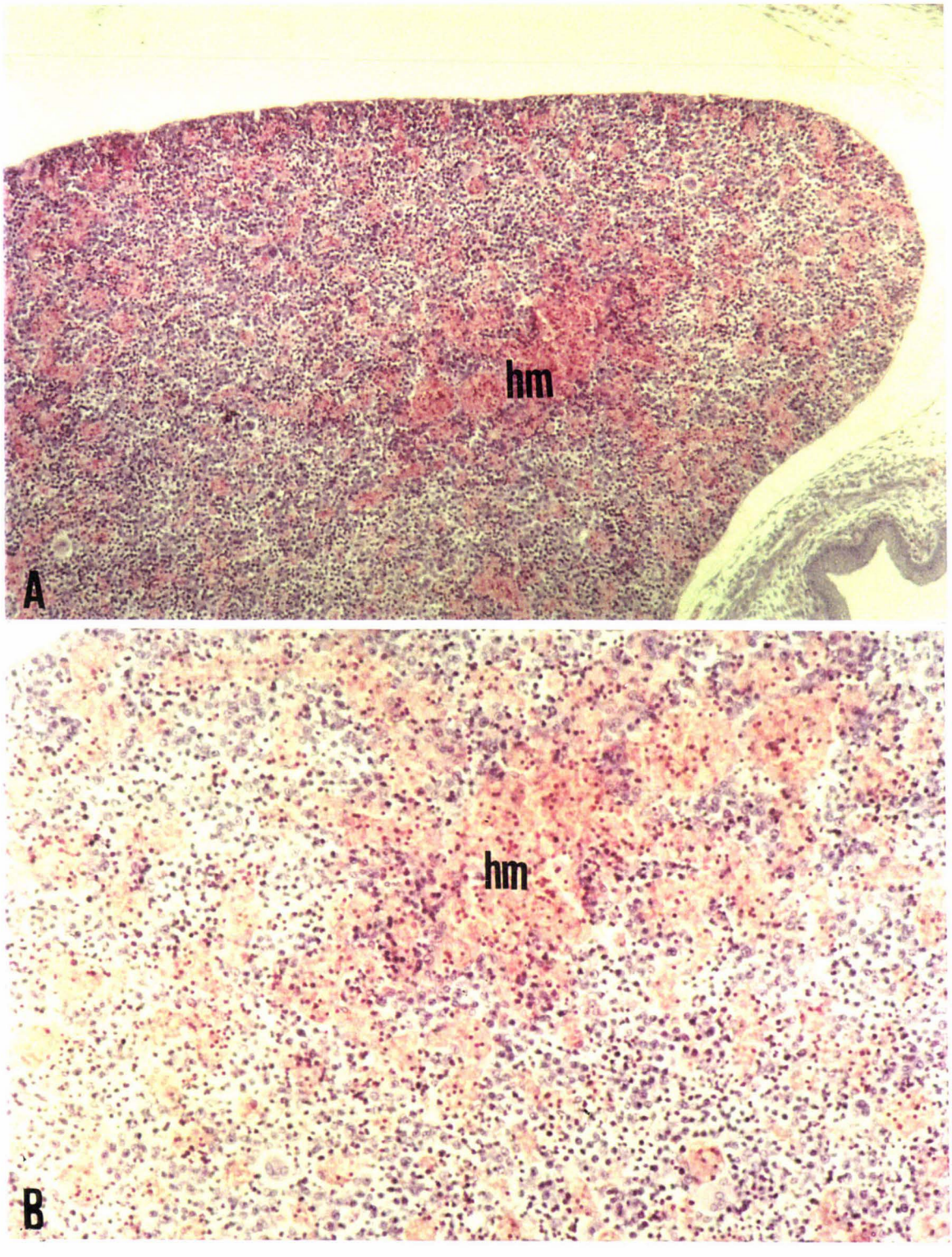

Figure 4.14 **Haemorrhage in the fetal liver.** Rat R20 (Fetus F3): (**A**) Magnification: x108. (**B**) Magnification: x215.
Haemorrhagic region (**hm**).
(Haematoxylin/Eosin staining).

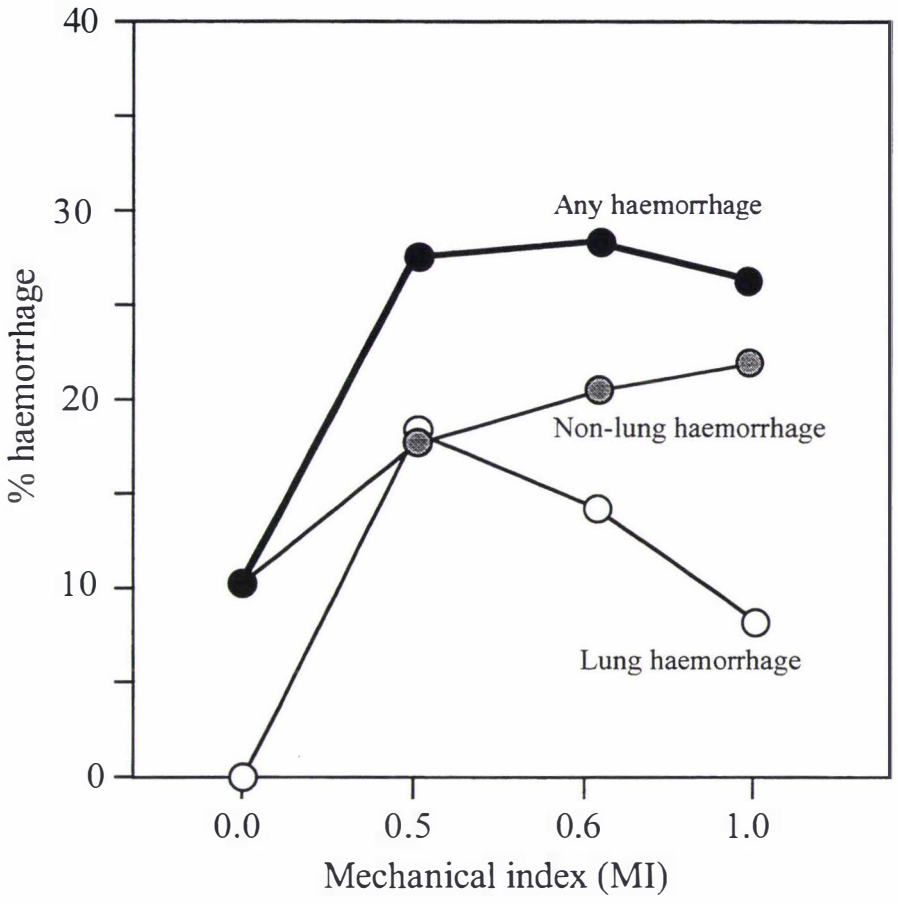

Figure 4.15 **Percentage of fetuses with haemorhage in the lung, in tissues other than lung and in all locations, both directly and indirectly exposed, at each level of mechanical index used.**

13 Oct 98 SPSS for MS WINDOWS Release 6.1

* * * * M U L T I P L E R E G R E S S I O N * * * *

Equation Number 1 Dependent Variable.. @_HM % HM

---------- Variables in the Equation ----------

A

Variable	B	SE B	95% Confdnce Intrvl B		Beta
MI	22.125443	9.092756	3.358916	40.891969	.401383
AGE	-7.219534	1.902921	-11.146970	-3.292097	-.627904
I_1____D	-5.935440	7.444338	-21.299799	9.428918	-.130083
(Constant)	152.356065	36.512395	76.998184	227.713945	

-2 Log Likelihood	176.501
Goodness of Fit	159.504

	Chi-Square	df	Significance
Model Chi-Square	12.211	2	.0022
Improvement	4.175	1	.0410

Classification Table for HM

		Predicted .00 (0)	Predicted 1.00 (1)	Percent Correct
Observed				
.00	0	114	7	94.21%
1.00	1	39	4	9.30%
			Overall	71.95%

---------- Variables in the Equation ----------

B

Variable	B	S.E.	Wald	df	Sig	R	Exp(B)
MI	-.3335	.1672	3.9762	1	.0461	-.1023	.7164
AGE	-.3445	.1158	8.8460	1	.0029	-.1905	.7085
Constant	6.1092	2.2298	7.5062	1	.0061		

---------- Model if Term Removed ----------

Term Removed	Log Likelihood	-2 Log LR	df	Significance of Log LR
MI	-90.338	4.175	1	.0410
AGE	-93.139	9.777	1	.0018

Figure 4.16 **SPSS logistic regression method applied to the results for any fetal haemorrhage in all fetuses (indirectly and directly exposed) for the 4 different levels of mechanical index MI.** (**A**) Effects of method of exposure on the incidence of any fetal haemorrhage per each exposure group; **I**: indirectly exposed fetuses, **D**: directly exposed fetuses (**B**) Effect of mechanical index, MI and fetal age on haemorrhage; **R**: regression coefficient; **Exp (B)**: logistic odds ratio.

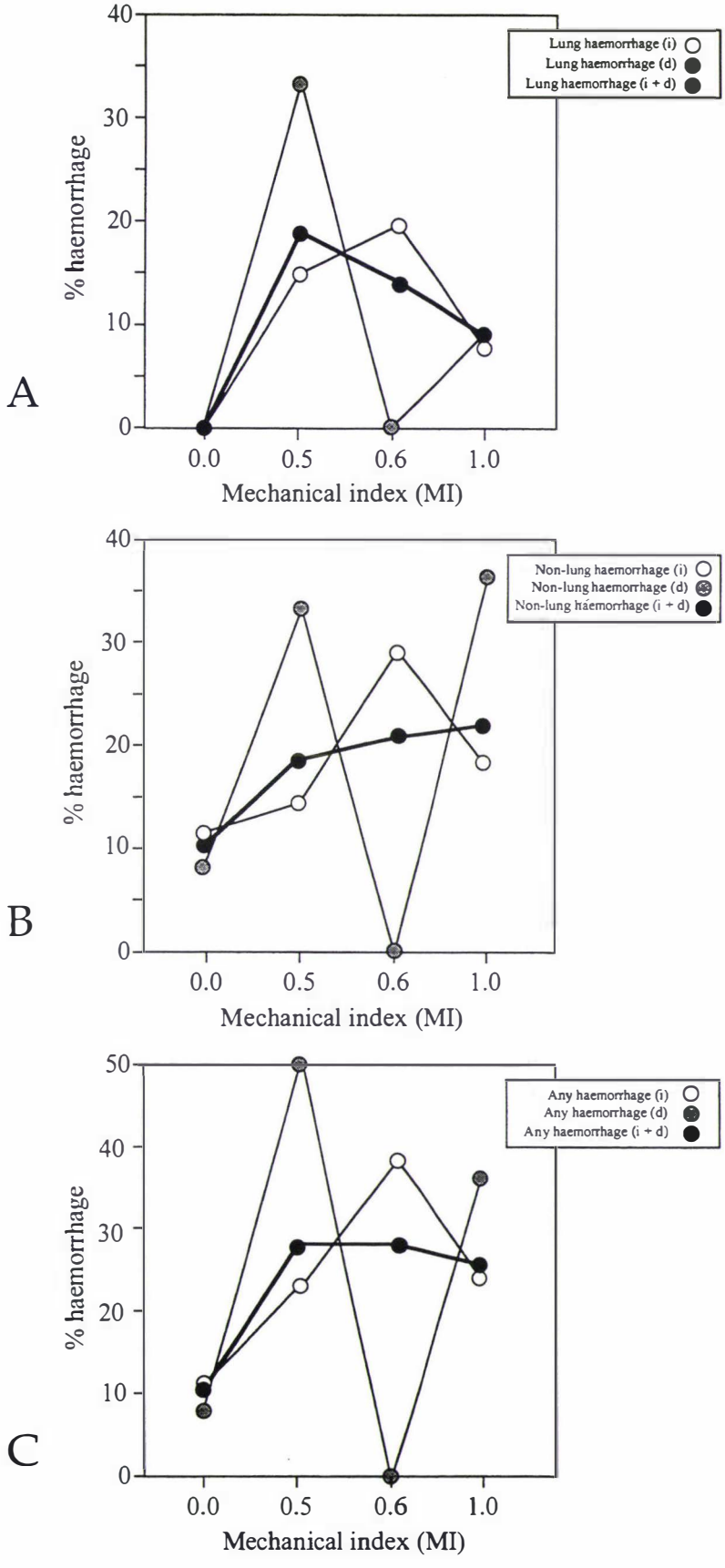

Figure 4.17 **The effect of method of exposure on the incidence of fetal haemorrhage.** Percentage of fetuses with haemorhage in the lung (A), in tissues other than lung (B) and in all locations(C), in indirectly (i), directly (d) and combined indirectly and directly (i+d) exposed fetuses at each level of mechanical index used.

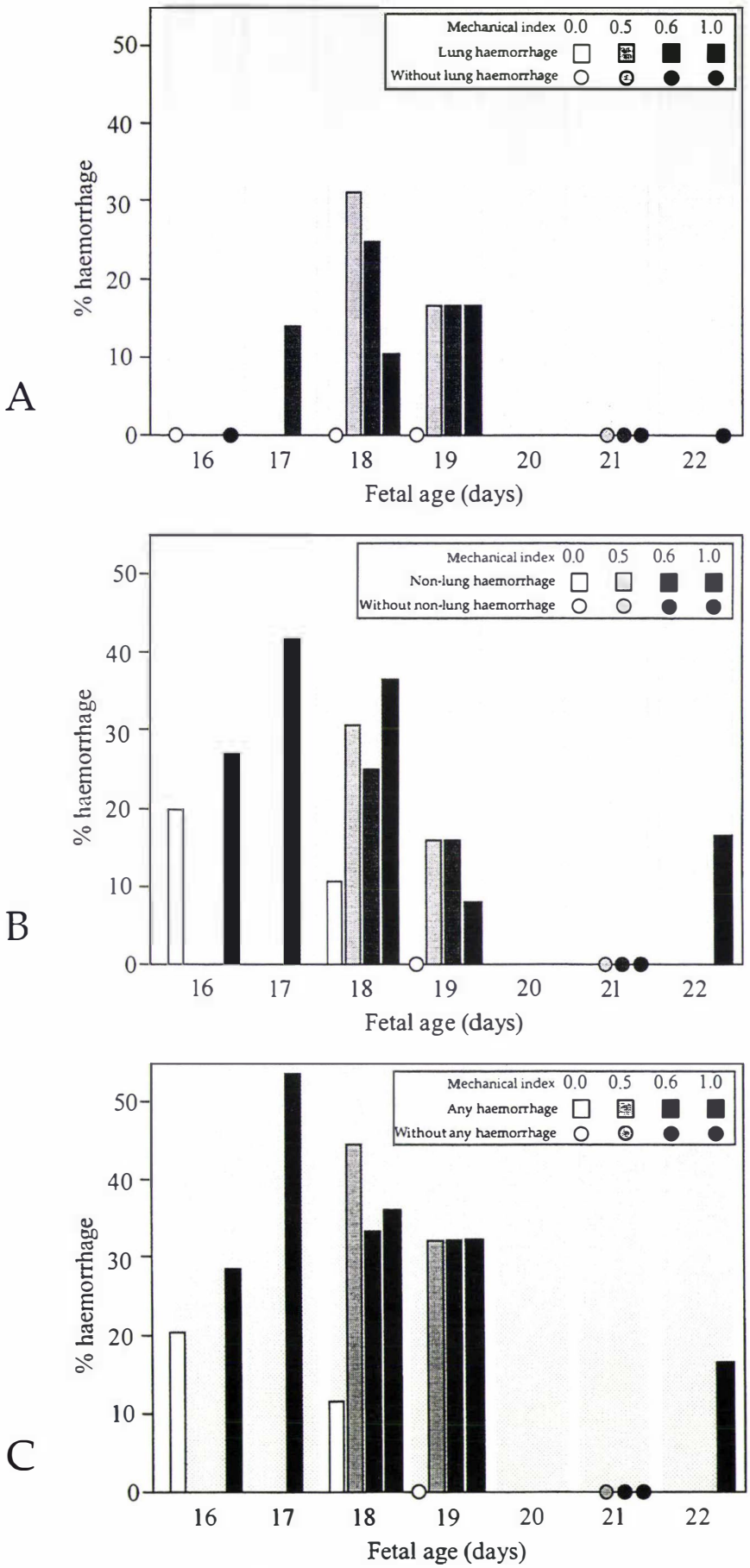

Figure 4.18 **Fetal age and the incidence of haemorrhage.**
The percentage of fetuses with lung (A), non-lung (B) and any haemorrhage (C) at different ages, and varying mechanical index.

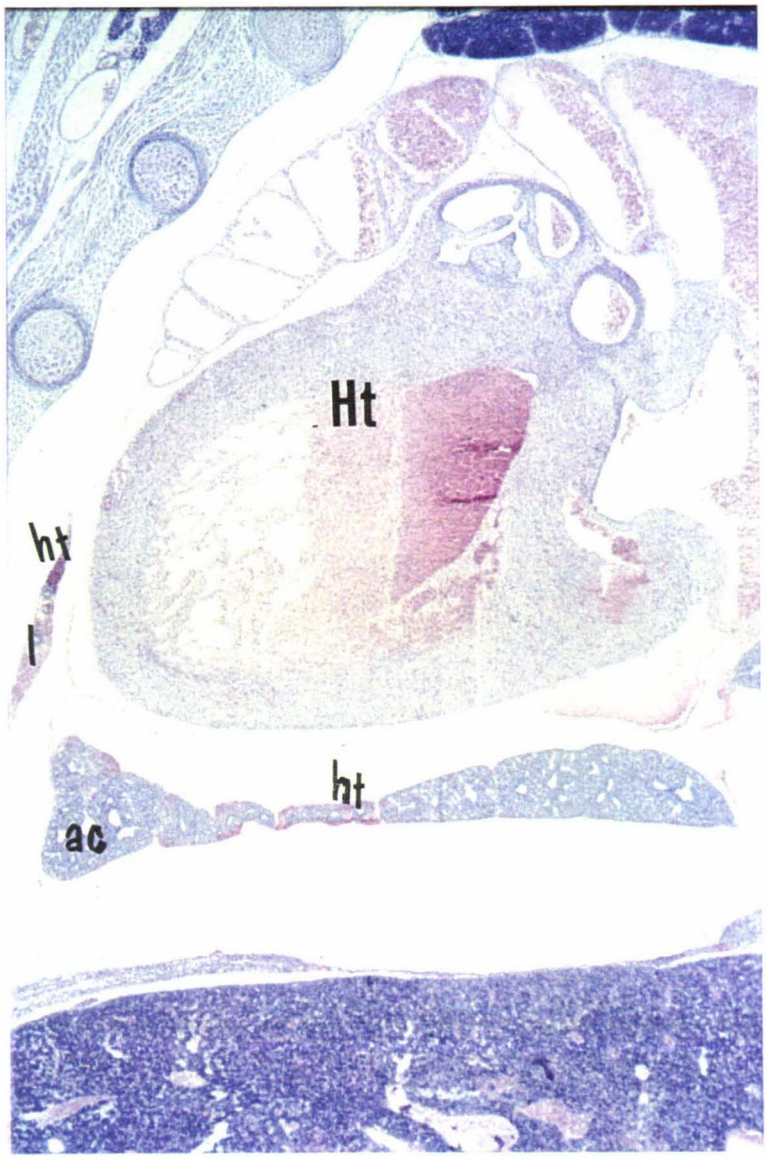

Figure 4.19 **Lung haemorrhage in a ventral trunk section of a serially sectioned fetus.** R16 (F3): Magnification: x26. Haemorrhagic focus (**hf**) in a thin ventral section of left lung (**l**) and accessory lobe (**ac**).
Heart (**Ht**).
(Haematoxylin/Eosin staining).

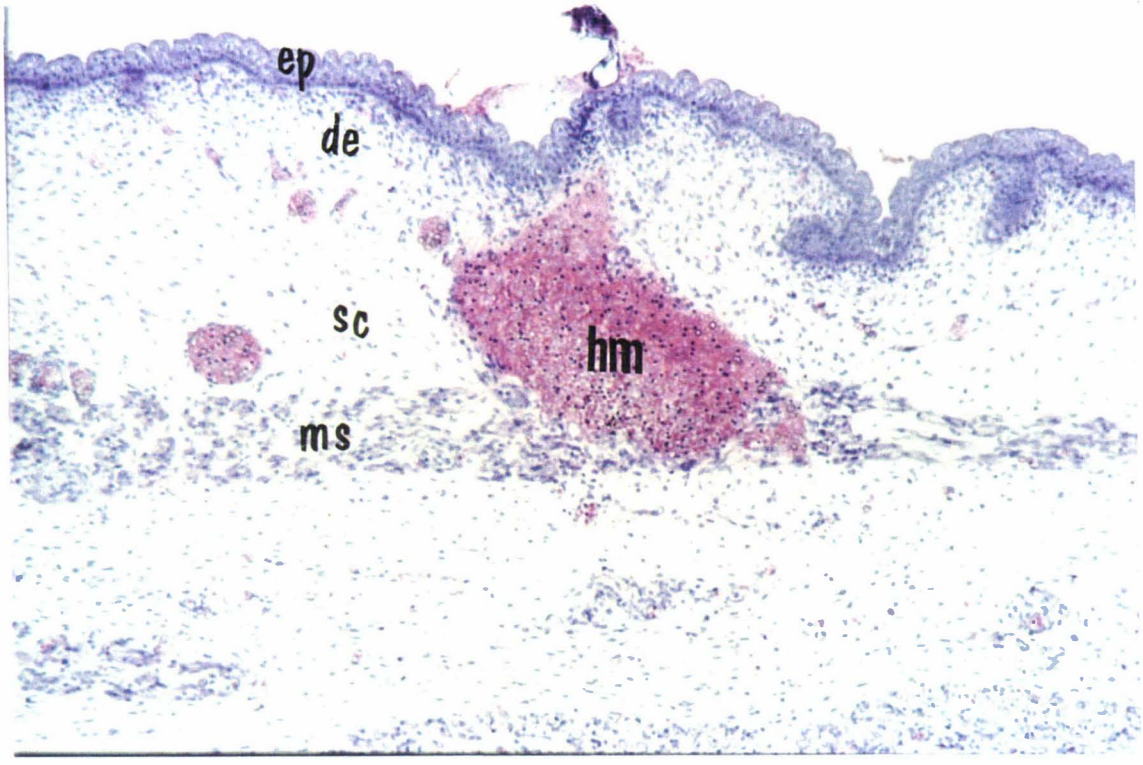

Figure 4.20 **Haemorrhage in the skin of a serially sectioned fetus.** Rd26 (F3): Magnification: x108. Haemorrhagic region (**hm**). Epidermis (**ep**), dermis (**de**), subcutis (**sc**) and muscle (**ms**). (Haematoxylin/Eosin staining).

Chapter 5

DISCUSSION

5.1 Experimental methods as a model of clinical conditions

5.1.1 Experimental equipment

Previous research on possible tissue damage caused by ultrasound has used a customised transducer under laboratory conditions, rather than a clinical machine. This study therefore differs from that of Child et al. (1990); Penney et al. (1993); Dalecki et al. (1997A) in that the transducer was manipulated by the controls of a regular machine that could also provide a screen image of the region being exposed. The transducers selected for this study were P5-3 and P7-4 which are commonly used in clinical diagnostic ultrasound examinations (Chapter 2).

The exposure levels were also typical for clinical use, regarding their type (pulsed Doppler), location (a model for echocardiography and obstetrical use) and duration.

5.1.2 Mechanical index (MI) as a threshold parameter

Previous studies on tissue effects measured acoustic pressure at the surface by a means of a hydrophone (Hartman et al., 1990 ; Dalecki et al., 1997A; Dalecki et al., 1997B; Coleman et al., 1998). This study has instead used mechanical index (MI). Ultrasound machines display this parameter, as a function of acoustic pressure and frequency of the sound wave, on the screen (Harris, 1996). It is calculated for the frequency and focal depth of each transducer type. By changing the setting on the machine, variations in MI sufficient to determine threshold levels of exposure are possible (AUIM, 1992). This method has the special advantage that it provides information to the ultrasonographer enabling control of the exposure levels.

5.1.3 Adjustment of the ultrasound machine for use with small laboratory animals.

The choice of the rat as an experimental model presented a special problem. The average depth of its chest (location of the lung surface) and abdominal wall (location of fetuses) is about 5mm. The desired intensity of ultrasound expressed as a varying value of MI has to be achieved at the focal depth of the transducer. However, the focal depth of any particular transducer is over 10mm. This problem was overcome by the use of standoff medium (Chapter 2) that effectively placed the desired focal point further from the transducer. The value of MI on the screen of an ultrasound

machine is calculated for average tissue (liver-like soft tissue) attenuation , which is assumed to be 0.3 dB cm^{-1} MHz^{-1} (derating factor) (AIUM, 1992). Because the standoff medium has an attenuation of essentially zero, MI values used in this study are underestimated for this derating factor. The extent of this error could not be estimated but will be small (AIUM, 92). Since it applies across all exposures, this error should not affect the significance of the results.

5.2 Damage in adult rat lungs

5.2.1 Lung haemorrhage

In this study lung haemorrhage, as seen by light microscopy, was a pathological change in exposed lung tissue. The threshold for this lung haemorrhage was considered to be between MI 0.5 and 0.6. Three aspects of the findings suggest that these haemorrhages are indeed due to ultrasound exposure:

i) There is a greater risk of haemorrhage with higher levels of exposure.

ii) The location of haemorrhages was commensurate with the position of the transducer on the dorsal surface of the thoracic wall, being predominantly in the right caudal lobe. Also the location within the lung was predominatly subpleural. Subpleural haemorrhage has previously been recorded as a result of ultrasound exposure in adult lung (Penney et al., 1993).

iii) The highest proportion of doubtful haemorrhage occurred at exposure levels immediately above the threshold. Since this was in part due to doubt in interpreting severe vasocongestion which might well precede haemorrhage in exposed lung tissue, this result could represent further evidence that ultrasound can cause lung haemorrhage.

Anaesthesia and lung haemorrhage

General anaesthesia affects both the dam and the fetus, and it is important to realize the consequences (Flecknell, 1996). The most obvious result is to induce hypoventilation of the dam (Dawes, 1968).

Pentobarbitol is the recommended anaesthetic for minimal cardiovascular depression (Fish, 1997; Wixson and Smiler, 1997; Chesterfield and Parton, 1997). Previous ultrasound research on anaesthetized animals has used mostly Ketamine (Hartman et al., 1990; Dalecki et al., 1997A ; Tarantal and Canfield, 1994) or Pentobarbitol (Dalecki et al., 1997B). The possibility that anaesthesia can contribute to haemorrhage has not previously been discussed. In the present study, as in earlier work, anaesthetized animals were used as sham controls and exhibited no significant rate of haemorrhage, suggesting that anaesthesia was not a significant contributing factor.

5.2.2 Possible sources of variations within experimental groups

Pregnancy

Most the rats used in this study were pregnant (Table 3.1). To reduce the number of experimental animals, pregnant rats were used to investigate the effects of ultrasound on both adult and fetal lungs. The number of nonpregnant rats used was insufficient to determine if pregnancy influenced the sensitivity of lung tissue to ultrasound. Haemorrhage could be more prevalent in lungs with a greater blood flow as in pregnancy (Weir and Reeves, 1989). Such a difference has been demonstrated in rats exposed to ozone, where lung damage is greater in pregnant rats (Gunnison and Finkelstein, 1997). Studies of the effect of pregnancy on lung damage due to ultrasound have not yet been made.

Variations in experimental procedures on experimental rats

Compared to other rats, those identified in Table 3.1 as " Rd " were under anaesthesia 30-40 minutes longer, because they had their fetuses exteriorised by laparotomy for direct exposure to ultrasound. The number of these rats (4 exposed and 2 controls) was too small to allow comparison of how this procedure may have influenced the results in their lungs. Although the bodies of pregnant rats overall were exposed several times, the lungs were exposed directly only once and the other exposures were on the fetuses. It is not expected that this difference could affect the results.

5.3 Damage in the tissues of rat fetuses

5.3.1 General observations

This study appears to be the first to observe a morphological effect by diagnostic levels of pulsed Doppler ultrasound exposure on fetal tissues, particulary lungs. Previous researchers (Dalecky et al., 1997A) induced haemorrhage in fetal lung and other fetal tissues by the much higher energy levels produced by a therapeutic ultrasound source used for lithotripsy. Also, the present study appears to be the first to apply a direct method of exposure to fetuses.

Since 188 rat fetuses were investigated in the present study, it was necessary to develop a method of sectioning the fetus for histology (Chapter 2) that could enable both lungs, and all adjacent tissues including the head, to be studied from a single section. A section of the fetus in the dorsal plane achieved this well with the additional advantage that the lungs were not disturbed by dissection. The time-consuming removal of the lungs aided by a dissection microscope, as by Dalecky et al. (1997A), was thereby avoided.

5.3.2 Fetal lung haemorrhage

Since neither MI setting, nor the directness of exposure of fetuses, had a consistent effect on the incidence of haemorrhage in the lung, even low levels of exposure appear to be effective in causing haemorrhage. That direct exposure of fetuses caused no more damage than indirect exposure was an unexpected result. Results from direct exposure of exteriorised fetuses have not been previously reported.

Dalecky et al.(1997A) exposed fetuses of mice late in gestation (18 days) with lithotripter ultrasound intensity. They found haemorrhages on the surface of the lungs which appeared as an evenly spaced row of dots correlated spatially with the areas of insertion of the ribs at either the sternum or vertebrae. The threshold for these haemorrhages was 1 MPa which is similar to the threshold for haemorrhage in adult mouse lung (Hartman et al., 1990). This result agrees with the present findings of petechial size haemorrhage, its sharp demarcation from surrounding tissue and its subpleural location. The finding that haemorrhage was located only in the caudal lobe of the lung could be explained by the attenuation of the thick muscle and reflection from the bones of the forelimbs. Also, advanced maturation of the cranial lobe in histological development (Farrell, 1982) could affect the result.

5.3.3 Haemorrhage in fetal tissues other than lungs

The risk of haemorrhage was significant in non-lung tissues as well as in lungs. Mostly, haemorrhage was located in the head (Table 4.2), in the skin and muscle. All haemorrhages in the head were located close to developing bones, as were those in the proximal forelimb, suggesting a reflection or boundary effect. Vykhodtseva et al. (1995) have found haemorrhage and tissue damage in rabbit brain produced by high power pulsed ultrasound (0,9-1.72 MHz). In the present study no haemorrhages were found in neural tissue, even though the brain had developed into a relatively large organ in the fetuses studied.

The liver was the second most common location of non-lung haemorrhage. Dalecki et al. (1997A) did not report liver damage. In the present study, haemorrhages in the liver, evidenced by irregular shaped collections of blood cells apparently enclosed within endothelial walls, were not easy to see.

5.3.4 The effect of age on fetal haemorrhage

All fetuses used in this study were in the last trimester, from 16 to 22 days old. Although there was a reasonably even distribution of ages over all fetuses used, this was not so within and between the levels of exposure (MI) and in the controls (Table 4.4). The results for all values of MI (0.5, 0.6 and 1.0) show that the highest risk of haemorrhage in the lungs was for fetuses at the canalicular stage of lung development, and that the number of lung haemorrhages declines subsequently.

The morphological events occurring in this period [Figure 4.2 (Chapter 4)] are:
(i) increasing vascularisation, characterised by completion of pre-acinar blood vessels within loose mesenchymal tissue and the invasion of the developing acini by capillaries (Farell, 1982). The vascularisation process occurs in a centripetal fashion, with the last phase having extension to the respiratory bronchioles.
(ii) The transition to the saccular stage of lung development (Plate 1) in which loose mesenchymal tissue is reduced and the saccular spaces are filled with "fetal pulmonary fluid".
(iii) The thoracic wall becomes thicker with development of intercostal muscle.
There was also no lung haemorrhage in the youngest fetuses, at 16 days of gestation. At this stage, the vascularisation of the mesenchyme was not apparent.

This study therefore suggests that the risk of haemorrhage from ultrasound exposure is greater at certain stages of lung development. Confirmation of this will require careful timing of gestational age in future experiments. Fetuses would be better studied at the time of most risk, apparently at 17 to 19 days. By standardising age, a better comparison of fetuses exposed to varying intensity of ultrasound would be possible.

Tissues other than lung were also less sensitive to haemorrhage in the older fetuses.

5.4 Possible pathophysiology of haemorrhage produced by ultrasound

The pathophysiology of ultrasound induced tissue damage is unknown, despite more than 30 years of using of ultrasound in medicine and several morphological studies on exposed animal models. Even in extracorporeal shock wave lithotripsy, the physical process by which kidney stone comminution is induced is not well understood (Cleveland et al., 1998).

5.4.1 Cavitation hypothesis

Cavitation includes a variety of phenomena and processes unique to biophysical ultrasonics (Miller et al., 1996). It may be considered generally as an interaction between an ultrasound field and any gaseous inclusion in a liquid medium (Miller and Thomas, 1995). For example, a form of cavitation called gas-body oscillation occurs when preexisting bodies of gas or gas bubbles are exposed to ultrasound. When the acoustic pressure varies rapidly, equilibrium between the pressure in the bubbles and the pressure in the liquid surrounding them may not have time to occur, and some bubbles will collapse producing a large gas pressure and marked local heating (Flint and Suslick, 1991).

Tissue damage is caused by the impact of high-speed liquid jets striking surfaces, producing tiny pits or craters on the different tissue layers with a mechanical lysis of the cells (Tavakkoli et al., 1997). Also there is evidence for production of free radicals during collapse of cavitation gas bubbles in ultrasound
exposed liquids which could have implications in cell injury (Christman et al., 1987).

The state of gas nucleation of tissues and organs *in vivo* is not well understood Miller et al., 1996). Because previous studies of adult and fetal mouse lung and intestine suggested that only tissues in which gas was present showed haemorrhage (Hartman et al. , 1990 ; Dalecki et al.; 1995) cavitation was a likely mechanism for tissue damage by ultrasound. Later, Dalecki et al. (1997A) found a significant proportion of ultrasound exposed fetuses with lung and non-lung haemorrhage. This result could not support cavitation as the only or primary pathomechanism of ultrasound produced tissue damage. As information accumulates it becomes less apparent that cavitation is responsible for lung haemorrhage (personal correspondence with Prof. Carstensen from the Rochester University Research Group, USA).

The results of the present study do not support cavitation as a primary cause of haemorrhage but this does not completely eliminate its possible involvement.
The highest proportion of haemorrhage was 64% in adult (MI 1.0) and 18.4 % (MI 0.5) in fetal rat lung. The result for fetal lung is based on finding haemorrhage from a tissue section at a single depth (Chapter 2). With serial sectioning to deep levels, more haemorrhage is likely to be located, and the actual incidence may be higher making cavitation, based on the presence of air interfaces, an even less likely cause.

The present study shows that because haemorrhage in fetal lung is age dependent, an experiment comparing adults with fetuses close to the full term (without haemorrhage) would be likely to support the cavitation hypothesis. An experiment using 18 day old fetuses would fail to support the concept, since they are likely to show lung haemorrhage.

In future, the development of a method to detect cavitation *in vivo* in different tissue exposed to ultrasound would be useful to check the cavitation hypothesis. The following methods have been used *in vitro*:
(i) The measurement of hydroxyl free radical concentration resulting from acoustic cavitation collapse in aqueous terephthalic acid solution (Christman et al., 1987).
(ii) Magnetic resonance imaging of ultrasound fields used to visualize longitudinal acoustic wave propagation in tissue, by mapping the minute particle displacement that accompanies propagating ultrasound waves (Walker et al., 1998).

5.4.2 Hypothesis on the association of developing bone with fetal haemorrhage.

Dalecki et al. (1997A) found a significant proportion of haemorrhage in 18 day but not 9 day old rat fetuses. The haemorrhages were found associated with tissues

near developing bone or cartilage. In 9 day fetuses there was no skeletal development and therefore no calcification of the primordial embryonic bone or cartilage.

In the present study, most fetal haemorrhage was also seen associated with developing bone or cartilage. However, the lack of haemorrhage in 21 day old fetuses and the low incidence in 22 day old fetuses indicate that presence of harder tissues does not have a primary influence on the incidence of haemorrhage.

5.4.3 Speculations on possible pathomechanisms

Vulnerability of tissues

The present study reports differences in the proportions of haemorrhage between adult lung and fetuses of different ages. This may occur because of effects of morphologically different tissues on propagation speed, attenuation and reflection of ultrasound waves (Chapter 1).

The fragility of blood vessels, when affected by ultrasound, may also depend on their support by the connective tissue matrix within the different tissues that they supply. Also, haemorrhage is likely to be more prevalent in tissues with a high capillary density, especially so in lung tissues (Astrand and Rodahl, 1986).

Adult lung with a mosaic of air-tissue interfaces will have many abrupt changes in propagation speed, and attenuation, and opportunities for reflection. Capillaries in fetal lung may be better supported at the saccular stage when they might be protected by fetal lung fluid.

Site of extravasation

Penney et al. (1993) provided light and electron microscopic evidence that haemorrhage in lung caused by ultrasound arose from capillaries within alveolar septa, resulting in blood cells free in alveolar spaces. This observation is confirmed in the present study although without the benefit of electron microscopy.

Heat

Petechia-like haemorrhages were seen in fetal lung in the present study, as well as in a study on mouse intestine by Miller and Gies (1998) using a low power level of continuous ultrasound (400 kHz) as used in physiotherapy. They considered that the petechiae were due to local heating. They also used low power pulsed ultrasound of the same frequency and produced haemorrhages larger than petechiae which were considered attributable to cavitation. Tissues such as muscle and liver, lacking gas bodies and marked interfaces, may be heated by ultrasound exposure (Miller and Gies, 1998). Heat is thus a possible factor in the pathomechanism of non-lung fetal haemorrhage found in present study. However to test a heating hypothesis, there are

difficulties inherent in measuring the heat produced, both during and following exposure, because of interference by the measuring device in the tissue.

Relative motion

A further hypothesis was advanced by Dalecky et al. (1997A), invoking the motion of partially ossified bones, especially ribs, relative to surrounding softer tissues. This relative motion may be sufficient to cause enough shear to tear fragile blood vessels in exposed mouse fetuses.

In the present study no lung haemorrhage was found in 21, 22 day rat fetuses in which the ribs and vertebrae are well ossified (Hebel and Stromberg, 1986).

Blast injury

Acoustic pressure is a unique physical property of a sound wave (Chapter 1) and it is used as a threshold parameter for ultrasound induced tissue damage. From this point of view a comparison of blast lung injury and ultrasound produced lung haemorrhage might be useful.

Blast injuries to lungs result in haemorrhages (Hirsch and Zumwalt, 1985). A sudden compression (pressure) wave propagates from a source through air (air blast) or water (hydro-blast). Injury to lungs is not a result of contusion from the impact of the ribs on the lung. Rather "extension strain forces" produced by distortion of the wave front in passing through the acoustically heterogeneous rib cage produce bands of lung haemorrhage corresponding to the intercostal region.

Dalecki et al. (1997A) concluded that fetal lung haemorrhage was associated with the ribs rather than intercostal spaces. Fetal lungs were examined grossly. In the present study, the relationships between the ribs and lung were maintained in the sections. Nevertheless there was no precise relationship apparent between the ribs and haemorrhage location (Figure 4.7). Haemorrhages did, however, occur subpleurally on the costal surfaces, but as foci rather than bands that might be compared to a blast injury effect from the ribs.

Reflection of ultrasound waves (Figure 1.4) from an ultrasound beam passing through an acoustically heterogeneous rib cage could focus ultrasound power on the exposed lung surface resulting in the type of multifocal lung haemorrhage found in adult and fetal rat lung in present study.

Rapid volume and pressure changes

Exercise-induced pulmonary haemorrhage commonly occurs in racehorses during severe exercise. Birks et al. (1997) have shown that it results from stress failure and disruption of pulmonary capillary endothelium, presumably caused by high pressures across capillary walls. The threshold value of the capillary pressure for the haemorrhage measured in that study was from 75 and 100mmHg. During exercise

when cardiac output may increase five times or more, pulmonary capillary pressure remains low because the pulmonary circulation has a remarkable ability to reduce its already low resistance (Widdicombe and Davies, 1991; Dawson et al., 1988).

Ultrasound induced haemorrhage is not attributable to a change in cardiac output, and it is local rather than generalised. Nevertheless, a comparable pulse of capillary pressure might occur by rapid vasoconstriction of pulmonary arterioles (Figure 3.4) resulting from ultrasound stimulation of their smooth muscle walls.

Hyninen et al. (1996) demonstrated that short (1 s), high-intensity focused ultrasound (1.49MHz) exposure can cause vascular spasm, and rupture with haemorrhage. Using the magnetic resonance and x-ray angiograms they showed that the vessel diameters relaxed back to their initial diameter during the first week after exposure.

In the present study vasostasis has been seen within capillaries in haemorrhagic regions of adult rat lungs, especially in association with doubtful haemorrhage (Chapter 3). As a result of sudden vasoconstriction, the pulse could be sufficient to rupture capillary walls in a manner similar to a 'water hammer" effect (Walshaw and Jobson, 1972). A lung capillary bed may be more susceptible than systematic capillaries, since flow regulation is different within lungs (Widdicombe and Davies, 1991).

The finding of free blood cells and plasma effusion within alveoli in localised parts of ultrasound exposed adult lungs in the present study is similar to the microscopical finding in lungs with pulmonary oedema (Kobzik et al., 1994). If the haemorrhage was located in well inflated lung the alveola septa would be expected to be obviously thickened were pulmonary oedema is present, but this was not so. Although plasma effusion to the alveoli was seen in adult lung in the present study, it was invariably associated with free blood cells and the situation is not similar to that of pulmonary oedema caused by circulatory interference (Kobzik et al.,1994). Production of surfactant is found to be important in lung fluid balance and the pathophysiology of pulmonary oedema. Its severe dilution with plasma effusion within alveoli could cause the collapse of the lung which is common in pulmonary oedema (Carlton and Bland, 1995; Morgenroth and Newhouse, 1988). Also, collapse of the haemorrhaged part of adult rat lung was a common finding in the present study. An increased secretion of surfactant occurs over the last third of fetal development, expecially in fetuses around birth (Wasowicz et al., 1996). This could have a protective role for the oldest fetuses, which did not show lung damage in the present study. But the presence of a combination of surfactant with gas within alveoli in adults could induce cavitation during ultrasound exposure. This could explain the finding of a higher risk to adult rat lungs than to fetal lung in 21-22 day old rat fetuses in the present study.

5.4.4 Ultrasound induced haemorrhage and the repair process

Local haemorrhage, such as that found in the present study, should be repaired in the same manner as other localised haemorrhages from various causes such as a common bruise. Following haemorrhage, the erythrocytes are phagocytised by macrophages and haemoglobin is eventually transformed to haemosiderin by lysosomal enzymes (Robbins et al., 1994).

After acute injury, repairs to the vascular wall and its endothelial lining are made by a physiological process. Sometimes, however, thickening as a healing response becomes exaggerated, resulting in intimal thickening hyperplasia, stenosis or occlusion of small and medium-sized blood vessels, and possibly a base for atherosclerosis (Schoen, 1994) or pulmonary hypertension (Rounds, 1989). In lungs with pulmonary oedema caused by ozone inhalation, a thickening of small pulmonary arteries was found as a long-term effect (Friedman, 1988).

Ultrasound produced haemorrhage appears to involve only capillaries. Were there to be a risk to health from the repairing of damaged endothelial walls, an epidemiological study of the first pre- and neonatally exposed humans born in the 1960s would be a check on the safety of ultrasound exposure.

5.4.5 The animal as a model for humans

One cannot infer that exposures to ultrasound which produce embryonic and fetal effects in the mouse and rat would have the same results in the human (Brent, Jensh and Beckman, 1991). Different animal species used as models are usually of different body size, and there are morphological differences in lungs as well as other organs. Apart from mice and rats there have been studies on non-human primates (Tarantal and Canfield, 1994) and rabbits and pigs (O'Brien and Zachary, 1996 and Baggs et al., 1996) that do not conclusively show that any species is especially relevant to humans However, mechanical injury is probably better extrapolated across species than are drug, metabolic, and toxicological effects for which animals are so often used.
Tarantal and Hendrickx (1989) investigated the potential teratological risk of diagnostic ultrasound on the fetuses of monkeys. Their equipment also closely modelled the situations in humans. No long-term effects were found in these fetuses.

5.5 Precautionary conclusion

This study, in common with studies on other animals, has shown tissue damage by ultrasound exposure, and a damage threshold has been indicated for adult rat lung. The results in fetuses emphasize the complexity of examining these issues. Further studies are required with more precise experimental design especially concerning fetal age, uniform level of exposure and fetal position. The fetuses of pigs and monkeys are recommended as models for humans in further studies, because of their larger size and closer physiological similarity to human infants (Tarantal et Hendrichx, 1994; Tarantal

and Canfield, 1994; O'Brien and Zachary, 1996).

A number of epidemiological studies (Brent et al., 1991) have shown no long term effects on exposed humans. The benefits of using ultrasound in medicine is enormous, and manufacturers of ultrasound machines continue to compete in technological development of new and more powerful machines.

The pathomechanisms of possible tissue damage by diagnostic and also by stone comminution by lithotripter (Cleveland et al., 1998) remain unknown, necessitating continued research into adult and fetal animal models.

In addition, the repair mechanism of damaged tissue, and the possible effects on nervous tissue (Vykhodtseva et al., 1995; Paneth, 1998) and DNA (Doida and Miller, 1992; Anon., 1999) warrant further investigation. Until these questions have been answered, care should be exercised in the use of ultrasound when it is used in patients with bleeding disorders and in pregnant women. Mechanical indices higher than 0.5 should be avoided during echocardiography and especially during obstetrical examination when pulsed Doppler ultrasound is used.

There is insufficient evidence to make recommendations for or against routine ultrasound examination of low risk women in the second trimester (Anon.,1997). The canalicular stage of human lung development happens in the second trimester from 16 to 26 weeks of pregnancy (Valdes-Dapena, 1979 and Farrell, 1982) and in the present study most fetal rat lung haemorrhages were found in this stage of lung development. Careful reference to the mechanical index display is necessary and if possible mechanical indices higher then 0.5 should be avoided during echocardiography and especially during obstretrical examination when pulsed Doppler ultrasound is used.

The results of research on experimental animals should not be ignored. Neither should researchers engender panic among the public with their results.

REFERENCES

Andrew, E. R.; Bydder, G.; Griffits, J; Iles, R.; Styles, P. (editors) Preface. In *Clinical magnetic resonance imaging and spectroscopy*. New York-John Willey and sons, **1990.**

Angles, J. M.; Walsh, D. A.; Barnet, S. B. Effects of pulsed ultrasound and temperature on the development of rat embryos in culture. *Teratology*. **42**:285-293, **1990.**

Anonymous Guide to clinical preventive services (Screening ultrasonography in pregnancy/recommendation. **http://text.nlm.nih.gov./cps/www/cps.42.html (1997).**

Anonymous Science, technology and health news. Research casts shadow on safety of ultrasound scans. *The Royal Society of New Zealand.* **http://www.rsnz.govt.nz/daily/y-1999/m-06/d-10/.**

AIUM, American Institute of Ultrasound in Medicine/National Electrical Manufacturers Association. Standard for real-time display of thermal and mechanical acoustic output indices on diagnostic ultrasound equipment. *AIUM/NEMA*, **1992.**

Astrand, P. O. and Rodahl, K. (editors) Respiration. In *Textbook of work physiology/physiological bases of exercise*, Third edition, pp. 209-272. New York-McGraw-Hill, **1986.**

Atkinson, D. E.; Sibley, C. P.; Williams, A. R. Effects of ultrasound on placental transfer during the last third of gestation in the rat. *Ultrasonics*. **28**:171-174, **1990.**

Baggs, R.; Penney, D. P.; Cox, C.; Child, S. Z.; Raeman, C. H.; Dalecki, D., and Carstensen, E. L. Threshold for ultrasonically induced lung hemorrhage in neonatal swine. *Ultrasound in Medicine and Biology*. **22**:119-128, **1996.**

Ball, R. and Moore, A. D. (editors) Ultrasound. In *Essential Physics for Radiographers*, Third edition, pp. 348-345. Blackwell Science, **1997.**

Birks, E. K.; Mathieu-Costello, O.; Fu, Z.; Tyler, W. S.; West, J. B. Very high pressures are required to cause stress failure of pulmonary capillaries in Thoroughbred racehorses. *Journal of Applied Physiology*. **82**:1584-1592, **1997.**

Boon, J. A. (editor) The physics of ultrasound. In *Manual of Veterinary Echocardiography*, pp. 17-25. Baltimore-Williams and Wilkins, **1998**.

Boyd, P. A.; Chamberlain, P.; Hicks, N. R. 6-year experience of prenatal diagnosis in an unselected population in Oxford, UK. *The Lancet*. **352**:1577-81, **1998**.

Brent, R. L.; Jensh, R. P.; Beckman, D. A. Medical sonography: reproductive effects and risk. *Teratology*. **44**:123-146, **1991**.

Breyer, B. and Andreic, Z. Fizika ultrazvuka. In *Ultrazvuk u klinickoj medicini*, pp. 1-3 (serbo-croation language). Edited by Kurjak, A. Zagreb-Naprijed, **1989**.

Brown, N. A. Nassiri, D.; Haar, G. Comments on "Effects of pulsed ultrasound and temperature on the development of rat embryos in culture" (Letter to editor). *Teratology*. **43**:551, **1991**.

Bude, R. O. and Rubin, J. M. Power Doppler sonography. *Radiology*. **200**:21-23, **1996**.

Carlton, D. P. and Bland, R. D. Surfactant and lung fluid balance. In *Surfactant therapy for lung disease*, pp. 33-46. Edited by Robertson, B.; Taeusch, H. W. New York-Marcel Dekker, **1995**.

Carnes, K. I. and Dunn, F. The effect of ultrasound *in utero* on the development of the fetal mouse testis: adult consequences. *Ultrasound in Medicine & Biology*. **21**:1247-57, **1995**.

Carstensen, E. L.; Campbell, D. S.; Hoffman, D.; Child, S.Z.; Ayme-Bellagarda, E. Killing of *Drosophila larvae* by the fields of an electrohydraulic lithotripter. *Ultrasound in Medicine & Biology*. **16**:687-698, **1990**.

Chesterfield, D. and Parton, K. Training and development: animal handling, research considerations and the biology and diseases of rats and mice. Massey University, **1997**.

Child, S. Z.; Hartman, C. L.; Schery, L. A.; Carstensen, E. L. Lung damage from exposure to pulsed ultrasound. *Ultrasound in Medicine and Biology*. **16**:817-825, **1990**.

Christman, C. L.; Carmichael, A.J.; Mossoba, M. M.; Riesz, P. Evidence for free radicals produced in aqueous solutions by diagnostic ultrasound. *Ultrasonics*. **25**:31-34, **1987**.

Cleveland, R. O.; Lifshitz, D. A.; Connors, B. A.; Evan, A. P.; Willis, L. R.; Crum, L. A. *In vivo* pressure measurements of lithotripsy shock waves in pigs. *Ultrasound in Medicine & Biology*. **24**:293-306, **1998**.

Coleman, A. J.; Draguioti, R.; Tiptaf, R.; Shotri, N.; Saunders, J. E. Acoustic performance and clinical use of a fibreoptic hydrophone. *Ultrasound in Medicine and Biology*. **24**:143-151, **1998**.

Cosgrove, D. The expanding role of ultrasound. *British Journal of Hospital Medicine*. **57**:7-9, **1997**.

Cotran, R. S.; Kumar, V.; Robbins, S. L. (editors) Hemodynamic disorders, thrombosis and shock. In *Robbins/Pathologic basis of disease*, Fifth edition, pp. 93-123. Philadelphia- W. B. Saunders, **1994**.

Culling, C.F.A.; Allison, RE.T.; Allison, R.T.; Barr, W. T. Decalcification. In *Cellular techniques*, pp 412-415. London- Butterworths,

Cutnell and Johnsoon (editors) Sound Intensity. In *Physics*, Volume I, pp. 471-474. New York-John Wiley and sons, **1998**.

Dalecki, D.; Raeman, C. H.; Child, S. Z.; Carstensen, E. L. Intestinal hemorrhage from exposure to pulsed ultrasound. *Ultrasound in Medicine and Biology*. **21**:1067-1072, **1995**.

Dalecki, D.; Raeman, C. H.; Child, S. Z; Carstensen, E. L. A test for cavitation as a mechanism for intestinal hemorrhage in mice exposed to a piezoelectric lithotripter. *Ultrasound in Medicine and Biology*. **22**:493-496, **1996**.

Dalecki, D.; Child, S. Z; Raeman, C. H.; Penney, D. P.; Mayer,R; Cox, C.; Carstensen, E. L. Thresholds for fetal hemorrhages produced by a piezoelectric lithotripter. *Ultrasound in Medicine and Biology*. **23**:287-297, **1997A**.

Dalecki, D.; Child, S. Z.; Raeman, C. H.; Cox, C.; Carstensen, E. L. Ultrasonically induced lung hemorrhage in young swine. *Ultrasound in Medicine and Biology*. **23**:777-781, **1997B**.

Dawes, G. S. (editor) Fetal O2 consumption and general anaesthesia. In *Fetal and neonatal physiology*, pp. 109-112. Chicago-Year Book Medical Publisher, **1968**.

Dawson, C. A.; Bronikowski, T. A.; Linehan, J. H.; Rickaby, D. A. Distributions of vascular pressure and resistence in the lung. *Journal of Applied Physiology*. **64**:274-284, **1988**.

Doida, Y., and Miller, M. W. Failure to confirm increase in unscheduled DNA synthesis in sonicated mammalian cells in vitro. *Ultrasonics*. **30**:35-9, **1992**.

Evans, J. A. Physics-the nature of ultrasound. In *Practical Ultrasound*, pp. 1-13. Edited by Lerski, R. A. Oxford-IRL press, **1998**.

Farrell, M. P. (editor) Morphological aspects of lung maturation. In *Lung development: biological and clinical perspectives*, pp. 13-25. London-Academic Press, **1982**.

Feigl, T.; Volklein, B.; Iro, H.; Schneider, T. Biophysical effects of high-energy pulsed ultrasound on human cells. *Ultrasound in Medicine and Biology*. **22**:1267-75, **1996**.

Fish, R. E. Barbiturates. In *Anaesthesia and analgesia in laboratory animals*, pp. 2-4 Edited by **Kohn, D. F.; Wixson, S. K.; White, W. J. and Benson, G. J.** New York-Academic Press, **1997**.

Fisher, J. E.; Acuff_Smith, K. D.; Schilling, M. A.; Vorhees, C. V.; Meyer, R. A.; Smith, N. B.; O'Brien, W. D. Teratologic evaluation of rats prenatally exposed to pulsed-wave ultrasound. *Teratology*. **49**:150-155, **1994**.

Flecknell, P. A. (editor) Anaesthesia of pregnant animals. In *Laboratory animal anaesthesia*, pp. 122-124. London-Academic Press, **1996**.

Flint, E. B. and Suslick, K. S. The temperature of cavitation. *Science*. **253**:1397-1399, **1991**.

Friedman, M. Effects of airborne pollution on endothelial cell metabolism. In *Toxicology of the lung*, pp. 269-283. Edited by Gardner, D. E.; Crapo, J. D., and Massaro, E. J. New York- Raven Press, **1988**.

Galperin-Lemaitre, H. and Kirsch-Volders, M. Ultrasound and mammalian D.N.A. *The Lancet*. **October 4**:662, **1975**.

Gunnison, A. F. and Finkelstein, I. Rat lung phospholipid fatty acid composition in prepregnant, pregnant, and lactating rats: relationship to ozone-induced pulmonary toxicity. *Lung*. **175**:125-137, **1997.**

Haar, G. Commentary: Safety of diagnostic ultrasound. *The British Journal of Radiology*. **69**:1083-85, **1996.**

Hande, M. P. and Devi, P. U. Effect of *in utero* exposure to diagnostic ultrasound on the postnatal survival and growth of mice. *Teratology*. **48**:405-411, **1993**.

Harding, L. K. Radiation protection - lessons from the past. *The British Journal of Radiology*. **70**:S10-S16, **1997**.

Harris. G. R. Are current hydrophone low frequency response standards acceptable for measuring mechanical/cavitation indices? *Ultrasonics*. **34**:649-54, **1996.**

Hartman, C.; Child, S. Z.; Mayer, R.; Schenk, E.; Carstensen, E. L. Lung damage from exposure to the fields of an electrohydraulic lithotripter. *Ultrasound in Medicine and Biology*. **16**:675-679, **1990.**

Hebel, R. and Stromberg, M. W.(editors) Embryology. In *Anatomy and embryology of the laboratory rat*, pp. 231-235. Worthsee (Federal Republic of Germany)-BioMedVerlag, **1986.**

Hirsch, C. S. and Zumwalt, R. E. Injuries caused by physical agents. In *Anderson's pathology*, pp. 128-136. Edited by Kissane, J. M. St. Louis- Mosby, **1990**.

Hyninen, K.; Chung, A. H.; Colucci, V., and Jolesz, F. A. Potential adverse effects of high-intensity focused ultrasound exposure on blood vessels *in vivo*. *Ultrasound in Medicine & Biology*. **22**:193-201, **1996.**

Jochle, K.; Debus, J.; Lorenz, W. J.; Huber, P. A new method of quantitative cavitation assessment in the field of lithotripter. *Ultrasound in Medicine and Biology*. **22**:329-338, **1996.**

Kay, J. M. Blood vessels of the lung. In *Comparative Biology of the Normal Lung*, Volume I, pp. 163-172. Edited by Parent, R. A. London-CRC Press, **1991.**

Kimmel, C. A.; Stratmeyer, M. E.; Galloway, W. D.; Brown, N. T.; Laborde, J. B.; Bates, H. K. Developmental exposure of mice to pulsed ultrasound. *Ultrasound in Medicine and Biology*. **40**:387-393, **1989**.

Kobzik, L., and Schoen, F. J. Diseases of vascular origin. In Chapter 15-The lung. In *Robbins/ Pathologic basis of disease*, 5th edition, pp. 676-681. Edited by Cotran, R. S.; Kumar, V.; Robbins, S. L. , and Schoen, F. J. Philadelphia- W.B. Saunders, **1994**.

Lockwood, G. R. A miniature high frequency array probe for medical ultrasound imaging. *The Whitaker Foundation Biomedical Enginering Grants May 1996*. **http://www.whitaker.org/abstract/rgmay96.html**

Lyons, E. A.; Dyke, C.; Toms, M.; Cheang, M.; Math, M. *In utero* exposure to diagnostic ultrasound: a 6-year follow-up. *Radiology*. **166**:687-690, **1988**.

McNeil, D. (editor) Mantel-Haenzel Methods. In *Epidemiological Research Methods*, pp. 95-123. New York- John Wiley and sons, **1996**.

McNeil, D. (editor) Logistic regression I. In *Epidemiological Research Methods*, pp. 125-129. New York- John Wiley and sons, **1996**.

Mercer, R. R. and Crapo, J. D. Architecture of the acinus. In *Comparative Biology of the Normal Lung*, Volume I, pp. 109-118. Edited by Parent, R. A. London-CRC Press, **1991**.

Miller, M. W.; Miller, D. L., and Brayman, A. A. A review of *in vitro* bioeffects of inertial ultrasonics cavitation from a mechanistic perspective. *Ultrasound in Medicine and Biology*. **22**:1131-1154, **1996**.

Miller, D. L. and Thomas, R. M. The role of cavitation in the induction of cellular DNA damage by ultrasound and lithotripter shock waves *in vitro*. *Ultrasound in Medicine and Biology*. **22**:681-687, **1996**.

Miller, D. L.; and Gies, R. A. The interaction of ultrasonic heating and cavitation in vascular bioeffect on mouse intestine. *Ultrasound in Medicine and Biology*. **24**:123-128, **1998**.

Morgenroth, K. and Newhouse, M. (editors) Adult respiratory distress syndrome. In *The surfactant system of the lungs*, **pp.** 91-108. Berlin- Walter de Gruyter, **1988**.

O'Brien, W. D. and Zachary, J. F. Comparison of mouse and rabbit lung damage from exposure to continuous wave 30-kHz ultrasound. *Ultrasound in Medicine and Biology*. **20**:299-307, **1994**.

O'Brien, W. D. and Zachary, J. F. Rabbit and pig lung damage comparison from exposure to continuous wave 30-kHz ultrasound. *Ultrasound in Medicine and Biology*. **22**:345-353, **1996**.

Paneth, N. Prenatal sonography-safe or sinister? *The Lancet*. **352**:5-6, **1998**.

Penney, D. P.; Schenk, E. A.; Maltby, K.; Hartman-Raeman, C.; Child, S. Z.; Carstensen, E. L. Morphological effects of pulsed ultrasound in the lung. *Ultrasound in Medicine and Biology*. **19**:127-135, **1993**.

Petergew, J. W. (editor) Preface. In *NMR: Principles and applications to Biomedical Research*, pp. v-viii. New York-Springer-Werlag, **1989**.

Pfeiffer, D. U. (editor) *Veterinary epidemiology - An introduction*, pp. 21-24, **1996**.

Plumb, D. C. (editor) Drug Monographs-pentobarbitol. In *Veterinary Drug Handbook*, p. 497. Iowa State University-Ames, **1999**.

Reef, V. B. (editor) Equine diagnostic ultrasound. W. B. Saunders, **1998**.

Rounds, S. I. S. Pulmonary circulatory control in lung injury. In *Pulmonary vascular physiology and pathophysiology*, pp. 403-443. Edited by Weir, K. E., and Reeves, J. T. New York- Marcel Dekker, **1989**.

Schneider, B. F. and Norton, S. Equivalent ages in rat, mouse and chick embryos. *Teratology*. **19**:273-278, **1979**.

Sears, F. W.; Zemansky, M. W., and Young, H. D. (editors) *University Physics*, Sixth edition. Addison-Wesley, **1982**.

Shoen, F. J. Blood vessels. In *Robbins/Pathologic basis of disease*, Fifth edition, pp. 467-472. Edited by Cotran, R. S.; Kumar, V., and Robbins. Philadelphia- W. B. Saunders, **1994**.

Steinhorn, R. H. Prenatal ultrasonography: first do no harm. *The Lancet*. **352**:1568-69, **1998**.

Tarantal, A. F. and Canfield, D. Ultrasound-induced lung hemorrhage in the monkey. *Ultrasound in Medicine and Biology*. **20**:65-72, **1994**.

Tarantal, A. F. and Hendrickx, A. G. Evaluation of the bioeffects of prenatal ultrasound exposure in the Cynomolgus Macaque (*Macaca fascicularis*): III. Developmental and hematologic studies. *Teratology*. **47**:159-170, **1993**.

Tavakkoli, J.; Birer, A.; Arefiev, A.; Prat, F.; Chapelon, J. Y.; Cathignol, D. A piezocomposite shock wave generator with electronic focusing capability: application for producing cavitation-induced lesions in rabbit liver. *Ultrasound in Medicine and Biology*. **23**:107-115, **1997**.

Thrusfield, M. (editor) Measures of association. In *Veterinary epidemiology*, Second edition, pp. 225-227. Oxford-Blackwell Scientific, **1995**.

Valdes-Dapena, M. A. (editor) Adult respiratory distress syndrome. In *The surfactant system of the lungs*, pp. 309-310. London- W. B. Saunders, **1979**.

Vrdoljak, J. and Japelj, I. Ultrazvucni pribor za luksacijsku manu kuka. In *Ultrazvuk u klinickoj medicini*, pp. 361 (serbo-croatian language). Edited by Kurjak, A. Zagreb-Naprijed, **1989**.

Vykhodtseva, N. I.; Hunynen, K., and Damianou, C. Histologic effects of high intensity pulsed ultrasound exposure with subharmonic emission in rabbit brain *in vivo*. *Ultrasound in Medicine & Biology*. **21**:969-979, **1995**.

Wagai, T. and Fukuda, M. (editors) The World Federation seminar on safety and standardization of diagnostic ultrasound in obstetrics. In *Ultrasound in Medicine & Biology*, International Congress Series, pp. 11-13. Excerpta Medica, **1988**.

Walker, C. L.; Foster, F. S., and Plewes, D. B. Magnetic resonance imaging of ultrasound fields. *Ultrasound in Medicine and Biology*. **24**:137-142, **1998**.

Walshaw, A. C. and Jobson, D. A. (editors) Water hammer. In *Mechanics of Fluids*, second edition, pp. 352-355. London- Longman, **1972**.

Wasowicz, M.; Kashima, K.; Yokoyama, S.; Nakayama, I. Pulmonary surfactant migrates into alveolar capillaries of newborn rats: An immunoelectron microscopic study. *Acta Anatomica*. **156**:11-21, **1996**.

Webb, S. (editor) In the beginning. In *The physics of medical imaging*, pp. 7-16. Bristol-Adam Hilger, **1988**.

Weil, F. S. Doppler Imaging. In *Ultrasound Diagnosis of Digestive Diseases*, pp.19-21. Springer, **1996.**

Weir, K. E. and Reeves, J. T. *Pulmonary vascular physiology and pathophysiology*. New York-Marcel Dekker, inc., **1989.**

Widdicombe, J. and Davies, A. (editors) Pulmonary circulation. In *Respiratory Physiology*, second edition, pp. 55-81. London-Edvard Arnold, **1991.**

Widdicombe, J. and Davies, A. (editors) Lung structure and function. In *Respiratory Physiology*, Second edition, pp. 1-16. London- Edward Arnold, **1991.**

Wilson, K. J. W. (editor) A lung structure and function. In *Ross and Wilson. Anatomy and physiology in health and illness*, seventh edition, pp 121-149. Edinburg-Churchill Livingstone, **1990**.

Wilson, L. M. and Waterhouse, J. A. H. Obstetric ultrasound and childhood malignancies. *The Lancet*. **November 3**:997-1000, **1984.**

Wixson, S. K. and Smiler, K. L. Parenteral general anesthetics. In *Anaesthesia and analgesia in labaratory animals*, pp. 173-175. Edited by Kohn, D. F.; Wixson, S. K.; White, W. J. and Benson, G. J. New York- Academic Press, **1997**.